THE UNIVERSITY OF CALGARY

DUAL DIVERSITY ANTENNAS FOR HAND-HELD RADIO

by

MARK GORDON DOUGLAS

A THESIS
SUBMITTED TO THE FACULTY OF GRADUATE STUDIES
IN PARTIAL FULFILLMENT OF THE REQUIREMENTS FOR THE
DEGREE OF MASTER OF SCIENCE

DEPARTMENT OF ELECTRICAL AND
COMPUTER ENGINEERING

CALGARY, ALBERTA

MARCH, 1993

ISBN 0-315-83136-7

Name MARK GORDON DOUGLAS

Dissertation Abstracts International is arranged by broad, general subject categories. Please select the one subject which most nearly describes the content of your dissertation. Enter the corresponding four-digit code in the spaces provided.

ELECTRONICS AND ELECTRICAL ENGINEERING | 0 5 4 4 | U·M·I

SUBJECT TERM | SUBJECT CODE

Subject Categories

THE HUMANITIES AND SOCIAL SCIENCES

COMMUNICATIONS AND THE ARTS
Architecture 0729
Art History 0377
Cinema 0900
Dance 0378
Fine Arts 0357
Information Science 0723
Journalism 0391
Library Science 0399
Mass Communications 0708
Music 0413
Speech Communication 0459
Theater 0465

EDUCATION
General 0515
Administration 0514
Adult and Continuing 0516
Agricultural 0517
Art 0273
Bilingual and Multicultural 0282
Business 0688
Community College 0275
Curriculum and Instruction 0727
Early Childhood 0518
Elementary 0524
Finance 0277
Guidance and Counseling 0519
Health 0680
Higher 0745
History of 0520
Home Economics 0278
Industrial 0521
Language and Literature 0279
Mathematics 0280
Music 0522
Philosophy of 0998
Physical 0523
Psychology 0525
Reading 0535
Religious 0527
Sciences 0714
Secondary 0533
Social Sciences 0534
Sociology of 0340
Special 0529
Teacher Training 0530
Technology 0710
Tests and Measurements 0288
Vocational 0747

LANGUAGE, LITERATURE AND LINGUISTICS
Language
- General 0679
- Ancient 0289
- Linguistics 0290
- Modern 0291

Literature
- General 0401
- Classical 0294
- Comparative 0295
- Medieval 0297
- Modern 0298
- African 0316
- American 0591
- Asian 0305
- Canadian (English) 0352
- Canadian (French) 0355
- English 0593
- Germanic 0311
- Latin American 0312
- Middle Eastern 0315
- Romance 0313
- Slavic and East European 0314

PHILOSOPHY, RELIGION AND THEOLOGY
Philosophy 0422
Religion
- General 0318
- Biblical Studies 0321
- Clergy 0319
- History of 0320
- Philosophy of 0322

Theology 0469

SOCIAL SCIENCES
American Studies 0323
Anthropology
- Archaeology 0324
- Cultural 0326
- Physical 0327

Business Administration
- General 0310
- Accounting 0272
- Banking 0770
- Management 0454
- Marketing 0338

Canadian Studies 0385
Economics
- General 0501
- Agricultural 0503
- Commerce-Business 0505
- Finance 0508
- History 0509
- Labor 0510
- Theory 0511

Folklore 0358
Geography 0366
Gerontology 0351
History
- General 0578
- Ancient 0579
- Medieval 0581
- Modern 0582
- Black 0328
- African 0331
- Asia, Australia and Oceania 0332
- Canadian 0334
- European 0335
- Latin American 0336
- Middle Eastern 0333
- United States 0337

History of Science 0585
Law 0398
Political Science
- General 0615
- International Law and Relations 0616
- Public Administration 0617

Recreation 0814
Social Work 0452
Sociology
- General 0626
- Criminology and Penology 0627
- Demography 0938
- Ethnic and Racial Studies 0631
- Individual and Family Studies 0628
- Industrial and Labor Relations 0629
- Public and Social Welfare 0630
- Social Structure and Development 0700
- Theory and Methods 0344

Transportation 0709
Urban and Regional Planning 0999
Women's Studies 0453

THE SCIENCES AND ENGINEERING

BIOLOGICAL SCIENCES
Agriculture
- General 0473
- Agronomy 0285
- Animal Culture and Nutrition 0475
- Animal Pathology 0476
- Food Science and Technology 0359
- Forestry and Wildlife 0478
- Plant Culture 0479
- Plant Pathology 0480
- Plant Physiology 0817
- Range Management 0777
- Wood Technology 0746

Biology
- General 0306
- Anatomy 0287
- Biostatistics 0308
- Botany 0309
- Cell 0379
- Ecology 0329
- Entomology 0353
- Genetics 0369
- Limnology 0793
- Microbiology 0410
- Molecular 0307
- Neuroscience 0317
- Oceanography 0416
- Physiology 0433
- Radiation 0821
- Veterinary Science 0778
- Zoology 0472

Biophysics
- General 0786
- Medical 0760

EARTH SCIENCES
Biogeochemistry 0425
Geochemistry 0996
Geodesy 0370
Geology 0372
Geophysics 0373
Hydrology 0388
Mineralogy 0411
Paleobotany 0345
Paleoecology 0426
Paleontology 0418
Paleozoology 0985
Palynology 0427
Physical Geography 0368
Physical Oceanography 0415

HEALTH AND ENVIRONMENTAL SCIENCES
Environmental Sciences 0768
Health Sciences
- General 0566
- Audiology 0300
- Chemotherapy 0992
- Dentistry 0567
- Education 0350
- Hospital Management 0769
- Human Development 0758
- Immunology 0982
- Medicine and Surgery 0564
- Mental Health 0347
- Nursing 0569
- Nutrition 0570
- Obstetrics and Gynecology 0380
- Occupational Health and Therapy 0354
- Ophthalmology 0381
- Pathology 0571
- Pharmacology 0419
- Pharmacy 0572
- Physical Therapy 0382
- Public Health 0573
- Radiology 0574
- Recreation 0575
- Speech Pathology 0460
- Toxicology 0383

Home Economics 0386

PHYSICAL SCIENCES
Pure Sciences

Chemistry
- General 0485
- Agricultural 0749
- Analytical 0486
- Biochemistry 0487
- Inorganic 0488
- Nuclear 0738
- Organic 0490
- Pharmaceutical 0491
- Physical 0494
- Polymer 0495
- Radiation 0754

Mathematics 0405
Physics
- General 0605
- Acoustics 0986
- Astronomy and Astrophysics 0606
- Atmospheric Science 0608
- Atomic 0748
- Electronics and Electricity 0607
- Elementary Particles and High Energy 0798
- Fluid and Plasma 0759
- Molecular 0609
- Nuclear 0610
- Optics 0752
- Radiation 0756
- Solid State 0611

Statistics 0463

Applied Sciences

Applied Mechanics 0346
Computer Science 0984

Engineering
- General 0537
- Aerospace 0538
- Agricultural 0539
- Automotive 0540
- Biomedical 0541
- Chemical 0542
- Civil 0543
- Electronics and Electrical 0544
- Heat and Thermodynamics 0348
- Hydraulic 0545
- Industrial 0546
- Marine 0547
- Materials Science 0794
- Mechanical 0548
- Metallurgy 0743
- Mining 0551
- Nuclear 0552
- Packaging 0549
- Petroleum 0765
- Sanitary and Municipal 0554
- System Science 0790

Geotechnology 0428
Operations Research 0796
Plastics Technology 0795
Textile Technology 0994

PSYCHOLOGY
General 0621
Behavioral 0384
Clinical 0622
Developmental 0620
Experimental 0623
Industrial 0624
Personality 0625
Physiological 0989
Psychobiology 0349
Psychometrics 0632
Social 0451

Nom ____

Dissertation Abstracts International est organisé en catégories de sujets. Veuillez s.v.p. choisir le sujet qui décrit le mieux votre thèse et inscrivez le code numérique approprié dans l'espace réservé ci-dessous.

______________________________ SUJET | □□□□ CODE DE SUJET | U·M·I

Catégories par sujets

HUMANITÉS ET SCIENCES SOCIALES

COMMUNICATIONS ET LES ARTS
Architecture 0729
Beaux-arts 0357
Bibliothéconomie 0399
Cinéma 0900
Communication verbale 0459
Communications 0708
Danse 0378
Histoire de l'art 0377
Journalisme 0391
Musique 0413
Sciences de l'information 0723
Théâtre 0465

ÉDUCATION
Généralités 515
Administration 0514
Art 0273
Collèges communautaires 0275
Commerce 0688
Économie domestique 0278
Éducation permanente 0516
Éducation préscolaire 0518
Éducation sanitaire 0680
Enseignement agricole 0517
Enseignement bilingue et multiculturel 0282
Enseignement industriel 0521
Enseignement primaire. 0524
Enseignement professionnel 0747
Enseignement religieux 0527
Enseignement secondaire 0533
Enseignement spécial 0529
Enseignement supérieur 0745
Évaluation 0288
Finances 0277
Formation des enseignants 0530
Histoire de l'éducation 0520
Langues et littérature 0279
Lecture 0535
Mathématiques 0280
Musique 0522
Orientation et consultation 0519
Philosophie de l'éducation 0998
Physique 0523
Programmes d'études et enseignement 0727
Psychologie 0525
Sciences 0714
Sciences sociales 0534
Sociologie de l'éducation 0340
Technologie 0710

LANGUE, LITTÉRATURE ET LINGUISTIQUE
Langues
- Généralités 0679
- Anciennes 0289
- Linguistique 0290
- Modernes 0291

Littérature
- Généralités 0401
- Anciennes 0294
- Comparée 0295
- Mediévale 0297
- Moderne 0298
- Africaine 0316
- Américaine 0591
- Anglaise 0593
- Asiatique 0305
- Canadienne (Anglaise) 0352
- Canadienne (Française) 0355
- Germanique 0311
- Latino-américaine 0312
- Moyen-orientale 0315
- Romane 0313
- Slave et est-européenne 0314

PHILOSOPHIE, RELIGION ET THÉOLOGIE
Philosophie 0422
Religion
- Généralités 0318
- Clergé 0319
- Études bibliques 0321
- Histoire des religions 0320
- Philosophie de la religion 0322

Théologie 0469

SCIENCES SOCIALES
Anthropologie
- Archéologie 0324
- Culturelle 0326
- Physique 0327

Droit 0398
Économie
- Généralités 0501
- Commerce-Affaires 0505
- Économie agricole 0503
- Économie du travail 0510
- Finances 0508
- Histoire 0509
- Théorie 0511

Études américaines 0323
Études canadiennes 0385
Études féministes 0453
Folklore 0358
Géographie 0366
Gérontologie 0351
Gestion des affaires
- Généralités 0310
- Administration 0454
- Banques 0770
- Comptabilité 0272
- Marketing 0338

Histoire
- Histoire générale 0578
- Ancienne 0579
- Médiévale 0581
- Moderne 0582
- Histoire des noirs 0328
- Africaine 0331
- Canadienne 0334
- États-Unis 0337
- Européenne 0335
- Moyen-orientale 0333
- Latino-américaine 0336
- Asie, Australie et Océanie 0332

Histoire des sciences 0585
Loisirs 0814
Planification urbaine et régionale 0999
Science politique
- Généralités 0615
- Administration publique 0617
- Droit et relations internationales 0616

Sociologie
- Généralités 0626
- Aide et bien-àtre social 0630
- Criminologie et établissements pénitentiaires 0627
- Démographie 0938
- Études de l' individu et de la famille 0628
- Études des relations interethniques et des relations raciales 0631
- Structure et développement social 0700
- Théorie et méthodes 0344
- Travail et relations industrielles 0629

Transports 0709
Travail social 0452

SCIENCES ET INGÉNIERIE

SCIENCES BIOLOGIQUES
Agriculture
- Généralités 0473
- Agronomie. 0285
- Alimentation et technologie alimentaire 0359
- Culture 0479
- Élevage et alimentation 0475
- Exploitation des péturages 0777
- Pathologie animale 0476
- Pathologie végétale 0480
- Physiologie végétale 0817
- Sylviculture et faune 0478
- Technologie du bois 0746

Biologie
- Généralités 0306
- Anatomie 0287
- Biologie (Statistiques) 0308
- Biologie moléculaire 0307
- Botanique 0309
- Cellule 0379
- Écologie 0329
- Entomologie 0353
- Génétique 0369
- Limnologie 0793
- Microbiologie 0410
- Neurologie 0317
- Océanographie 0416
- Physiologie 0433
- Radiation 0821
- Science vétérinaire 0778
- Zoologie 0472

Biophysique
- Généralités 0786
- Medicale 0760

SCIENCES DE LA TERRE
Biogéochimie 0425
Géochimie 0996
Géodésie 0370
Géographie physique 0368
Géologie 0372
Géophysique 0373
Hydrologie 0388
Minéralogie 0411
Océanographie physique 0415
Paléobotanique 0345
Paléoécologie 0426
Paléontologie 0418
Paléozoologie 0985
Palynologie 0427

SCIENCES DE LA SANTÉ ET DE L'ENVIRONNEMENT
Économie domestique 0386
Sciences de l'environnement 0768
Sciences de la santé
- Généralités 0566
- Administration des hipitaux 0769
- Alimentation et nutrition 0570
- Audiologie 0300
- Chimiothérapie 0992
- Dentisterie 0567
- Développement humain 0758
- Enseignement 0350
- Immunologie 0982
- Loisirs 0575
- Médecine du travail et thérapie 0354
- Médecine et chirurgie 0564
- Obstétrique et gynécologie 0380
- Ophtalmologie 0381
- Orthophonie 0460
- Pathologie 0571
- Pharmacie 0572
- Pharmacologie 0419
- Physiothérapie 0382
- Radiologie 0574
- Santé mentale 0347
- Santé publique 0573
- Soins infirmiers 0569
- Toxicologie 0383

SCIENCES PHYSIQUES
Sciences Pures
Chimie
- Généralités 0485
- Biochimie 487
- Chimie agricole 0749
- Chimie analytique 0486
- Chimie minérale 0488
- Chimie nucléaire 0738
- Chimie organique 0490
- Chimie pharmaceutique 0491
- Physique 0494
- PolymÇres 0495
- Radiation 0754

Mathématiques 0405
Physique
- Généralités 0605
- Acoustique 0986
- Astronomie et astrophysique 0606
- Electronique et électricité 0607
- Fluides et plasma 0759
- Météorologie 0608
- Optique 0752
- Particules (Physique nucléaire) 0798
- Physique atomique 0748
- Physique de l'état solide 0611
- Physique moléculaire 0609
- Physique nucléaire 0610
- Radiation 0756

Statistiques 0463

Sciences Appliqués Et Technologie
Informatique 0984
Ingénierie
- Généralités 0537
- Agricole 0539
- Automobile 0540
- Biomédicale 0541
- Chaleur et ther modynamique 0348
- Conditionnement (Emballage) 0549
- Génie aérospatial 0538
- Génie chimique 0542
- Génie civil 0543
- Génie électronique et électrique 0544
- Génie industriel 0546
- Génie mécanique 0548
- Génie nucléaire 0552
- Ingénierie des systàmes 0790
- Mécanique navale 0547
- Métallurgie 0743
- Science des matériaux 0794
- Technique du pétrole 0765
- Technique minière 0551
- Techniques sanitaires et municipales 0554
- Technologie hydraulique 0545

Mécanique appliquée 0346
Géotechnologie 0428
Matières plastiques (Technologie) 0795
Recherche opérationnelle 0796
Textiles et tissus (Technologie) 0794

PSYCHOLOGIE
Généralités 0621
Personnalité 0625
Psychobiologie 0349
Psychologie clinique 0622
Psychologie du comportement 0384
Psychologie du développement 0620
Psychologie expérimentale 0623
Psychologie industrielle 0624
Psychologie physiologique 0989
Psychologie sociale 0451
Psychométrie 0632

THE UNIVERSITY OF CALGARY

FACULTY OF GRADUATE STUDIES

The undersigned certify that they have read, and recommend to the Faculty of Graduate Studies for acceptance, a thesis entitled, "Dual Diversity Antennas for Hand-Held Radio", submitted by Mark Gordon Douglas in partial fulfillment of the requirements for the degree of Master of Science.

Ronald H Johnston

Dr. R.H. Johnston, Supervisor
Dept. of Electrical and Computer Engineering

Michel Fattouche

Dr. M. Fattouche
Dept. of Electrical and Computer Engineering

Dr. A. Sesay
Dept. of Electrical and Computer Engineering

K. Duckworth.

Dr. K. Duckworth
Dept. of Geology & Geophysics

Date: March 10, 1993

Abstract

Cellular telephony is currently facing many challenges, one of which is the ability to provide consistent high-quality voice or data amidst the multipath fading effects inherent in the mobile environment. The use of diversity antennas at the mobile receiver can overcome some of the fading effects. For this thesis, three microstrip antennas are presented. Each of them is designed to provide polarization diversity near the 800 MHz cellular frequency band. The last antenna works very well and has some commercial potential. Measured scattering parameters and radiation patterns show that the vertically-polarized and horizontally-polarized modes radiate independently with good return losses and very low coupling between them. Future research should include reducing its size for hand-held units and evaluating how well it improves the received signal level.

Acknowledgements

I wish to first thank Dr. Ron Johnston for his guidance, support and helpful suggestions during the course of my work as well as the University of Calgary and TR*Labs* for their financial and educational support.

I am also indebted to my colleagues at NovAtel: David Goulbourne for his enthusiasm and expertise in antenna modeling, Dan Harrison for his time and patience in the Antenna Test Range, and Andy McGirr for convincing me to come to Calgary.

At TR*Labs*, I would like to thank John McRory for his helpful assistance and proofreading of this thesis and to the rest of the staff, students and professors for all of the discussion, levity and good will during this seemingly unending process.

Table of Contents

List of Tables

List of Figures

List of Symbols and Abbreviations

Γ	reflection coefficient
ε_r	relative permittivity of dielectric substrate
η	efficiency
θ	phase angle of the reflection coefficient of the calibrated antenna
θ_1	phase angle of the reflection coefficient of an uncalibrated antenna
θ_{open}	phase angle of the reflection coefficient of an open circuit
θ_{HP}	half-power beamwidth in the vertical plane
λ	wavelength of radiation
ρ	correlation coefficient
ϕ_{HP}	half-power beamwidth in the horizontal plane
ATR	Antenna Test Range
AUT	Antenna Under Test
BW	bandwidth
cm	centimetres
d	distance between the outside edge of the square patch and the feed point
D	directivity
DC	direct current

dB	decibels
dBi	decibel gain over an isotropic antenna
E_h	horizontal component of the electric field
E_v	vertical component of the electric field
E_x	x component of the electric field
E_y	y component of the electric field
E_z	z component of the electric field
F_1	feed point 1
F_2	feed point 2
f_{ri}	resonant frequency of slot i
G	antenna gain
GHz	gigaHertz
H_x	x component of the magnetic field
H_y	y component of the magnetic field
H_z	z component of the magnetic field
IF	Intermediate Frequency
j	the imaginary number (square root of -1)
ℓ	screw length below the square patch antenna
ℓ	length of the NEC model of the patch antenna
LC	inductor-capacitor
LPDA	Log-Periodic Dipole Array antenna
MHz	MegaHertz
mm	millimetres
NEC	Numerical Electromagnetics Code
nH	nanoHenries

P_0	output power from the signal generator
P_1	sample of the reflected power from the AUT
P_{1open}	sample of the reflected power from an open circuit
P_2	coupled power through the AUT
P_{2A}	P_2 - 20 dB
P_3	sample of the output power, P_0
P_{3open}	sample of the output power when open-circuit terminated
$P_{absorbed}$	antenna loss due to absorption
$P_{avg\ AUT}$	average radiated power of the AUT
$P_{coupled}$	power coupled from one port of the AUT to another port
pF	picoFarads
P_{in}	input power fed into an antenna
$P_{m\ AUT}$	maximum radiated power of the AUT
$P_{m\ ref}$	maximum radiated power of the reference antenna
$P_{radiated}$	power radiated by the antenna
$P_{reflected}$	power reflected at the input port of the antenna
Q	quality factor
RF	Radio Frequency
S parameter	Scattering parameter
S_{11}	return loss at port 1 of the antenna
S_{11open}	measured return loss of an open circuit
$S_{11uncal}$	return loss of an uncalibrated antenna
S_{21}	coupling from port 1 of the antenna to port 2
S_{12}	coupling from port 2 of the antenna to port 1
S_{22}	return loss at port 2 of the antenna

SWR	Standing Wave Ratio
w	base width of triangle patch
w	width of a patch of the U patch antenna
W	Watt
Z_{in}	input impedance

Chapter 1 Fads, Phones and Fading

1.1 Object of Investigation

It is no wonder that the cellular telephone has become the latest status symbol in our culture. It is probably the single most popular yet unattainable technology of the twentieth century. From Dick Tracy to Captain James Kirk and Agent Maxwell Smart, popular culture has marveled at the magical presence of the portable communicator, the definitive technology of some far distant future.

Yet in the early 1980s, the industrialized world was finally informed that the future had arrived. Science and ingenuity had boldly gone where only Star Trek had gone before, and it was only a matter of time before every man, woman and child would wear a personal telephone on their wrist, on their chest, or even in their shoe if they were so inclined. Those who could afford them quickly scrambled to buy the prohibitively expensive first generation of cellular telephones to show that they were indeed part of this glorious future. The rest of society patiently waited.

Ten years later, the technology of the mobile telephone has slowly advanced but is far from keeping its daring promises. Still very few people own these systems and the rest of society has all but given up waiting.

Meanwhile, in the dark corridors of university electrical engineering departments and in the looming office towers of cellular telephone designers, engineers and scientists are working to level some of the mountainous obstacles that still stand between the present technology and the phone systems of the future.

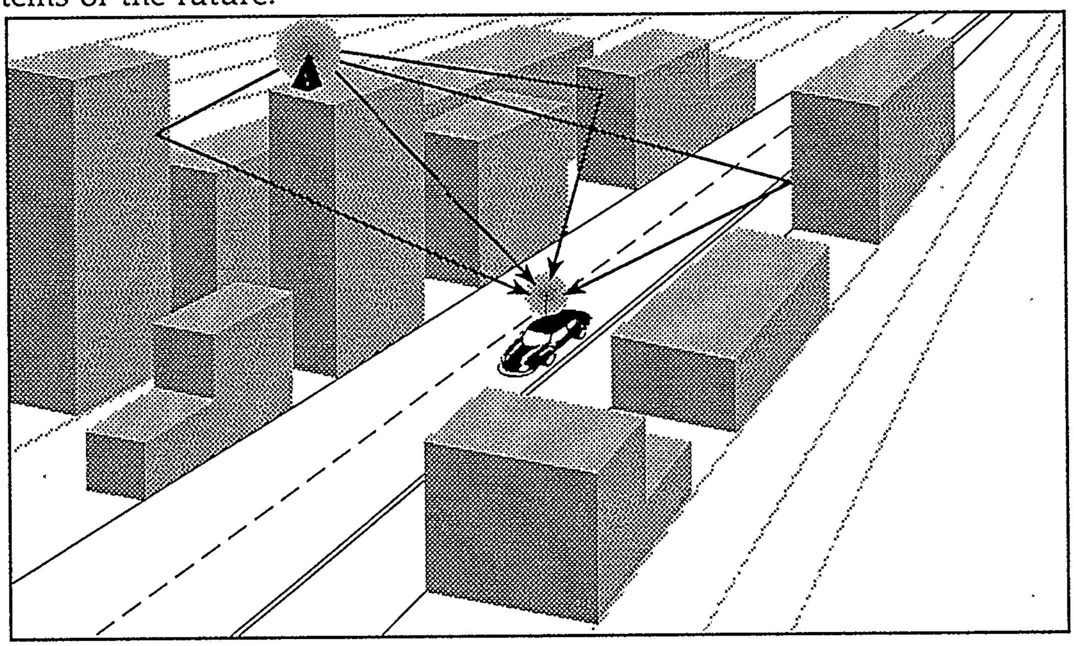

Fig. 1.1 Signals arriving from a base station.

Communicating electrically through the air between two devices the size of a wallet at practically any locations on earth with only a couple of watts of power has always been thought to be difficult, especially if those devices are moving. For instance, if one of the devices is traveling in an automobile through a busy downtown area, the signal arriving at its antenna will have a power level that fluctuates in time, according to the environments around it and the transmitter, and according to the obstacles in the path between them. As shown in Fig. 1.1, the signal from a base station antenna can travel along a large number of paths before reaching a mobile telephone.

Each component of the signal may be reflected, refracted, partially absorbed and otherwise degraded before arriving with random phase and amplitude at the receiver. The power level of the total vector sum of these signals will have a "multipath" fading characteristic as shown in Fig. 1.2.

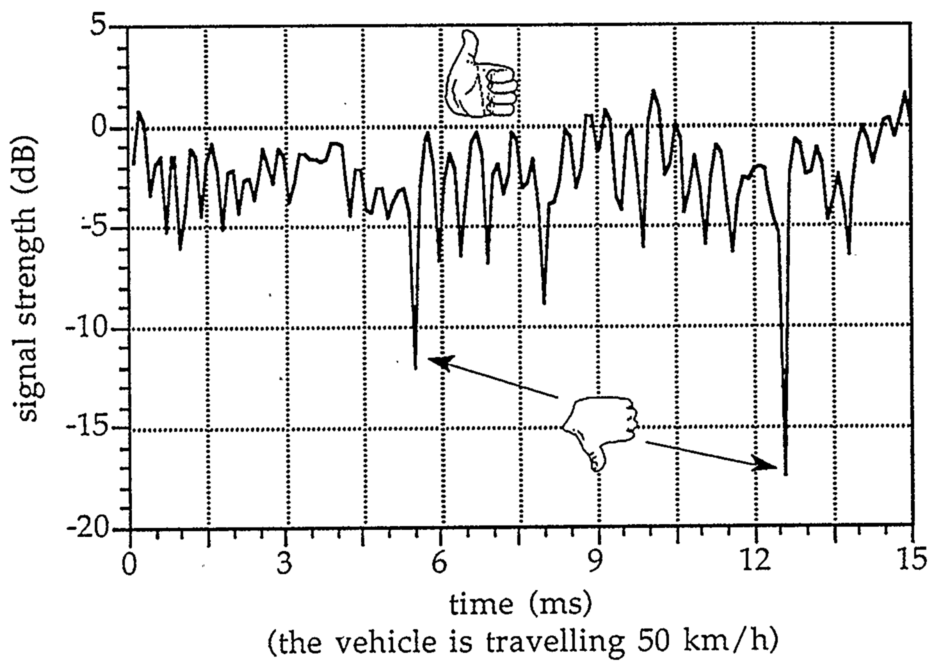

Fig. 1.2 Multipath fading characteristic [1.1].

During the deep fades, highlighted in Fig. 1.2, the signal level is so low that communication is nearly impossible. Luckily the deep fades are brief in duration, but they occur often enough to degrade the overall voice quality heard at the receiver of the mobile telephone.

The obvious question to be asked is therefore, "How can this fading be removed?" The answer, unfortunately, is, "It can't," but the probability of fading can be reduced, which is what diversity reception is designed to do.

To reduce the probability of signal fading at a cellular telephone receiver, two or more antennas are used to receive the signal instead of one. If the system is designed properly, there is a low probability that when one antenna experiences fading, the others also experience fading. With the receiver designed to either combine the received signals or switch between them, the received signal fades far less frequently than the signal from one antenna alone. This system of two or more antennas is called a "diversity antenna."

Although diversity reception has not yet been used on mobile receivers in cellular communication, there is widespread interest in using it in future generations of the medium. Tests have shown that when diversity receivers are used instead of traditional receivers, a signal improvement of 6dB is measured [1.2].

This thesis is a study of different diversity antenna designs for the next generation of cellular telephones. Such antennas must be small enough to fit inside the wallet-sized communicators and effective enough to make diversity worthwhile. These two factors are usually in competition with each other and therefore, innovative designs are necessary to take this into account.

The antennas covered in the thesis were designed, built and then tested to determine various properties such as efficiency, radiation pattern and signal polarization. These properties indicate how well the diversity antennas perform.

1.2 Historical Background

"Rome was not built in a day," according to an anonymous scribe who either was not a Christian or had forgotten about a very important book that states that the entire universe was created slightly under a week. Nevertheless, this statement withstood the tests of time and criticism, becoming a testimony to the idea that great inventions do not just appear, but are the result of sweat and sacrifice.

The same can be said of the cellular telephone and the microstrip antenna. In fact, it can be said that neither of them are great inventions at all. Instead, they are technologies that have gradually evolved over time through a little inspiration, a lot of perspiration, and a clever mistake or two.

This section is a brief discussion of the history of these technologies.

1.2.1 Cellular Telephony

As stated in the last section, it is difficult to physically realize the concept of communication between two wallet-sized, wireless, personal communicators. Such a concept requires the prerequisite inventions of other technologies, namely the telephone and the radio.

The telephone provided a communication hierarchy, together with its circuit switching and traffic handling capabilities, that made it possible for personal communication to work. The radio allowed for the transmission of signals through space, thus liberating communications from being fixed into a network of copper wire.

These two inventions evolved along largely divergent paths which crossed only occasionally to bring such innovations as dispatch systems, citizens' band radio, amateur radio and the car radio-telephone. The first car phone was conceived in 1946. It was this development that very slowly became today's cellular telephone.

However, to say that the cellular telephone is merely a merging of the radio and the telephone is an over simplification; mobile communication has its own set of challenges which requires some technological innovation.

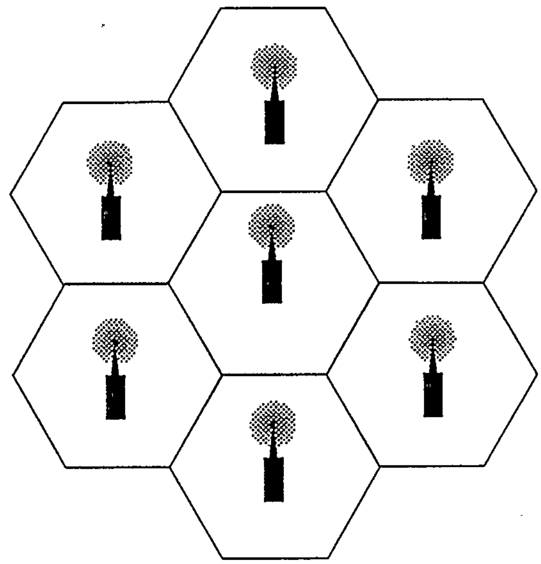

Fig. 1.3 Simple cellular coverage

(hexagons give a rough indication of cell boundaries).

Take, for instance, the very narrow frequency spectrum allotted by regulatory agencies to mobile communications. Only 50 MHz is allocated for the cellular 800 system (compared to 400 MHz for television channels 2 to 69), which makes it difficult for the system to supply enough radio channels to a large city like New York if traditional radio broadcasting is used. Reducing the channel bandwidth can increase the number of channels in the spectrum, but only by a limited amount. Mobile telephone designers therefore employed a channel-reuse scheme. With this scheme, a city uses a large number of low-powered transmitters instead of one high-powered transmitter (see Fig. 1.3). Each of the smaller transmitters covers only a small area (called a "cell") within the city*. Because of the lower power of a cell, two signals can be transmitted on the same channel from two distant transmitters without significantly interfering with each other. Therefore, the number of

* In concentrated urban districts such as downtown New York, some transmitters cover less than one square kilometre.

available radio channels is more dependent on the number of cells than it is on the allocated frequency spectrum.

However, this leaves one unanswered question, "How many channels will be required in a city, and therefore, how many transmitters should be installed?" The answer to this question is difficult to find, as the number of mobile telephone users changes over time. This query lead engineers to a second innovation in cellular communications - *cell splitting* (see Fig. 1.4).

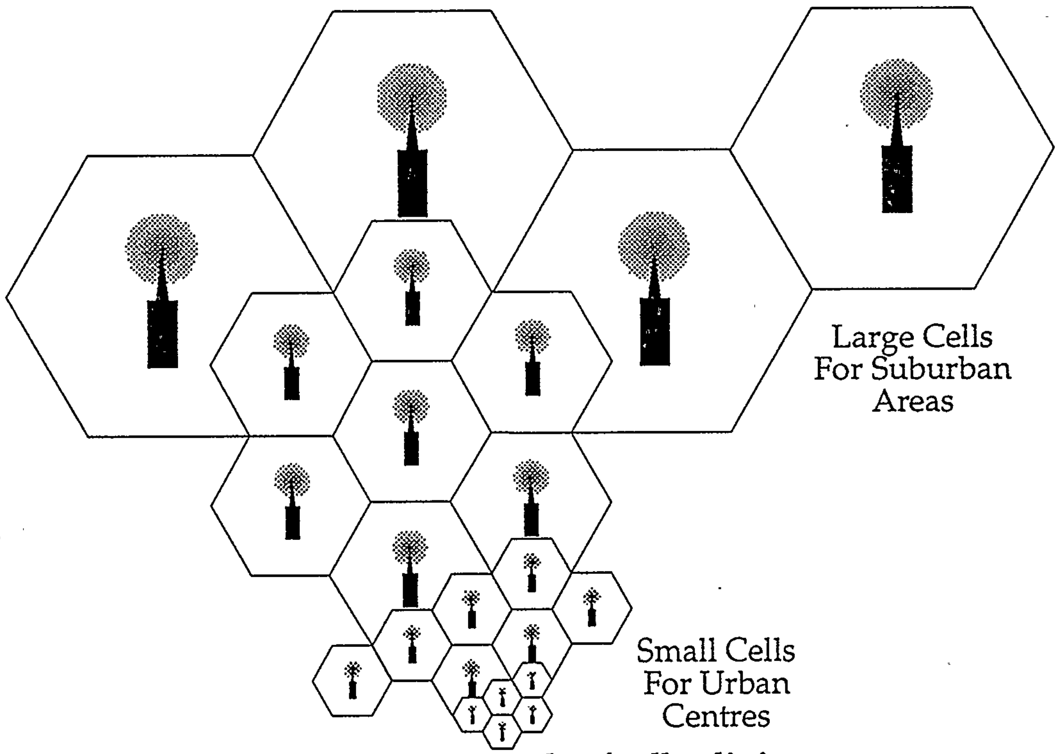

Fig. 1.4 An example of cell splitting.

(From "Digital Cellular Radio," by Calhoun, pg. 43.)

Instead of installing a fixed number of cell sites in a city, cell sites can be added gradually whenever the demand for more channels arises. An area may start with one high-powered transmitter, and as the need for more radio channels arises, the cell is subdivided into a number of lower-powered cells, each with its own set of channels. When one of those smaller cells becomes saturated it too can be subdivided. The process is repeated as necessary until either all of the channels are supplied or the maximum cell density is reached.

While cell splitting alleviates the problem of limited service and allows the system to gradually evolve, it creates another problem. The smaller a cell becomes, the greater the chance that a call will not be completed within the boundaries of a single cell. A vehicle traveling on a highway may pass through several cells during a single conversation.

To handle this problem, the hand-off procedure was developed. Just like it sounds, hand-off allows a call to be handed off from one cell site to its neighbour as the vehicle moves between the two. Using the signal strength from the vehicle as measured at the cell site, a mobile-telephone switching office determines when the vehicle is moving from one cell to another and commands the cell sites to hand off the call.

Today, cellular communication is a working technology that has gained considerable acceptance over the past ten years. there are, however, some obstacles preventing it from achieving its potential. Among them is the problem of multipath fading which is prohibiting cellular communication from providing a consistent quality of voice and data transmission. This problem can be alleviated by using diversity reception.

1.2.2 Microstrip Antennas

The microstrip antenna appears to be a natural inclusion into the evolution of cellular communications. As mobile telephones become smaller and more portable, their antennas must also shrink. Microstrip antennas, unlike conventional monopole antennas, lend themselves well to this aim.

A microstrip antenna is essentially a printed circuit, with the radiators photo-etched on one side of the board, and a metallic ground plane on the other side. Matching networks, phasing circuits and power splitters may also be built into the planar construction of the dielectric and conductors. A simple configuration is shown in Fig. 1.5. Its planar geometry allows the microstrip antenna to be used where space is limited and gives it the ability to be molded to conform to the shape of a structure such as the tip of an aircraft wing or the roof top of a car.

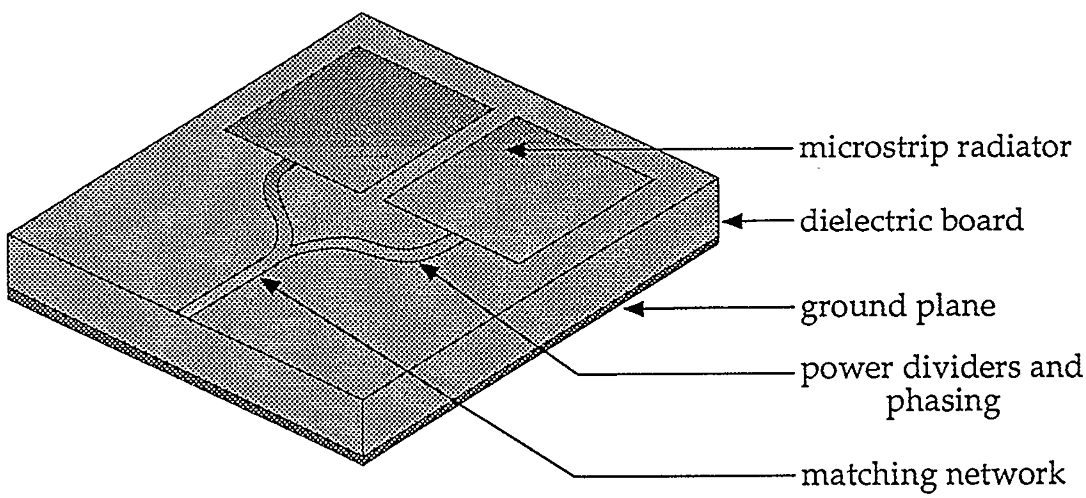

Fig. 1.5 Simple microstrip antenna configuration.

The microstrip radiator was not always looked upon favorably, however. In the early days of microstrip circuit design, radiation was something only to be avoided, as it represented a loss in the circuit. Engineers were therefore busy designing circuits that suppressed radiation as far as possible. But in 1953, Deschamps [1.3] thought that this radiation could be utilized and introduced the concept of microstrip circuits as antennas. A revolutionary concept in microstrip circuit design perhaps, but a concept that was virtually ignored for twenty years.

The first practical use of microstrip antennas was in warfare. In the early 1970s, the United States military realized that because of the flat geometry and low profile of these antennas, they could be installed on the sides of guided rockets and missiles without disturbing their aerodynamics. This interest provided the funds necessary to fuel the microstrip antenna's initial developments.

Such developments led the microstrip antenna out of its dark beginnings and into more commercial use by the late 1970s. More recently, the revolution in electronic circuit miniaturization, brought about by progress in large scale integration, fiber optics and sensor technology, has allowed microstrip antenna technology to advance even further.

The microstrip antenna has many advantages over other designs which makes it the preferred choice in many applications. These advantages include

- light weight, compact size and planar geometry, which allow it to be used where small size is important or conformity with a structure is required
- manufacturing that is inexpensive and accurate, therefore making it readily amenable to mass production. Feed lines and matching networks can also be fabricated simultaneously with the antenna structure
- compatibility with integrated circuits, which can be mounted directly on the board

Along with these advantages, the microstrip antenna also has inherent limitations which include

- narrow bandwidth

- dielectric loss, hence somewhat lower gain
- lower power handling capability
- complicated electrical properties, which make microstrip antennas difficult to analyze in the general case
- possible excitation of surface waves
- poor isolation between the feed and the radiating elements
- radiation into a half space only

For many uses, the limitations of microstrip antennas are far outweighed by their advantages. Therefore, it is expected that in the future, microstrip antennas will replace conventional antennas for many applications [1.4]. Today, microstrip antennas are used in a variety of areas, including satellite communication, Doppler and other radars, environmental instrumentation, remote sensing and biomedical radiators.

Cellular telephony is another field in which there is increasing interest in microstrip antennas. Bandwidth, power handling capability and full-plane radiation are not critical here, and the light weight, compact size and simple manufacturing make these antennas attractive to designers and manufacturers of cellular telecommunications equipment.

1.3 Multipath Effects in Cellular Communications

In these increasingly fast-paced, highly-mobile times, the portable communicator is sometimes viewed as a great liberator, allowing near-instant accessibility to people and information without wires to keep us tied to a fixed location. However, accessibility has its costs. Before wires are to be done away with completely, some of the problems of radio communication need to be addressed.

Section 1.1 briefly described that a signal arriving at a portable communicator has a power level that fluctuates in time, exhibiting a multipath fading effect. In this section, further detail is given regarding the causes and effects of the multipath phenomenon.

Communicating through a wire, however limited it may be, is at least predictable. Once a wire network is fixed in place, its characteristics are known and, with the exception of weathering and the occasional accident, they are not expected to change significantly. Some cross talk, echoing and line loss may exist, but a caller is reasonably assured of clear, two-way communication.

The same cannot be said of cellular communication. Here, a signal must pass through the air between the portable phone and the cell site's base station antenna. Along the way, the signal will experience free-space loss, terrestrial loss and perhaps some Doppler frequency shifting if the caller is moving. Most importantly, it will encounter multipath effects. Between the phone and the base station, the signal will travel along several different paths (see Fig. 1.1), some of which may encounter obstacles which can scatter, refract, absorb, reflect or re-polarize them. In outdoor communication, these obstacles are typically trees, buildings, cars and the terrain. For indoor communication, they are desks, people, walls and partitions.

Some of the signal components arrive at their destination, but with different amplitudes, phases, polarizations and arrival times. Signal components with different phases may destructively interfere, resulting in the signals partially or wholly canceling each other out. In addition, the polarizations of some of the signal components may be different from the polarization of the receive antenna, giving rise to further power loss.

The final received signal has an amplitude and phase that are difficult to predict and fluctuate in time as the personal communicator moves and the mobile environment changes (see Fig. 1.6). Therefore, it is very difficult for cellular communications to assure the caller of clear, two-way communication.

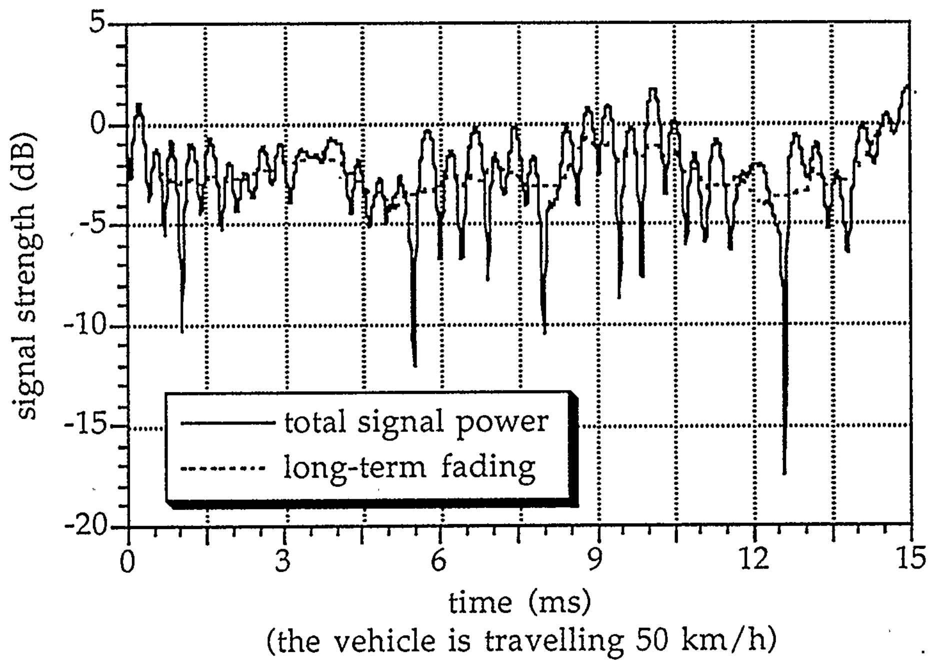

Fig. 1.6 Multipath fading characteristic showing long term fading [1.1].

Some efforts are currently being made to alleviate this problem. The total multipath fading characteristic can be broken up into long-term and short-term fading components. The long-term component (shown with the total fading characteristic in Fig. 1.6) is caused by gradual variations in the mobile environment, such as terrain (for outdoor communication) or corridors (for indoor communication). It can be averaged out at the receiver using an automatic gain control circuit. The short-term fading, on the other hand, is impossible to remove completely, but diversity reception can significantly reduce it.

1.4 Diversity Reception

In simple terms, diversity reception is a modern extension to the age-old phrase, "two heads are better than one." Like most age-old phrases, this one comes with a set of provisions: two heads are better than one only if each can think independently and agrees to cooperate with the other. In cellular telephony, two *antennas* are better than one provided that they both receive statistically independent signals and the receiver that they are connected to can use them cooperatively.

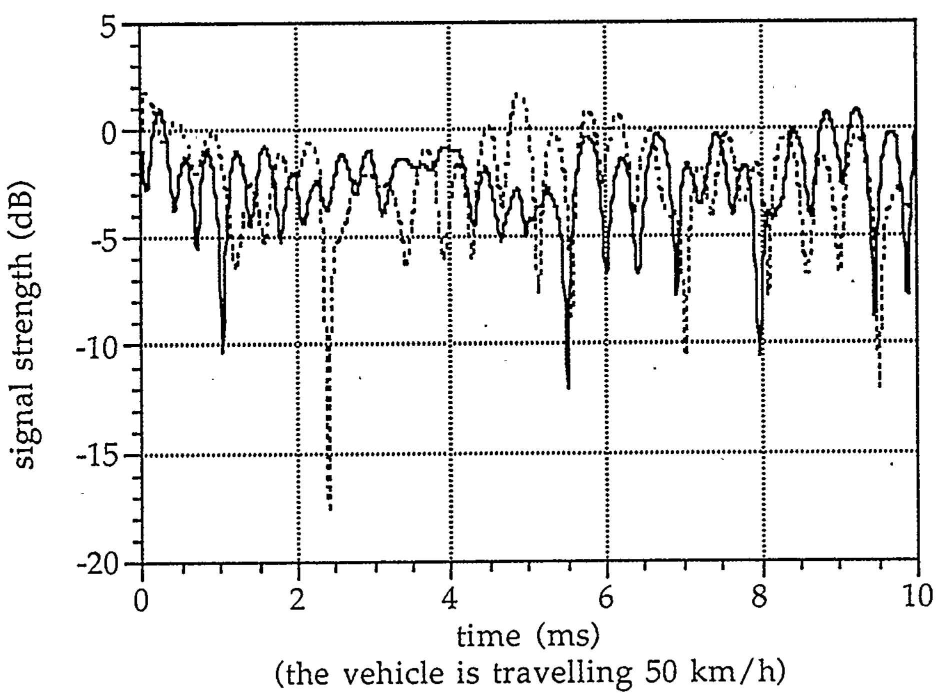

Fig. 1.7 Received signals from two antennas [1.1].

As was seen in the last section, a mobile telephone with one antenna receives a signal that has a multipath fading pattern. If the same mobile telephone is instead connected to two antennas, it will receive two signals, each having a statistically-similar type of fading pattern (see Fig. 1.7).

The advantage of using two antennas is that the receiver can either select which signal to receive, based on which has the higher signal strength at that time, or somehow combine the two signals. Either way, the resultant signal fades less frequently and less severely than either of the individual signals. Fig. 1.8 illustrates this point. It represents the sum of the two signals of Fig. 1.7.

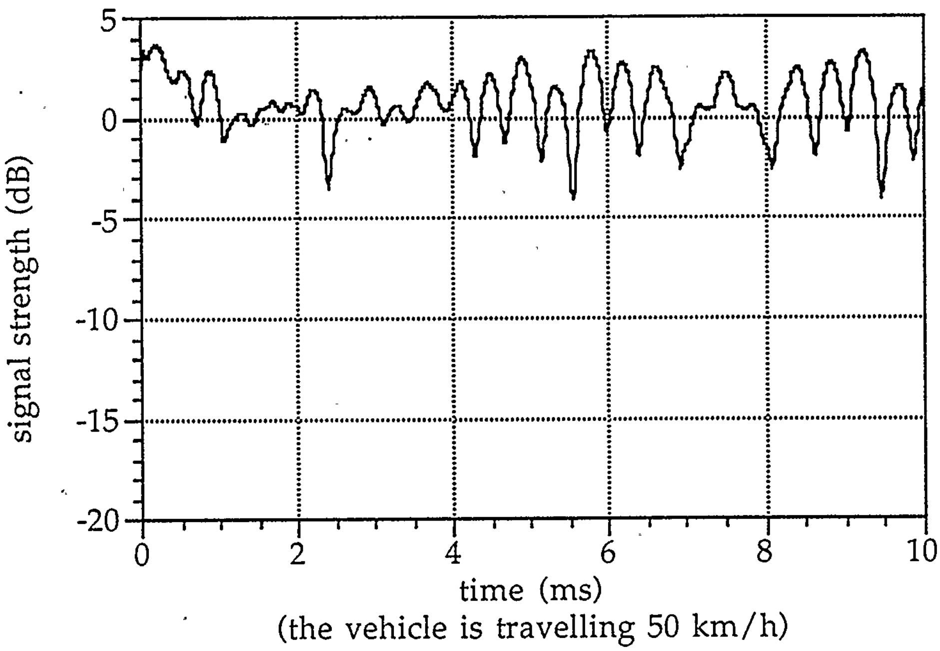

Fig. 1.8 Additively combined signals of Fig. 1.7.

As Fig. 1.8 illustrates, there is still some fading in the resultant received signal, which occurs when both individual antennas (collectively known as a "diversity antenna") experience fading simultaneously. The key to designing a diversity antenna is therefore to ensure that the two received signals are not likely to fade at the same time (or, in other words, the fading patterns of the two signals are statistically independent).

A number of different diversity methods can be employed to ensure a reasonable amount of statistical independence. Six of these methods are:

space diversity, frequency diversity, time diversity, angle diversity, field component diversity and polarization diversity. Each method is briefly described and evaluated below.

1.4.1 Space Diversity

In this method, the two antennas are spaced sufficiently far apart that the short-term components of the received signals are statistically independent. Results have shown that the minimum antenna separation for reasonably independent statistics is $\lambda/2$, where λ is the free space wavelength [1.5].

At 880 MHz (the median receive frequency in the cellular 800 system), $\lambda/2 = 17$ cm. This separation is too large for a diversity antenna built into a handset. Even at 1800 MHz (indoor cordless), $\lambda/2 = 8.33$ cm, which is still impractical for a handset antenna.

1.4.2 Frequency Diversity

Two signals with very different carrier frequencies are "possibly independent" [1.6]. The independence increases with frequency separation; however, even for a very large separation it is not good enough for some applications. Another disadvantage of this method is that it requires extra bandwidth, a commodity that is already scarce in cellular communications.

1.4.3 Time Diversity

If the cellular telephone is moving, then the mobile environment is varying in time. Therefore, two time-delayed transmissions of the same signal may be statistically independent. The minimum time delay for diversity depends on how quickly the mobile environment is varying, which is usually measured from the speed of the mobile: the faster it moves, the shorter the delay.

Although time diversity has the advantage that only a simple antenna is needed, there are some strong arguments against using it. For it to work, the base station must have knowledge of the mobile's speed to decide when to send the second transmission. From the system's perspective, this makes time diversity more complicated than the other methods. Also, when the mobile is stationary the time delay becomes infinite, so time diversity will not work. This is especially a problem with hand-held systems, where the unit is likely stationary or moving very slowly.

1.4.4 Angle Diversity

Multipath fading is largely the result of the destructive interference of signal components arriving from different signal paths. If these components can be isolated before they interfere, multipath fading will be much less severe. Angle diversity makes use of the observation that most of the signals arriving from different signal paths also have different angles of arrival. In most cases, the signals from different arrival angles will have fading patterns that are statistically independent. Diversity can therefore be achieved using directional antennas to isolate the signal components.

The more directional each antenna is, the more independent each received signal is. Fig. 1.9(a) illustrates the case when three highly directional antennas are placed on top of a car. Unfortunately, using highly directional antennas also results in less coverage area and therefore low average received signal power. There may also be deep fades when no signals arrive in the directions of the antenna beams. Widening the antenna beamwidths (as shown in Fig. 1.9(b)) generally increases the signal power and coverage but may reduce the statistical independence. As a result, the beamwidth of the antennas must be adjusted to find an optimum tradeoff between statistical independence and signal coverage.

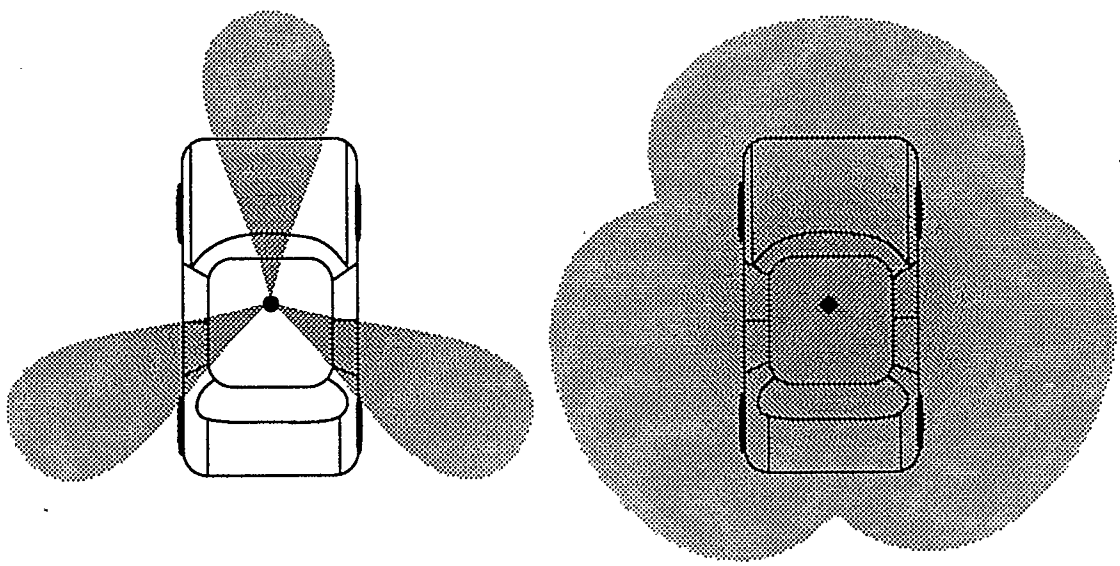

(a) (b)

Fig. 1.9 Angle diversity with three directional antennas, using (a) narrow beamwidths and (b) wide beamwidths.

1.4.5 Field Component Diversity

A wave traveling in space has a maximum of six field components, three for the electric field (E_x, E_y and E_z) and three for the magnetic field (H_x, H_y and H_z). In an ideal mobile environment, where the waves propagate close to the ground, the vertically-polarized electric field (E_z) and the horizontally-polarized magnetic fields (H_x and H_y) are the most significant [1.7]. Each of the three components for a single wave is interdependent on the other two, but in a multipath environment where a measured signal is the combination of several waves, each combined component can be shown to be statistically independent of the others [1.7]. An energy density antenna, one which receives E_z and one or both of H_x and H_y independently, provides field-component diversity.

1.4.6 Polarization Diversity

Polarization diversity is a specific form of field component diversity where the received components are of the same field. It usually refers to the separate reception of a vertically-polarized and horizontally-polarized electric field. This type of diversity works in most cases, although, as was stated in section 1.4.5, only the vertically-polarized electric field is significant in an ideal mobile environment. Many studies have been done on polarization diversity, and the results conclude that polarization diversity offers a substantial improvement in outdoor systems in suburban areas and in indoor systems where there is no line-of-sight propagation.

Bergman and Arnold [1.9] tested polarization diversity indoors at 816 MHz using a cross-polarized microstrip patch antenna. Measurements were taken in an office building (where both the transmitter and receiver were indoors) and in a house (with the transmitter outside and the receiver inside). The results indicate that the vertically- and horizontally-polarized electric fields are only weakly independent (the correlation coefficient, ρ, is 0.5) when there is a strong line of sight but are strongly independent (ρ = 0.01) when there is no line of sight.

The improvement due to polarization diversity for indoor systems was studied by Davies [1.2]. A cross-polarized dipole antenna was used in hallways and a gymnasium at 915 MHz. Selective combining of the vertically- and horizontally-polarized signals gave an average improvement of 6 dB (improvement is defined as the increase in gain of the deepest fades after the long-term fading is removed). After removing the long-term fading, the different polarizations were found to be statistically independent ($\rho = 0.1$ max).

Measurements conducted by Lee [1.8] show that the local mean levels of the horizontally- and vertically-polarized electric fields received at a mobile antenna are similar in suburban areas. In urban centres, however, Lee states that the vertical component is slightly stronger:

> In comparing the local means of E_v and E_h in a suburban area, there are no gross differences between the average local mean levels of E_v and E_h. However, on the basis of measured data recorded within a 3-mi radius of the base station located in the Keyport-Strathmore area of New Jersey, it was noted that E_v was slightly higher than E_h.

The antennas studied here use a combination of polarization diversity and angle diversity. They are described in more detail in Chapter 4.

Although diversity reception has the advantage of substantially increasing the received signal power at a mobile, it also has some drawbacks. A more complex receiver structure is required to receive the diversity signals and combine them. This requires extra parts which makes the wireless phone more expensive and less compact. Due to recent advances in circuit mass production and miniaturization, however, this is becoming less of a problem.

1.5 Previous Work

Most of the diversity antenna research to date employs space diversity, as mentioned in section 1.4.1, which is impractical for use in hand held radios because the distance between the antennas is so large. There is, however, some important work in this area that concentrates on antenna designs with a flat profile.

Nishikawa et al. have designed two flat antennas -- one a table antenna, the other resembling a folded F antenna -- that operate in diversity when separated by more than 0.4 wavelengths [1.10]. Although this design is too large for a handset, it can be mounted on a vehicle, replacing the traditional monopoles which can bend or break and may not be aesthetically pleasing.

Tsunekawa has created a working diversity system using two planar inverted-F antennas [1.11]. By combining space and angle diversity, he was able to reduce the distance between the antennas to 0.1 λ, but the antennas are only weakly independent ($\rho = 0.43$).

Some important work in single, compact diversity antenna design is provided by Arai et al [1.12]. Their antenna consists of a centre-fed disk above a ground plane with four slots cut radially into the disk. In the plane of this flat-profile antenna, the disk receives an electric field component while the slots receive a magnetic field component. Thus, field component diversity is achieved in one integrated unit. However, with a diameter of over 0.6 λ, this antenna is also impractical for use in a handset.

A simple polarization diversity scheme was proposed by Lalezari et al over 10 years ago [1.13]. Two feed line networks independently feed a pair of square microstrip patches. This system provides horizontal and vertical polarizations independently and is said to minimize the coupling between the feed ports, but again, size is a problem. To isolate the patches and make room for the two feed networks, the structure must be 0.95 λ long.

Chapter 2
Background Theory

As microwave circuit design is a very specialized field, some background theory will help the reader appreciate the remaining work of this thesis.

This chapter contains two sections, the first describing the basic operation of microstrip antennas. Topics discussed here include the excitation and radiation of electric fields, methods of theoretically analyzing microstrip antennas and ways of manipulating an antenna's physical and electrical properties to change its measured characteristics.

The Smith chart is briefly described in Section 2.2. This graphical design tool is indispensable in microwave circuit design.

2.1 Microstrip Antenna Theory

At first sight, the microstrip antenna appears to be a remarkably simple device. It is merely a printed circuit on a dielectric with a ground plane underneath (see Fig. 2.1). The top surface is accessible, so it is easy to mount discrete devices on it and make modifications to it. Its simple configuration allows the patch radiators to be designed to any flat shape and enables it to be molded to wrap around a structure.

However, despite its simple appearance, the microstrip antenna is often not used because of its complex electrical properties. The radiation mechanism of microstrip circuits is complicated because the radiating patch rests between two different materials: air and a dielectric.

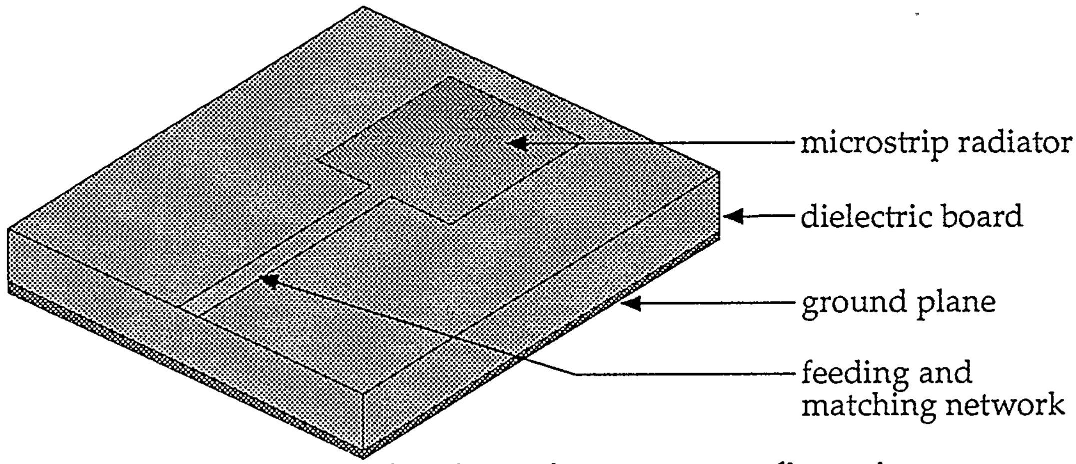

Fig. 2.1 Simple microstrip antenna configuration.

Fig. 2.2 gives a cross-sectional view of the microstrip antenna of Fig. 2.1, showing its electric and magnetic fields. In this case, the microstrip patch is at a voltage potential above the ground plane, exciting an electric field between them. At the centre of the patch, the electric field acts vertically between the patch and the ground plane, but towards the patch edges, the field is not as concentrated and tends to fringe outwards. Some of the fringing electric fields separate from the circuit and become radiation fields. As the radiation fields are essential for an antenna, they can be enhanced by choosing the proper patch shape, dielectric thickness and dielectric constant.

The difficulty in making these choices lies with the fact that, unlike most antennas, the microstrip antenna radiates into both the air and a dielectric medium. The use of the dielectric medium adds losses. It also results in the bending and refraction of electric fields. All of these are difficult to analyze. As a consequence, although patch conductors can be designed to any flat shape, the difficulty in analyzing these shapes generally restricts them to conventional shapes (rectangles, circles and triangles).

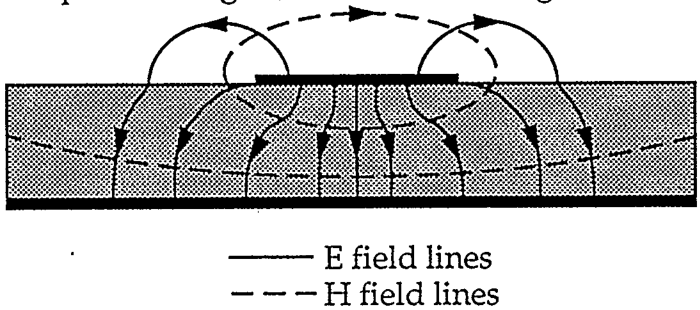

Fig. 2.2 Side view of microstrip circuit showing field lines.

Many methods exist to analyze microstrip antennas (ie., determine the radiation pattern, input impedance, gain, bandwidth, beamwidth, efficiency, losses and Q factor), but none of them are exactly comparable to practice. Some of these methods are described below [2.1]:

- One of the more rigorous methods is the Vector Potential Approach where the mode theory of wave propagation is used to numerically evaluate the fields of the antenna based on the fields of a dipole antenna.
- The Dyadic Green's Function Technique uses Maxwell's equations together with a superposition integral and the appropriate boundary conditions to determine the radiated fields.
- If the microstrip antenna radiation can be thought to come mainly from an open-circuited end of the patch, the Radiating Aperture Method can be used.
- Another method is the Cavity Model, where microstrip antennas are treated as cavities in microstrip lines and the fields in the antenna are assumed to be those of the cavities.
- A simple method for rectangular patches is the Transmission Line Model where the radiator element is represented as two radiating slots separated by a length of transmission line.

- The Wire Grid Model is a generalized method of analyzing the radiation mechanism of any antenna that can be described as a matrix of straight wires. This method first solves for the currents on the wires and then derives the radiation pattern and other characteristics from those currents.

The Wire Grid Model [2.1] is the method of analysis used during the thesis work. It is provided by Numerical Electromagnetics Code [2.2], a computer program described in section 3.2.1.

During the design and testing stages, it is also important to know some general principles of microstrip antennas, such as how the patch size, dielectric thickness, dielectric constant and feed point design affect its electrical properties.

The size of the patch affects the resonant frequency, field polarization and efficiency. For most designs, a size on the order of half a wavelength achieves the best performance. Patches smaller than required reduce the antenna's efficiency, while larger patches increase the efficiency but introduce higher-order modes, distorting the fields [2.3]. As well as being undesirable in a small hand-held radio, larger patches also tend to reduce the antenna beamwidth. Size is a very critical parameter because of the narrow bandwidth of microstrip antennas.

The thickness of the dielectric determines the antenna's bandwidth and efficiency. Thick dielectrics typically allow larger bandwidths and greater antenna efficiency.

The substrate's dielectric constant is a very critical parameter also, as it affects the size, bandwidth, efficiency and most other parameters. Materials with large dielectric constants ($\varepsilon_r \approx 10.0$) allow the antenna size to be reduced and still operate at the same frequency. Unfortunately, this also reduces the bandwidth, gain and efficiency. The substrate dielectric constant also determines which parameter tolerances will affect the antenna's resonant frequency. For substrates with low dielectric constants ($\varepsilon_r \approx 2.5$), the resonant frequency is strongly affected by tolerances in the antenna size. For antennas with high dielectric constant substrates, tolerances in the dielectric constant become a strong influence on the resonant frequency.

Feeding the antenna is as important as designing the antenna itself. Choosing the proper feed point location can provide some input impedance matching. The geometry of the feed point should also be carefully selected to reduce unwanted inductive effects. For example, if a coaxial feed is chosen in preference to a microstrip transmission line feed, then the thickness and shape of the post should be taken into consideration. Matching circuits may also be required at the feed point to provide further impedance matching.

2.2 The Smith Chart

One graphical and analytical tool indispensable to RF design is the Smith chart. Developed by P.H. Smith in the late 1930s, it is still widely used today as a graphical method to solve impedance transformation problems in RF circuit design.

The idea for the Smith chart came from the need to provide a simple method of plotting impedances on a polar plot. The input impedance of a microwave circuit can be plotted in polar form by first converting it to a reflection coefficient. An example of this is shown in Fig. 2.3(a), where the input impedance is $Z_{in} = 15 + j25$ ohms on a 50 ohm line. The mismatch between the line impedance and circuit input impedance produces a reflection, with a reflection coefficient of [2.4]

$$\Gamma = 0.62\, e^{j123.4°}\,. \tag{2.1}$$

The polar plot has a maximum radius of one, and angles are measured counter-clockwise from the positive real axis.

The advantage of a polar representation of impedances is that all possible values of impedance can be plotted on the same chart. However, the numerical conversion from impedance to reflection coefficient is time consuming and tedious to the RF designer who will be doing it often.

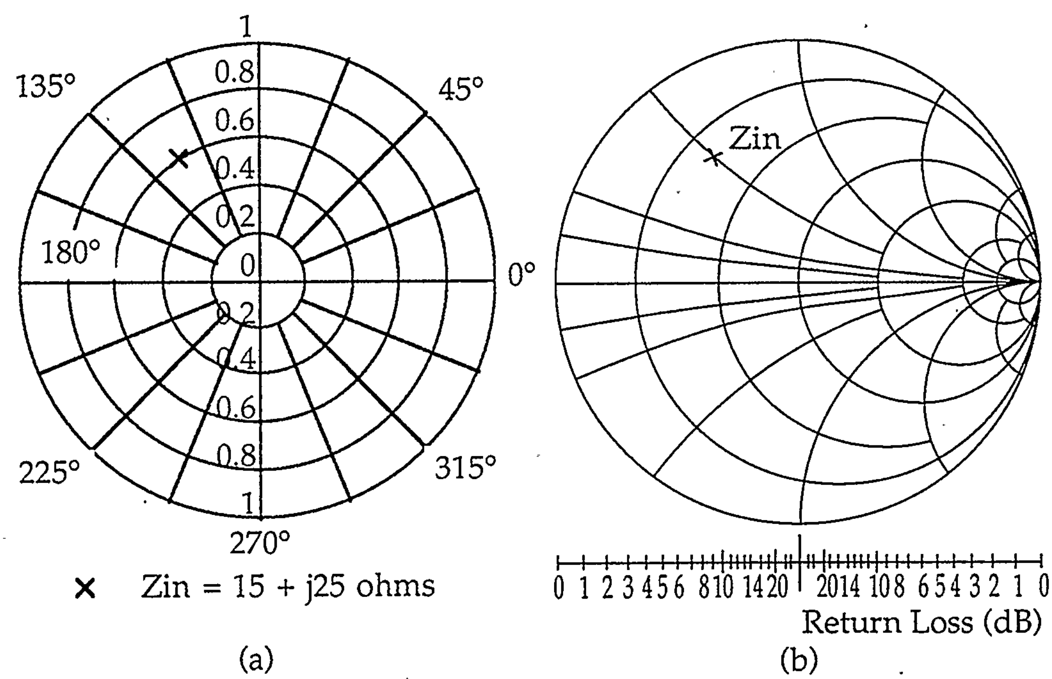

Fig. 2.3 Two representation of impedances: (a) polar and (b) Smith chart.

Fortunately, this numerical conversion can be avoided if a graphical conversion is provided on the graph itself. With this new graph, the Smith chart, impedances can be plotted directly. Fig. 2.3(b) shows how this is done with the same input impedance, $Z_{in} = 15 + j25$ ohms. The input impedance must first be normalized to the 50 ohm system impedance before being plotted

$$\frac{Z_{in}}{Z_o} = \frac{15 + j25}{50} = 0.3 + j0.5\,, \tag{2.2}$$

where Z_o is the system impedance. The value 0.3 + j0.5 is easily plotted by following the circles of constant resistance and arcs of constant reactance, shown respectively on Figs. 2.4(a) and 2.4(b).

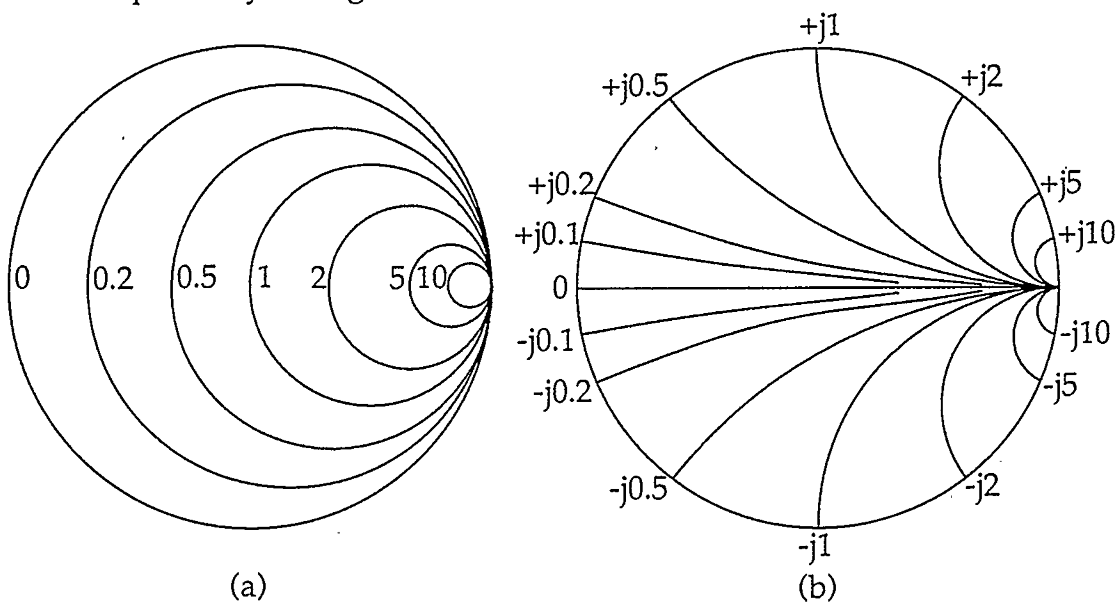

Fig. 2.4 Partial Smith charts showing (a) constant resistance circles and (b) constant reactance arcs.

Other parameters of the circuit can also be easily read from the Smith chart. These include the standing wave ratio, the transmission loss, the reflection loss and the return loss. A scale for the return loss is shown beneath the Smith chart of Fig. 2.3(b). Notice how the return loss improves substantially as the input impedance moves closer to the centre of the chart.

In other words, the return loss is greatest when the circuit impedance is matched to the line impedance.

Chapter 3 Design and Measurement

Many electrical engineers not familiar with microwave circuit design refer to it as a "black magic." As "proof," they point to the three-dimensional partial derivatives and closed-loop integrals of Maxwell's equations and speak of the difficulty in comprehending the invisible electromagnetic waves that propagate in all directions at the same time.

However, as the knowledge of this complex field increases and better tools are developed to design and measure microwave circuits, engineers are bringing this science down to a more understandable level.

This chapter describes some of the tools which are indispensable in designing and measuring diversity antennas. The design tools are described in section 3.2 and the measurement system is outlined and evaluated in section 3.3. Before this, however, the parameters important in designing and measuring antennas are described in section 3.1.

3.1 Diversity Antenna Parameters

To evaluate a diversity antenna, one must decide which antenna parameters are most significant. These parameters should provide a quantitative basis for an evaluation of the antenna's ability to overcome signal fading effects in a multipath environment.

The two (or more) antennas constituting a diversity antenna must radiate efficiently, must have the desired radiation patterns and polarization and must be reasonably uncorrelated in a multipath environment. These three criteria are explained in the following subsections.

It is important to note that although these criteria are sufficient in evaluating a diversity antenna, they cannot measure system improvements such as the improvement of the signal strength at a mobile receiver. Such system improvements are outside the scope of this thesis.

3.1.1 Efficiency

The input power to an antenna is transformed into one of four other forms. It is

- reflected at the input port
- coupled through to the other port(s)
- absorbed via dielectric loss or copper loss
- radiated

In equation form, this can be written

$$P_{in} = P_{reflected} + P_{coupled} + P_{absorbed} + P_{radiated} \tag{3.1}$$

The first three loss mechanisms are undesirable, and an efficient antenna is therefore one in which all of the input power is radiated. To evaluate how well an antenna radiates, its efficiency is defined

$$\eta = \frac{P_{radiated}}{P_{in}} \tag{3.2}$$

Looking at equation (3.2), it is apparent that one method of finding antenna efficiency is to measure the radiated power, $P_{radiated}$, relative to the input power, P_{in}. The radiated power can be determined from the antenna's radiation pattern (as described in section 3.1.2), but this method is not favoured, as it is time consuming and computationally intensive.

An alternative is to find the efficiency indirectly, measuring the energy lost in the other three mechanisms, $P_{reflected}$, $P_{coupled}$, $P_{absorbed}$, relative to P_{in}, substituting them into equation (3.1) and rearranging (3.1) to get

$$\eta = 1 - \frac{P_{reflected} + P_{coupled} + P_{absorbed}}{P_{in}} \tag{3.3}$$

The first two mechanisms, $P_{reflected}$ and $P_{coupled}$, are found directly by measuring the antenna's scattering parameters (S parameters). For a two-antenna diversity system, scattering parameters S_{11} and S_{22} are the return losses of the first and second antennas, respectively, while the second and first antennas, respectively, are terminated in a 50 ohm impedance. S_{21} and S_{12} describe the power coupled from one antenna to the other. The normalized power coupled from antenna 1 to antenna 2 is S_{21} and S_{12} measures the power coupled from antenna 2 to antenna 1. In equation form, the four scattering parameters are defined

$$|S_{11}|^2 = \frac{P_{reflected1}}{P_{in1}} \tag{3.4}$$

$$|S_{21}|^2 = \frac{P_{coupled1}}{P_{in1}} \tag{3.5}$$

$$|S_{12}|^2 = \frac{P_{coupled2}}{P_{in2}} \tag{3.6}$$

$$|S_{22}|^2 = \frac{P_{reflected2}}{P_{in2}} \tag{3.7}$$

Note that numerical subscripts have been added to $P_{reflected}$, $P_{coupled}$ and P_{in} to indicate which of the two antennas is being measured.

The third unwanted mechanism, $P_{absorbed}$, can be estimated from microstrip transmission line measurements. In some cases the absorbed power, which is mainly described by copper losses and dielectric losses, is small enough to be insignificant. Equation (3.3) can therefore be rewritten as

$$\eta_1 \approx 1 - |S_{11}|^2 - |S_{21}|^2 \tag{3.8}$$

$$\eta_2 \approx 1 - |S_{22}|^2 - |S_{12}|^2 \tag{3.9}$$

where η_1 is the efficiency of antenna 1 and η_2 is the efficiency of antenna 2. However, it is bad practice to assume that absorbed power is negligible. If it is necessary to calculate the efficiency, the absorbed power must be measured.

For this thesis, the absorbed power was not measured and so the efficiency was not calculated. Instead, the antennas were evaluated by comparing the scattering parameters to accepted standards. An acceptable diversity antenna should have at most -20 dB coupling between antennas [3.1] and 25 MHz of bandwidth at the resonant frequency [3.2]. The bandwidth is defined as that range of frequencies where the return loss is -9.54 dB at most (in other words, the SWR is 2 or less).

3.1.2 Radiation Pattern and Polarization

Although S parameters indicate how well the antenna radiates, they cannot fully describe the mechanisms of radiation. It is also important to know in what directions the antenna radiates and how the fields are polarized. The radiation patterns and field polarizations of the antenna must therefore be measured.

To understand electromagnetic wave propagation in a multipath environment, it is useful to describe the wave in terms of phasor quantities. If the directions and magnitudes of the electric and magnetic fields are represented with phasors, then simple physical laws of reflection and refraction can be used to examine how the fields change in the environment.

Wave polarization is a way of categorizing the direction and movement of these phasors through space. Three categories are used: linear, circular and random polarization.

Linear polarization exists if the phasors maintain the same orientation as they travel in time and space. In the example shown in Fig. 3.1, a wave traveling in the z direction is composed of mutually-orthogonal electric and magnetic fields. The amplitudes of the fields vary sinusoidally as they travel in space but are always oriented in the same direction. By convention, the type of polarization is based on the direction and movement of the electric field [3.3]. Therefore, because the electric field is always vertical, Fig. 3.1 describes what is more specifically known as a vertically-polarized wave. In the general case, a linearly-polarized wave could be oriented in any direction.

If the electric field vector has a constant amplitude but rotates in space instead of having a sinusoidal amplitude that is fixed in space, then the wave is described by circular polarization. The rotation of the electric field traces out a corkscrew pattern which looks like a circle if viewed normal to the xy plane.

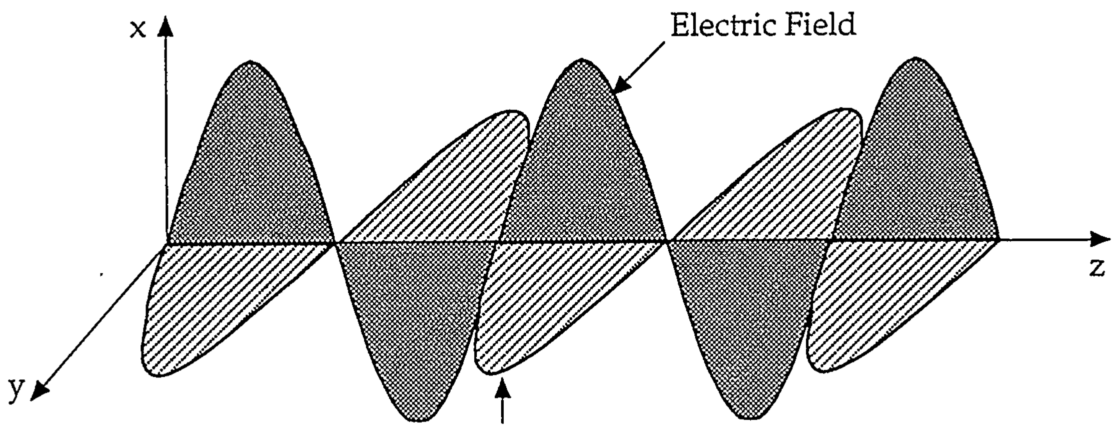

Fig. 3.1 Linearly-polarized wave.

Linear and circular polarization are both special cases of elliptic polarization, where the electric field traces out an ellipse when viewed normal to the xy plane [3.4]. One method of generating elliptic polarization is to combine two orthogonal, linearly-polarized waves 90° out of phase. If the amplitudes of the two waves are equal, the polarization is circular; if one wave has zero amplitude (or both are cophasal), the polarization is linear. Between these two extremes, the wave is elliptically polarized.

Radiation from radio stars and the sun exhibit random polarization, where, as the name implies, the orientation of the electric field vector varies randomly through space and time.

Microstrip antennas can be made to radiate circular-polarized waves, but they are most often designed for linear polarization. One mechanism for the creation of linearly-polarized waves was described in section 2.1. The fringing electric fields between the microstrip patch and the ground plane are approximately vertical in Fig. 2.2 (as viewed from the side of the antenna). As they separate from the antenna and become radiation fields, they remain vertical.

Linearly-polarized waves are also created if an electric field is excited across a slot between two patches, as shown in Fig. 3.2. The electric field is excited when the two patches are fed at different voltage potentials. Those fields that fringe above and away from the antenna will create linearly-polarized waves.

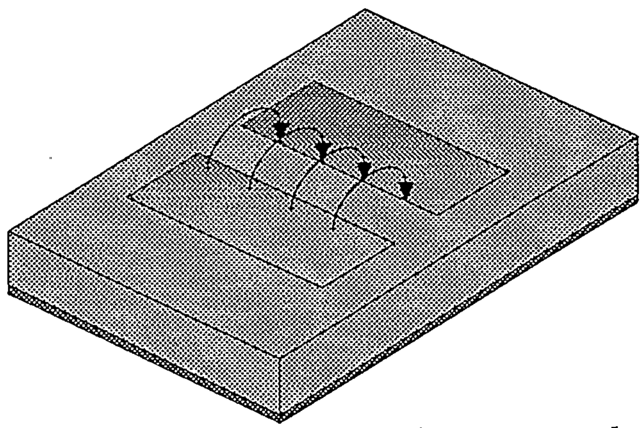

Fig. 3.2 Linear polarization between patches.

Both of the above mechanisms are used in the antennas designed for this thesis.

A radiation pattern illustrates how well an antenna radiates in all directions. The three-dimensional radiation pattern of a vertical, half-wavelength slot antenna is shown in Fig. 3.3. The radiation pattern is in the shape of a doughnut or toroid with its hole closed up. It illustrates that the slot radiates best in all horizontal directions but not at all vertically.

More can be understood about the radiation pattern with the help of some definitions.

Antenna gain, G, is a standard reference used to compare the maximum radiated power of the antenna under test (AUT), $P_{m\,AUT}$, to the maximum radiated power of a reference antenna, $P_{m\,ref}$. In equation form, this is expressed

$$G = \frac{P_{m\,AUT}}{P_{m\,ref}} \tag{3.10}$$

where $P_{m\,AUT}$ and $P_{m\,ref}$ are expressed in Watts. By convention, the reference antenna is usually a theoretical isotropic antenna that radiates 1 W of power with a constant power density in all directions.

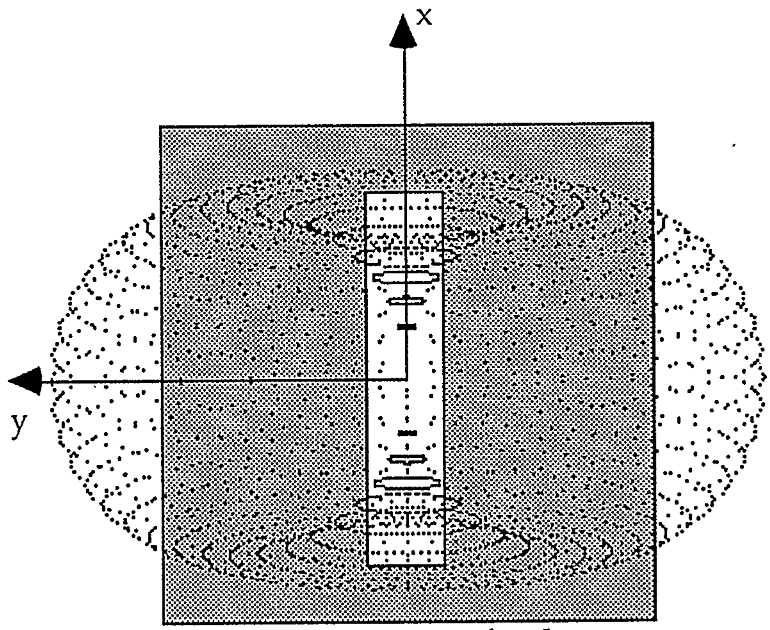

Fig. 3.3 Radiation pattern of a slot antenna.

The directivity and beamwidths indicate the antenna's ability to focus its radiated power in certain directions. The directivity, D, is defined

$$D = \frac{P_{m\,AUT}}{P_{avg\,AUT}} \tag{3.11}$$

where $P_{avg\ AUT}$ is the average radiated power. Directivity is always greater than one*, and the higher it is, the more focused is the beam.

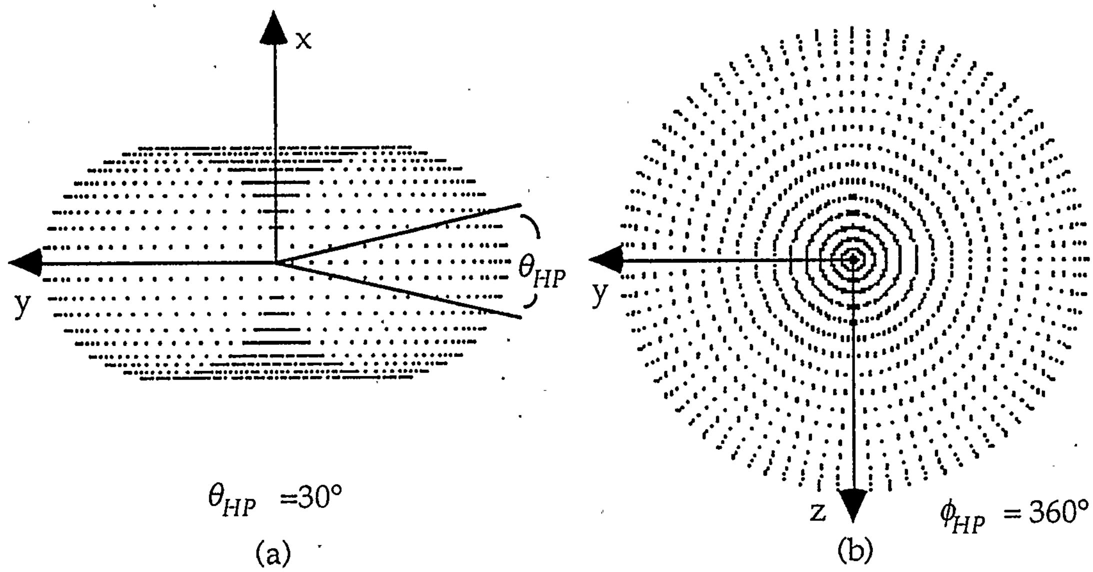

Fig. 3.4 Beamwidths of a slot antenna radiation pattern in the (a) θ plane and (b) ϕ plane.

The beamwidth for a given plane (θ or ϕ plane) is the angle over which the radiated power is at least half of the maximum radiated power. The two beamwidths of the slot antenna radiation pattern are shown in Fig. 3.4. Fig. 3.4(a) is the side view of the radiation pattern of Fig. 3.3. At 15° above and below the horizontal, the power decreases to half of the maximum, giving a θ-plane beamwidth of 30°. In the ϕ plane, shown by the top view of the radiation pattern of Fig. 3.3, the radiation is constant and therefore its beamwidth is 360°.

For cellular communications, the mobile antenna should transmit or receive in all directions between the horizontal and roughly 30° above the

* Directivity can never equal one unless the antenna is a theoretical isotropic antenna, which is impossible to construct in reality.

horizontal [3.5] (because antennas are reciprocal devices, they transmit and receive with equal ability). Therefore, θ_{HP} should be no less than 30°. Flat microstrip antennas can be designed to have any beamwidth. Typically for rectangular patches, this beamwidth lies between 60° and 160° in the θ plane* [3.6] and can be increased by reducing the size of the patch [3.7]. Increasing the beamwidth has the effect of decreasing the gain and directivity but does not affect the efficiency.

3.1.3 Diversity

Diversity antenna measurements would not be complete without some test to determine the received signal improvement using the diversity antenna versus a single antenna in mobile environments.

One such test is to install the diversity antenna in a mobile telephone and operate it in a number of typical multipath environments. In each environment, the received signal power of both antennas in diversity are measured and a standard selection or combining method is used to determine the signal improvement due to diversity (in dB). The same data can also be used to evaluate the correlation between the two signals. Such information indicates whether or not the two signals are statistically independent enough for the diversity antenna to be worthwhile. Although these tests are ideal, they are so time consuming and resource intensive that they have been the subject of an entire Master's thesis on their own [3.8].

A simpler method is to estimate the theoretical correlation between the two received signals, using an accurate computer model. Such a model

---

* assuming that the antenna lies in the yz (or ϕ) plane.

calculates the correlation from known parameters of the diversity antenna which are more easily measured. The computer model method has the advantage of speed but is often less reliable because of the simplifications and assumptions used. The results of such a model, therefore, can only be used to provide a reasonable estimate of the received signal improvement using a diversity antenna. Such a computer model was written by the author as a project for a computer programming course [3.9]. It was intended for use with this thesis work, but time constraints and programming bugs prevented this.

3.2 Software Design Tools

Building and modifying antennas is often time consuming and laborious. Weeks of time can be spent measuring, modifying and measuring again an antenna design that, for seemingly supernatural reasons, will not work.

In contrast, software design and software testing can be performed very quickly. This makes them attractive replacements for hardware testing in the initial debugging stages. Hardware testing, however, must still be used in the end to verify that the concept works in reality.

The remainder of this section describes NEC, a software package that was used to analyze some of the antennas in this thesis. The results of the NEC analyses were not reliable and thus were not used to complement the hardware design, but so much time was spent using NEC that it justifies a brief mention in the thesis.

3.2.1 Numerical Electromagnetics Code

Numerical Electromagnetics Code (NEC) is a computer program used to theoretically analyze the electromagnetic properties of any object that can be described as a structure composed of a finite number of wires and/or enclosed objects made of planar surfaces [3.10]. The analysis relies on the numerical solution of integral equations for induced currents. Once the currents are derived, radiation patterns, impedances and node voltages can be found.

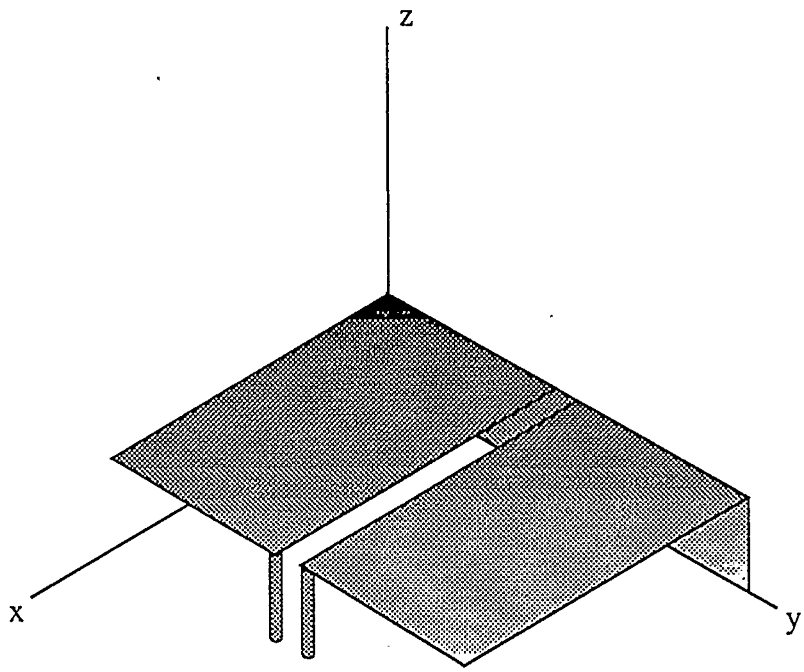

Fig. 3.5 The U-patch antenna.

The structure can include lumped elements (resistors, inductors and capacitors), transmission lines and perfect or imperfect conductors. It may be modeled over a ground plane that is either a perfect or imperfect conductor and can be excited by voltage sources on the structure and/or incident plane waves of any non-random polarization.

As an example of its use, the U-patch antenna of Fig. 3.5 is depicted as it would be modeled by NEC in Fig. 3.6. Each copper surface of the antenna is represented as a rectangular wire mesh, and the feed points are represented by thick wires. The ground plane is not shown, but it is modeled as infinitely large along the xy plane.

The density of the mesh and the radii of wires are up to the designer's discretion. There is no optimum mesh density, although NEC algorithms work best when the wires are less than 10 per cent of the wavelength apart. An optimum wire radius has been found using the "Equal-Area Rule" algorithm [3.11]. Unfortunately, NEC is unable to model dielectric materials, but this limitation can be transcended by using capacitors between the conducting patches and the ground plane.

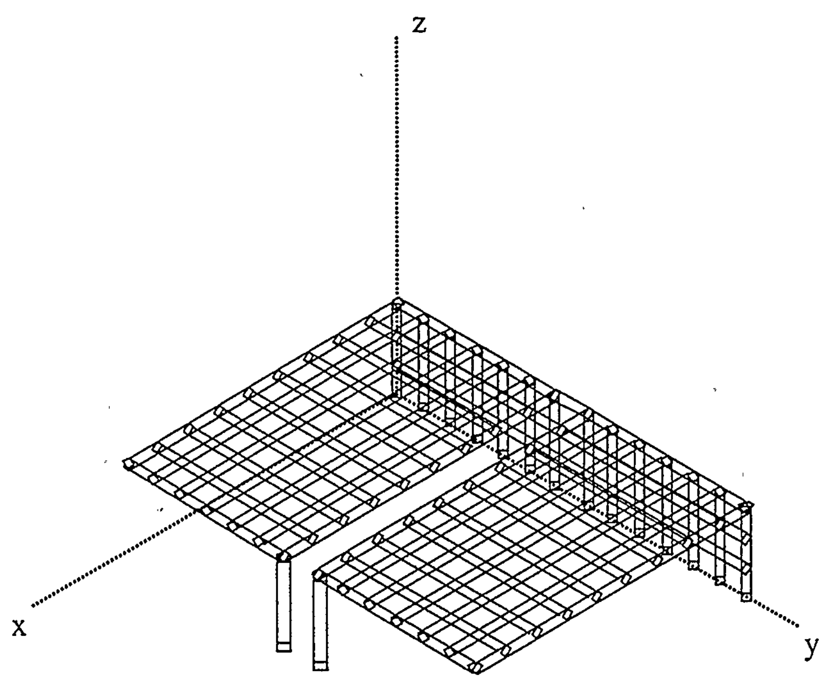

Fig. 3.6 Wire grid model of the U-patch antenna.

To automate the design and modification of the models, short programs were written by the author. These programs allow design changes to be made in a few seconds. A NEC analysis of this model normally took 30 to 40 minutes on a DEC™ minicomputer to either find the input impedance over a frequency range of 600 MHz to 900 MHz or the radiation pattern at one frequency.

After the analysis is complete, the input impedances and radiation patterns are viewed in order to decide whether further design changes should be made.

NEC was used in this thesis with the hope that it would complement experimental results, particularly in the initial antenna design stages. However, after five months of use, the results were not reliable enough to justify using NEC. The appendix provides some of the results of the NEC program and compares them to experimental measurements.

3.3 Measurement and Analysis

In section 3.1, it was determined that the important characteristics of a diversity antenna are efficiency, radiation pattern, radiation polarization and diversity. The devices used to measure all of these characteristics except diversity are described in this section. During the course of this thesis work, the hardware facilities at the newly-formed TR*Labs* were quickly evolving. Thus, later antenna designs were tested with much more efficient and reliable equipment than early designs. The square patch antenna was tested with somewhat crude hardware set-ups which are described in sections 3.3.1, 3.3.2 and 3.3.4. The apparati used to measure the other antennas are discussed in sections 3.3.3 and 3.3.5.

3.3.1 Return Loss and Coupling Measurement Apparatus

The S parameters of an antenna, described in section 3.1.1, are instrumental in understanding where the power into the antenna is flowing. With a network analyzer, described in section 3.3.3, the S parameters are measured very quickly. Unfortunately, one was not readily available when the square patch antenna was being developed. Two other measurement apparati were used instead. The magnitude and phase of S_{11} were observed with a vector voltmeter set-up (shown in section 3.3.2) and the magnitudes of S_{11} and S_{21} were read from the power meter apparatus, described in this section and shown in Fig. 3.7.

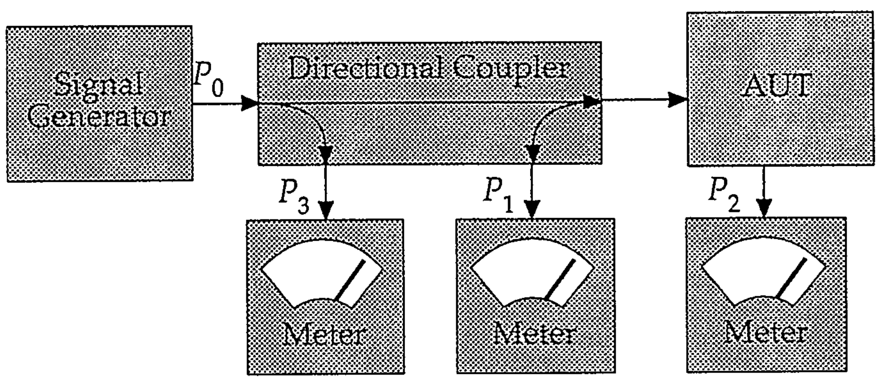

Fig. 3.7 Power meter apparatus.

The power meter apparatus consists of a Marconi® 2202 signal generator, one Narda® Microline 3020A bi-directional coupler, the antenna under test (AUT) and three Hewlett Packard® 436A power meters. From the signal generator, energy flows through the directional coupler and is split into two paths. Most of the power propagates straight through the main branch of the coupler to the antenna, but a small portion (20 dB down) is coupled to one of the power meters. This power, P_3, acts as a reference. It tracks the output power of the signal generator, which one should not assume is constant over all frequencies. The power to the antenna is either reflected, coupled, absorbed or radiated, as discussed in section 3.1.1. The portion that is coupled is recorded as P_2 by one power meter, and the reflected power propagates backwards through the directional coupler, where a 20 dB portion is read by the third power meter as P_1. Substituting P_1, P_2 and P_3 into equations 3.4 and 3.5, the forward S parameters are calculated

$$|S_{11}|^2 = \frac{P_1}{P_3} \tag{3.12}$$

$$|S_{21}|^2 = \frac{P_{2A}}{P_3} \tag{3.13}$$

where P_1, P_{2A} and P_3 are given in Watts. With powers measured in decibels, the above equations become

$$|S_{11}| = P_1 - P_3 \tag{3.14}$$

$$|S_{21}| = P_{2A} - P_3 = P_2 - 20\text{ dB} - P_3 \tag{3.15}$$

where $P_{2A} = P_2$ - 20 dB. Note that only the forward S parameters, S_{11} and S_{21}, are measured. Because the square patch antenna is symmetric, the backward S parameters, S_{22} and S_{12}, should be very similar to their forward counterparts. This fact is verified in section 4.1.3.

3.3.2 Input Impedance Measurement Apparatus

To plot the input impedance on a Smith chart, both the magnitude and phase of S_{11} must be measured. Power meters are, however, only capable of measuring magnitude, so a different set-up from the one described in the last section must be used. This instrument is the vector voltmeter, shown connected in the measurement apparatus in Fig. 3.8.

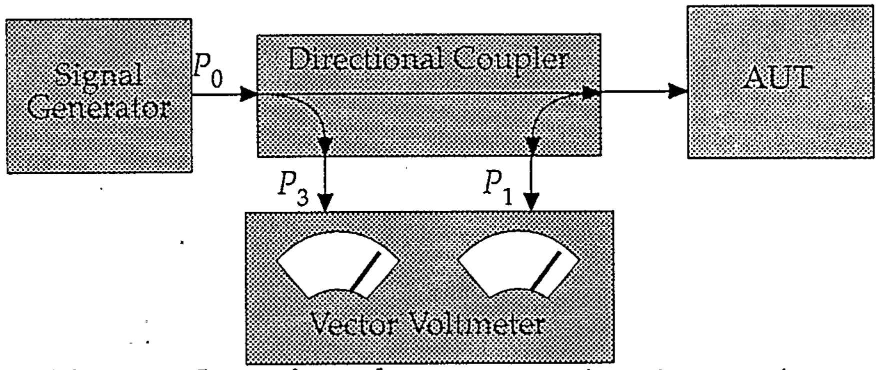

Fig. 3.8 Input impedance measurement apparatus.

This apparatus is very similar to that of Fig. 3.7. The main difference is that the coupled source power, P_3, and reflected power from the input port of the antenna, P_1, are both measured by the same vector voltmeter, rather than separate power meters (the vector voltmeter measures power in decibels in addition to rms voltage). Three values are measured by the vector voltmeter: the magnitudes P_1 and P_3 and the phase angle θ_1 between them. An uncalibrated return loss, $S_{11\mathrm{uncal}}$, is calculated from these measurements as follows

$$S_{11uncal} = |S_{11uncal}| \angle \theta_1 \tag{3.16}$$

where $|S_{11uncal}| = P_1 - P_3$ and P_1 and P_3 are measured in dB. This uncalibrated value is not the true return loss, however. To find the true return loss, the system must be calibrated. Using an open circuit termination in place of the AUT, the same measurements are repeated. The new values, P_{1open}, P_{3open} and θ_{open} are recorded and the return loss of the open circuit is calculated

$$S_{11open} = |S_{11open}| \underline{/\theta_{open}} \tag{3.17}$$

where $|S_{11open}| = P_{1open} - P_{3open}$. In a calibrated system, both $|S_{11open}|$ and θ_{open} are zero, but this is never the case in reality. To account for this, the return loss is corrected

$$S_{11} = |S_{11}| \underline{/\theta} \tag{3.18}$$

where $|S_{11}| = |S_{11uncal}| - |S_{11open}|$ and $\theta = \theta_1 - \theta_{open}$.

3.3.3 HP 8510C Network Analyzer

The HP 8510C Network Analyzer became available for use at TR*Labs* after the square patch antenna was developed. It was used to measure the S parameters of the remaining antennas.

Vector network analyzers like the HP 8510C are used to measure the magnitude and phase characteristics of devices such as amplifiers, filters and antennas. The HP 8510C system consists of a series synthesized sweeper, an S-parameter test set, an IF/detector, and a display/processor [3.12].

The sweeper provides the RF signal. The test set contains the input/output ports to connect to the antenna under test (AUT) and the signal separation and mixing required to provide the incident, reflected and transmitted signals. These signals are then sent to the IF/detector which converts them to a lower intermediate frequency (IF) so that the signal levels and phase differences can be measured directly. The resulting S parameters are finally sent to the display/processor, where they are displayed on a video screen in a variety of formats.

The HP 8510 is capable of linear network analysis between 45 MHz and 50 GHz in both the frequency domain and the time domain. For further technical information, consult the HP 8510C operating manual [3.12].

3.3.4 Polarization Measurement Apparatus

The S parameters of an antenna determine how well matched and isolated the feed points are, and they indicate, in an indirect way, how efficiently the antenna radiates, but little is known about the antenna's radiating behaviour until the radiation is measured directly.

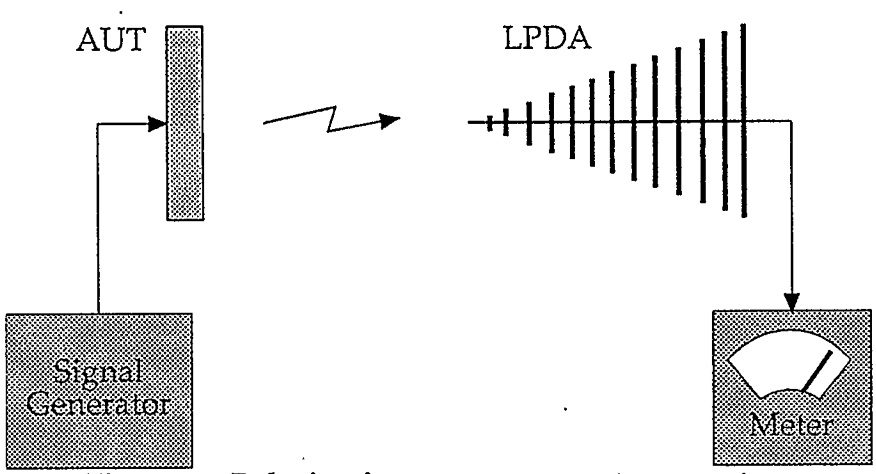

Fig. 3.9 Polarization measurement apparatus.

Two methods of measuring radiation were used in this thesis. For the U patch antenna, the entire far field radiation pattern was measured at a single frequency using the Antenna Test Range at NovAtel. This system is described in some detail in section 3.3.5. For the square patch antenna, a more crude system was used. Radiation over a band of frequencies in two polarizations but only in one direction from the antenna was measured. The experimental apparatus for this measurement is illustrated in Fig. 3.9.

The signal is supplied to one port of the diversity antenna over the 500 MHz to 900 MHz frequency range by a Marconi® 2202A signal generator. The unused port of the antenna is terminated with a 50 ohm impedance. At a distance of 49 centimetres from the diversity antenna, the log-period dipole array (LPDA) antenna receives the far field radiation which is then measured by a Hewlett-Packard® 436A power meter.

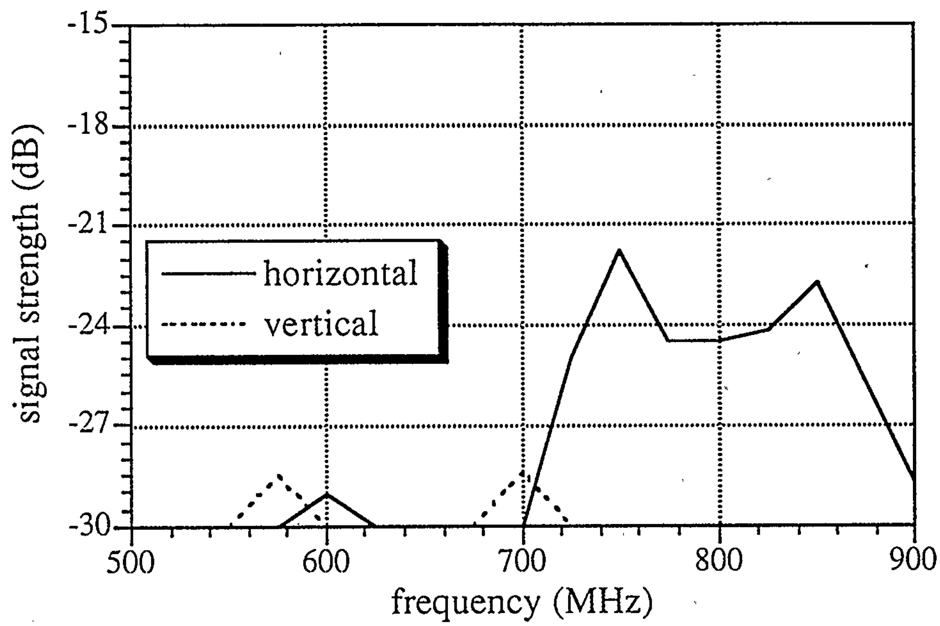

Fig. 3.10 Vertical and horizontal polarization of a horizontally-oriented dipole antenna.

The LPDA (model CLP 5130-2 by Creative Design Co. Ltd.) is a wide band antenna (105 to 1300 MHz for SWR < 2) with linear polarization and 10 dBi to 12 dBi gain in the forward direction (the direction pointing towards the AUT). For a given set of measurements, it is oriented to receive either the vertical polarization (as shown in Fig. 3.9) or the horizontal polarization. It only receives energy in the direction normal to the radiating copper patch of the test antenna, so information such as beamwidth and directivity are impossible to determine. These measurements can, however, illustrate whether the antenna radiates with the polarization that it was designed to in that direction.

When making radiation measurements, it is important to have the LPDA antenna only receiving power directly from the test antenna. Just as in a cellular environment, if radiation is allowed to reflect off of walls and equipment in the laboratory, some of the reflected signals could arrive at the receive antenna with different phases, polarizations, etc. than the signal directly from the test antenna. These signals would thus adversely affect the measurement results, and so microwave absorbing material was placed around the experimental apparatus to prevent reflected signals.

To evaluate the measurement set-up and verify that reflected signals were not significant, a dipole antenna with horizontal polarization and a centre frequency of 800 MHz was measured, taking the place of the AUT. As shown in Fig. 3.10, the reflected signals were not significant. The horizontal polarization dominated around 800 MHz, and the vertical polarization was almost insignificant across the entire frequency band.

3.3.5 Antenna Test Range

Far-field radiation patterns of the U patch antenna were measured at NovAtel's Antenna Test Range (ATR) [3.13]. The ATR was developed by the Antennas/Propagation group at NovAtel Communications Ltd. with the purpose of measuring the entire far field radiation patterns of small antennas for cellular telephones and Global Positioning Systems.

The ATR, shown in Fig. 3.11, consists of a large anechoic chamber where the antenna under test (AUT) and a linearly-polarized receiving antenna are placed. Low-dielectric materials and microwave absorbing foam are used in the ATR to approximate a free-space environment and reduce the effects of electromagnetic interference. The AUT is connected to a battery-powered transmitter and mounted in the centre of a test jig which rotates the AUT to any angular orientation via two stepper motors. As the AUT is rotating, its emitted radiation is sampled by the receive antenna at points on a spherical surface surrounding the AUT. The sampled radiation pattern is then processed and displayed in two- or three-dimensional plots.

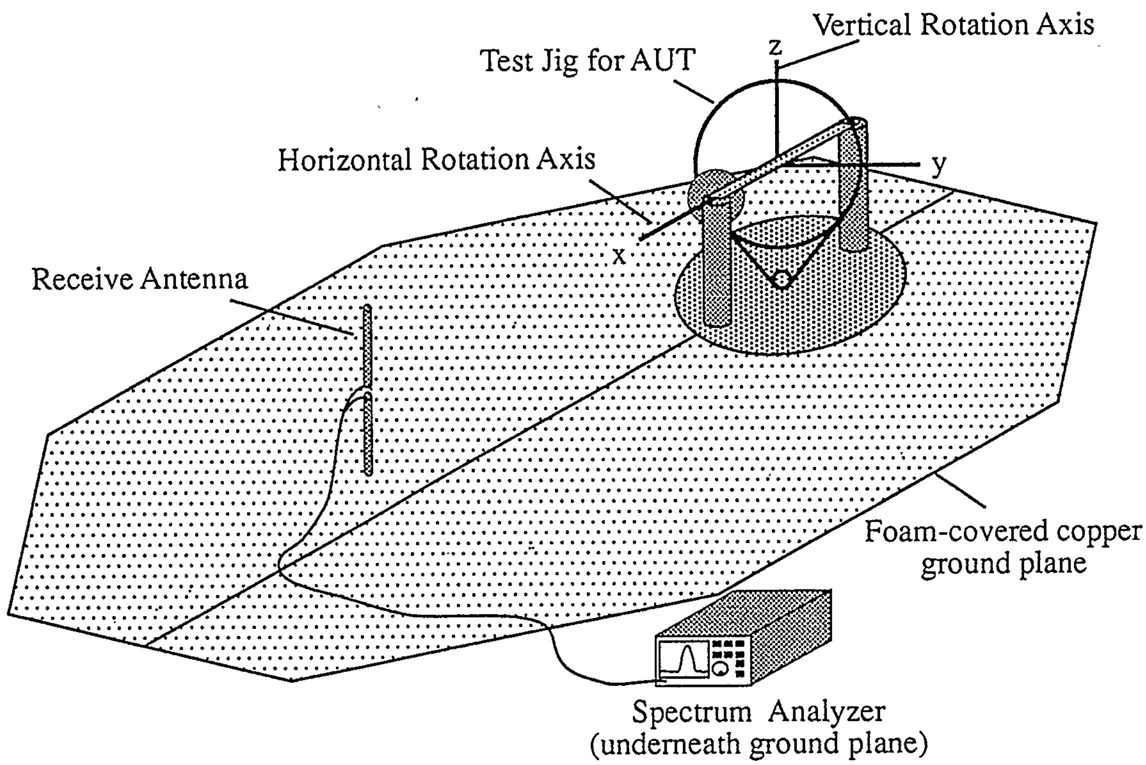

Fig. 3.11 Antenna Test Range configuration.

A block diagram of the ATR is shown in Fig. 3.12. As the stepper motors rotate the AUT, a spectrum analyzer measures the radiation incident at the receive antenna and an SDK-85 microprocessor kit records the AUT's angular position. Both sets of information are sent to the controller, where they are stored on a personal computer.

The personal computer mediates each test run, sending initialization commands to all other instruments of the Antenna Test Range, storing the received data and manipulating it to create the radiation pattern plots. It is connected, via an RS-232 bus, to an IoTech Micro 488 Bus Controller. The Bus Controller simply allows the personal computer to be connected to the spectrum analyzer and SDK-85 through a general purpose interface bus (GPIB).

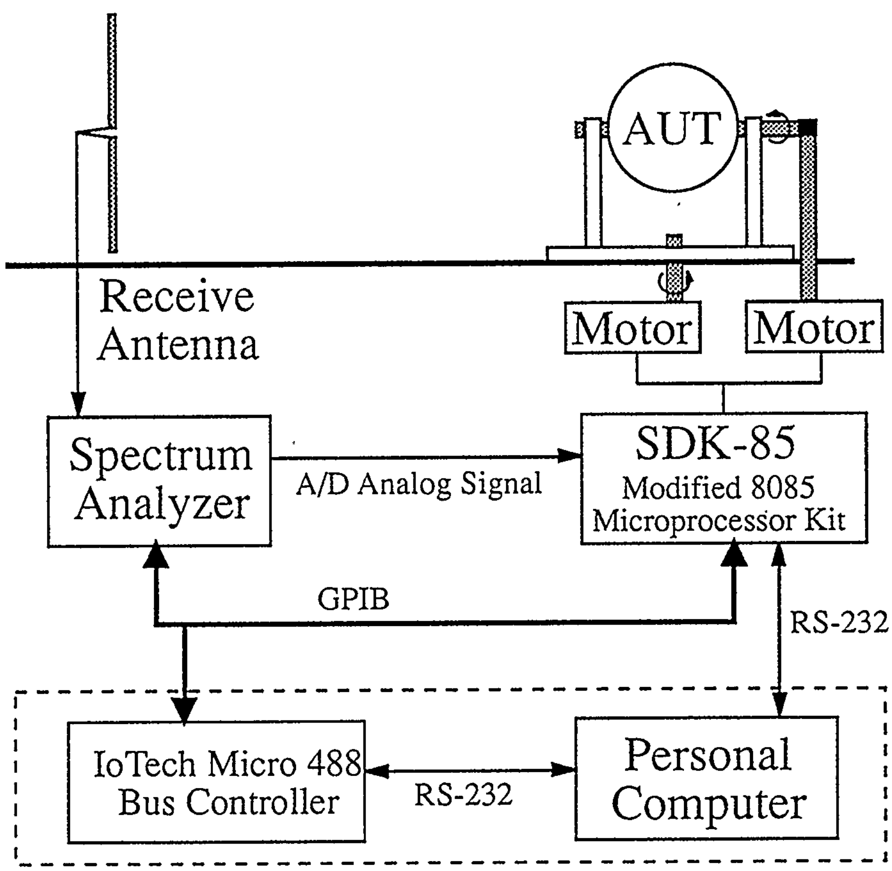

Fig. 3.12 Block diagram of the Antenna Test Range.

Besides recording the angular position of the AUT, the SDK-85 is also responsible for zeroing the motors before a test run, setting the spatial resolution of the run and controlling the motors.

To measure the vertically-polarized, horizontally-polarized and total radiation patterns, three measurement runs are performed, each with the receive antenna in a different position. For the first two runs, the antenna is oriented to receive vertical and horizontal polarization. A third run, with the antenna oriented 45 degrees from the horizon, is necessary to resolve any ambiguity as to the true direction of the total electric field vector.

The automation of the Antenna Test Range allows a measurement run to be performed within half an hour.

Chapter 4
Results

All of the antennas developed during the course of this thesis use two orthogonally-polarized slots to provide polarization diversity. The simplest device that uses orthogonally-polarized slots is the cross slot antenna shown in Fig. 4.1.

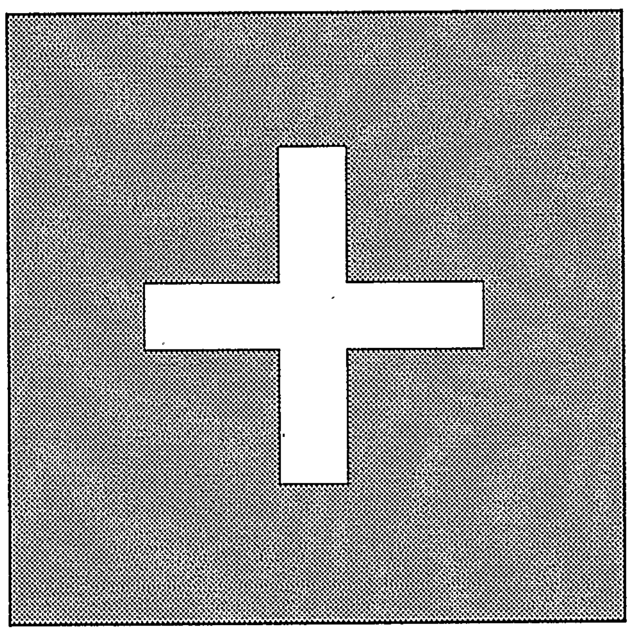

Fig. 4.1 Cross slot antenna.

A vertical slot and a horizontal slot are cut into a square sheet of copper. Each slot can be excited independently by creating an electric potential across the long sides at the proper frequency. The electric potential forces an electric field to act across the slot and radiate into space with a linear polarization and radiation pattern as described in section 3.1.2.

The cross slot antenna provides a valid form of polarization diversity and can be used in mobile cellular systems where size is not restricted. However, for hand-held cellular telephones, this antenna is normally too large. Each slot must be one half of a wavelength long at the resonant frequency which is roughly 17 cm for the 800 MHz cellular systems.

Antenna designs that provide polarization diversity based on the cross slot antenna but are smaller to be practical in hand-held cellular systems must be found. Three such designs are studied in this chapter.

4.1 Square Patch Antenna

4.1.1 General Description

A wire dipole antenna must be one half of a wavelength long at its resonant frequency, but from basic antenna theory it is well known that this length can be halved if a ground plane is inserted in the middle.

The same principle applies with the slot antenna; its resonant length can be halved when one side is grounded. As a consequence, if one side of each slot is grounded, an antenna can be built that has the action of a cross slot antenna but with an area equal to one quarter of the original area.

It is this idea that created the first of the antenna designs, the square patch antenna. As shown in Fig. 4.2, this antenna consists of a square microstrip patch stuck onto a thick dielectric material which is glued atop a copper ground plane. Each side of the square patch is 6.1 cm long, which is equivalent to one quarter of a wavelength at the resonant frequency. It is made of copper tape that is cut to shape, peeled from its backing and adhered to the dielectric material. Compared to photo etching, copper tape is much easier to work with and makes antenna modifications very simple. The tradeoff, however, is that copper tape is not as reliable due to the electrical properties of the glue, air bubbles underneath the surface and frayed edges. But these tradeoffs are likely to be slight at the low frequencies used (near 1 GHz).

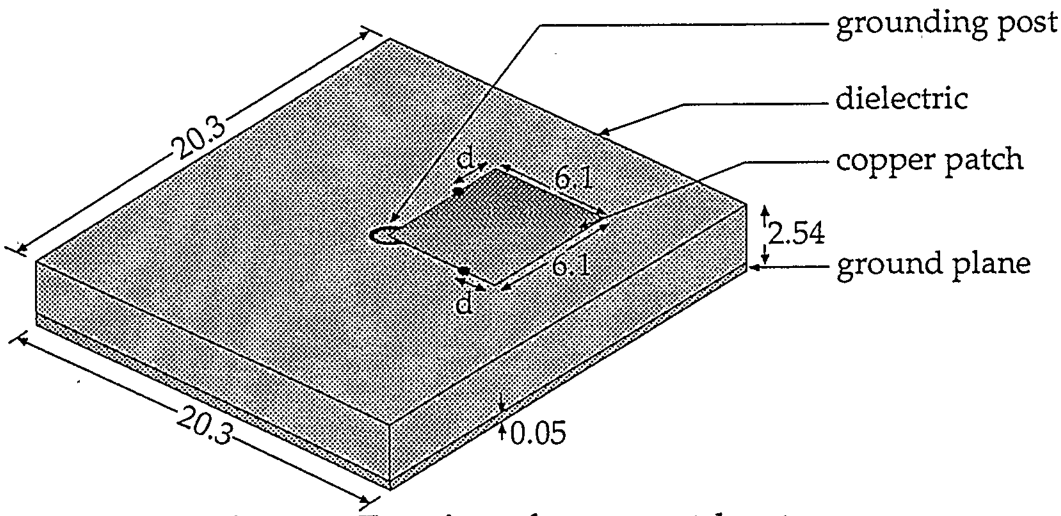

Fig. 4.2 Top view of square patch antenna (all dimensions are in centimetres).

One corner of the square patch is short circuited to the ground plane using a thick brass screw (8.3 cm long with a 1.0 cm outer diameter). The brass screw extends a distance ℓ below the nut under the screw. Each of the two feed points is a 22 gauge wire (approximately 0.05 cm in diameter) that extends vertically through the dielectric connecting a BNC connector underneath the antenna (as shown in Fig. 4.3) to an edge of the microstrip patch on top of the antenna. The feed points are each a distance d away from opposite corners of the patch. This distance d is variable, depending on the required input impedance at each feed point.

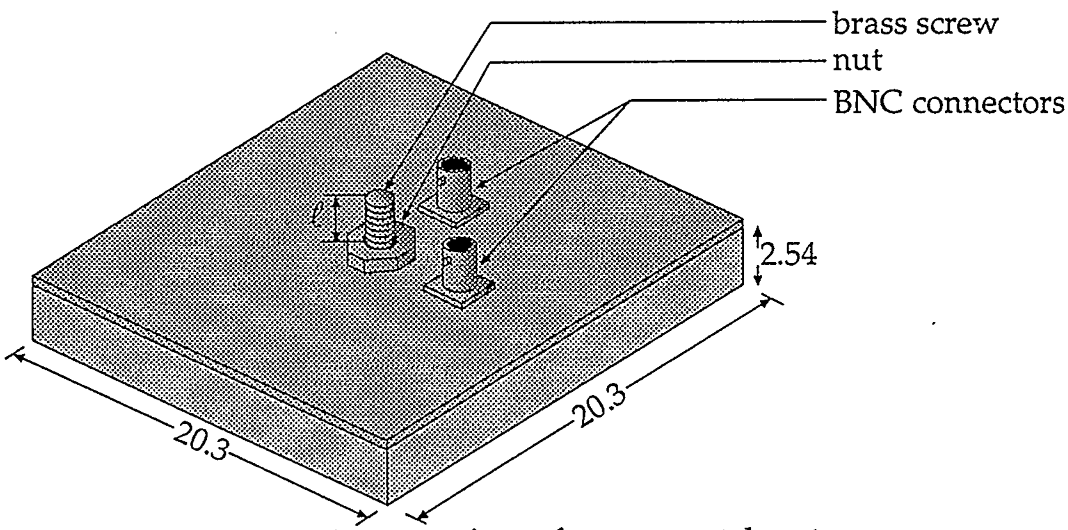

Fig. 4.3 Bottom view of square patch antenna (all dimensions are in centimetres).

4.1.2 Theory of Operation

On its own, a square patch has no slots. It may therefore seem impossible for it to act like the cross slot antenna of Fig. 4.1. That is why the addition of the ground plane is essential. As explained in sections 2.1 and 3.1.2, a linearly-polarized wave radiates when an electric potential is created between the edge of a microstrip patch and ground. With the square patch antenna, the slot is not created by a gap in a copper patch but rather, it is created between one edge of the patch and the ground plane.

Each of the feed points (labeled F_1 and F_2 in Fig. 4.4) excites a linear polarization from the patch by feeding current along the closest outside edge to it (the two outside edges of the patch are defined as those not connected to the grounding post). Seen from the top in Fig. 4.4, feed point F_1 feeds current to the right-most vertical edge of the square patch and F_2 feeds current to the lower horizontal edge.

The operation of the square patch antenna relies on the assumption that when one feed point is in operation (F_1, say), the edge of the patch that connects the other feed point (F_2) to the grounding post is close to zero potential. This assumption is supported by three observations: the grounding post is very close to zero potential (the brass screw is thick so as to reduce its inductance to ground); when one feed point is in operation, the other feed point can be thought of as short circuited due to the superposition principle; the distance between the grounding post and the second feed point is small and therefore the whole edge that connects them together can be assumed to be at ground potential.

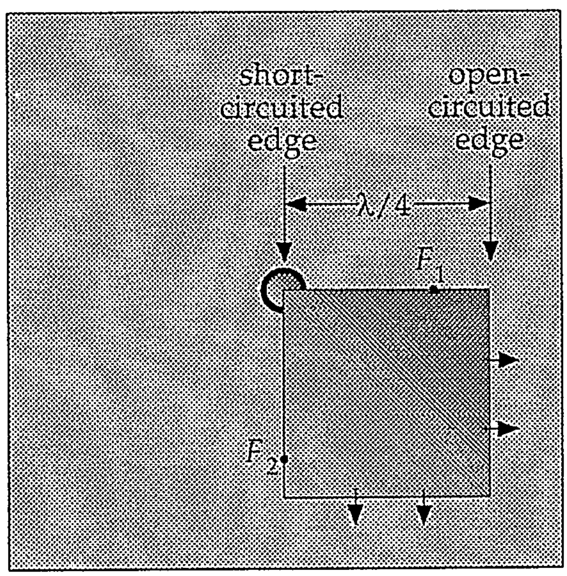

Fig. 4.4 Top view of square patch antenna, showing the radiating edges and polarizations.

One quarter of a wavelength ($\lambda/4$) away, the opposite edge experiences an open circuit so that current there cannot flow across the patch to the short-circuited edge. Current can therefore only travel along the open-circuited edge. This current excites an electric field between that edge and the ground plane which radiates a horizontally-polarized wave as seen from Fig. 4.4. In a similar manner, point F_2 excites an electric field between the bottom edge of the microstrip patch and ground, creating a vertically-polarized wave.

The operation of this antenna would not change if the feed points were moved to the corners of the patch adjacent to the grounding post (so that d in Fig. 4.2 is zero). Moving them in by a distance d only serves to change the input impedance. For symmetry, both feed points must be moved in by the same amount.

Section 2.1 explained that the bandwidth of an antenna is proportional to the dielectric thickness and inversely proportional to the dielectric permittivity. Therefore, to keep the bandwidth of the antenna large, a thick dielectric (thickness = 2.54 cm) with a low permittivity ($\varepsilon_r = 2.5$) was used.

The square patch antenna was designed to operate in the 800 MHz to 900 MHz range. With a length of 6.1 cm being equivalent to one quarter of a wavelength at resonance, the free space wavelength is 24.4 cm. Without the dielectric then, the antenna should resonate at 1.23 GHz. But this frequency is reduced with the inclusion of the dielectric. A relative dielectric constant of 2.5 gives an effective dielectric constant between 2.0 and 2.2 (taking the air above the antenna into account) so that the resonant frequency is reduced to between 829 MHz and 870 MHz.

4.1.3 Results

There were three versions of the square patch antenna, named

Kutzmayteen, Clayoquot and Carmanah*. Perspective views of the antennas are shown with S-parameter measurements in Figs. 4.5, 4.7 and 4.9. Only the return loss at port 1 (S_{11}) and the coupling from port 1 to port 2 (S_{21}) were measured (F_1 was fed and F_2 was terminated in a 50 ohm impedance). The other two S parameters were assumed to be similar due to the symmetry of the antenna. None of the three antennas performed very well, but the observations made when designing and measuring the square patch antennas were important when designing the next antennas.

The first antenna, Kutzmayteen, had a long brass tube inserted vertically into the dielectric half of the way down at the grounding point of the square patch. The tube was soldered to the patch but did not touch the brass screw nor the ground plane. Therefore, the air gap between the tube and the screw acted like a capacitor in series with the inductance of the screw. By turning the screw inside the tube, the capacitance can be varied until it cancels the screw's inductance. At this point, the corner of the patch attached to the tube should be at ground potential.

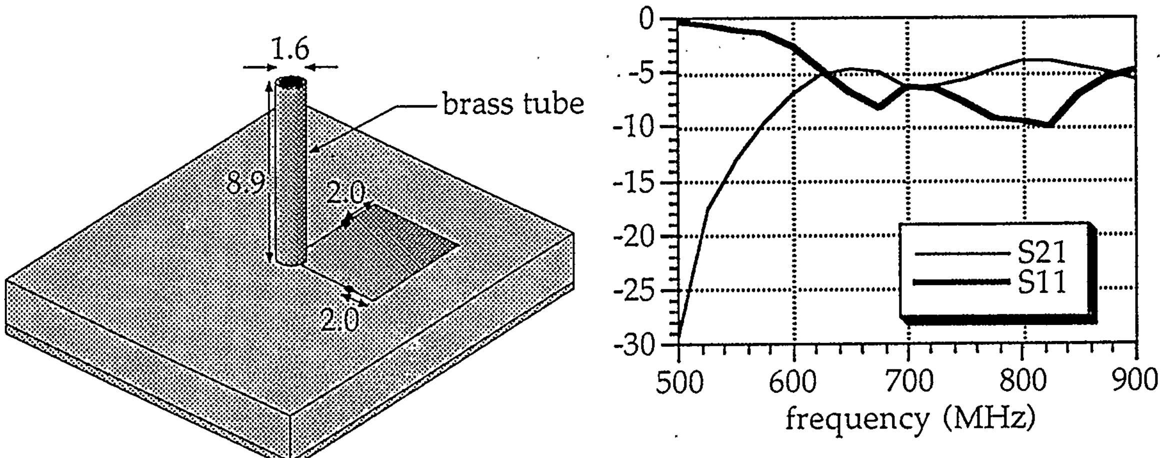

Fig. 4.5 Kutzmayteen antenna with S parameters for $\ell = 2.5$ cm.

---

* The antennas in this thesis, with the exception of the triangle patch antennas, are named after rivers.

As it is difficult to tell when the corner of the patch is grounded, measurements were made at a number of different screw settings. The best results were found when the screw length, ℓ (as shown in Fig. 4.3) was 2.5 centimetres.

As witnessed by the measurements presented in Fig. 4.5, Kutzmayteen was a very inefficient antenna. The return loss is poor over most of the frequency range and even where it improves, the coupling degrades. For example, the frequency where the return loss is best (-10.06 dB at 825 MHz) is also where the coupling is the worst (-3.93 dB).

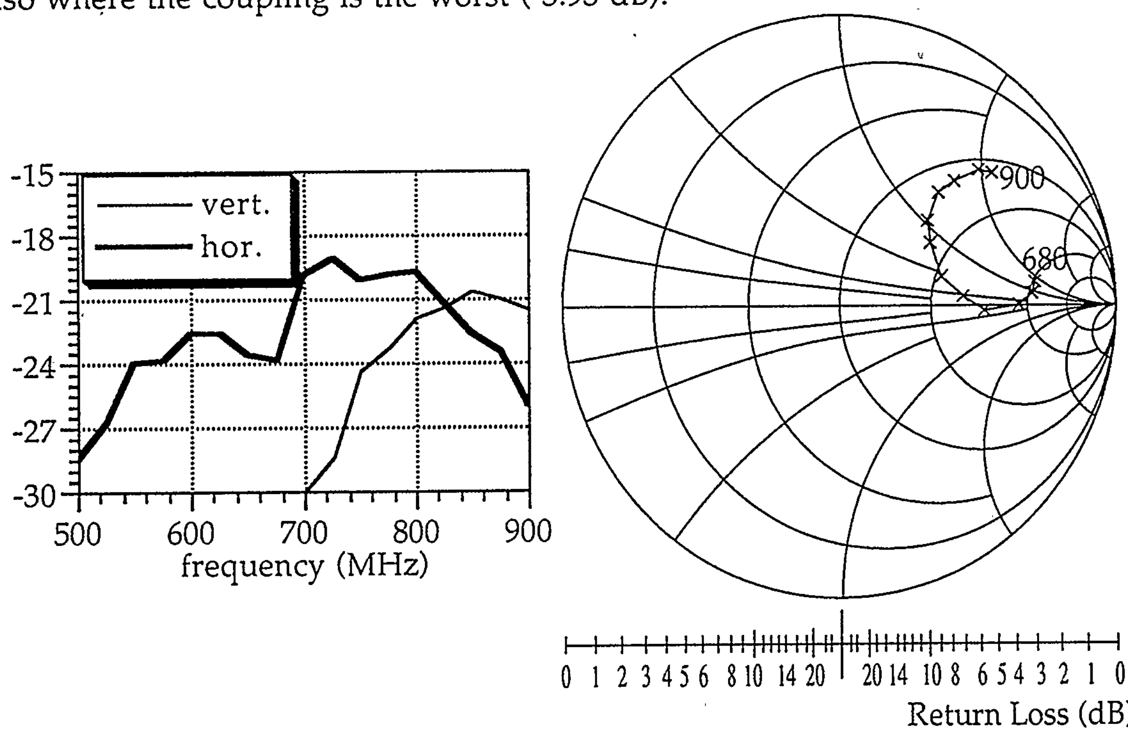

Fig. 4.6 Polarization and input impedance of Kutzmayteen.

Kutzmayteen has no obvious resonant frequency, but the power sum of the return loss and coupling is lowest (-2.85 dB) at 750 MHz*. The input

* This is likely not the true resonance frequency if the antenna performed well, as it was designed for a resonance frequency between 829 MHz and 870 MHz.

impedance of Kutzmayteen was measured from 680 MHz to 900 MHz in 20 MHz steps and is shown in Fig. 4.6 (a screw length of 4 centimetres was used in this measurement. No measurements were taken when ℓ = 2.5 cm, but other measurements suggest that they should be very close to those obtained with ℓ = 4 cm, particularly above 800 MHz. Also, the results are shown for the case when F_1 was fed and F_2 was terminated with 50 ohms, the same way that S parameters were measured). The impedance characteristic is very tight about a mean impedance of 2.4 + j1.4 ohms. Both the inductance and resistance are high. The resistance can be lowered by moving the feed points closer to the grounding post and the inductance can be tuned out with capacitors on the feed points.

The measured power in the vertically and horizontally polarized waves of Kutzmayteen when feed point F_1 was fed are also shown in Fig. 4.6 (this measurement was explained in section 3.3.4). The horizontal polarization dominates at low frequencies but is quickly overtaken by the vertical polarization above 825 MHz. At the 750 MHz 'resonant' frequency, the horizontal polarization is only 4 dB stronger than the vertical. This strong vertical component around the resonant frequency skews the polarization away from the horizontal. There are a number of possible explanations for this. One explanation is that the brass tube was also radiating. Because the tube was so long (almost one quarter of a wavelength at 750 MHz) there was no guarantee that the entire tube was at ground potential even if the tube was grounded near the patch. In fact, using crude measurements (running a finger along the tube and noting the change in S parameters) it was determined that parts of the tube near the top were not at ground potential (the human body is an RF absorber, so if the S parameters change significantly when parts of the antenna are touched, then those parts are not near ground potential). The tube may therefore have acted like a monopole antenna, radiating various polarizations as seen when looking down at the top of the antenna along a line of sight coincident with the tube axis.

There is also a strong possibility that currents from F_1 were flowing along the bottom of the square patch (when viewed as in Fig. 4.4) causing vertically-polarized energy to radiate from the lower edge. This observation stems from the idea that the edge of the square patch between F_2 and the grounding post may not have been as close to ground potential as necessary when F_1 was fed. The distance between feed point F_2 and the grounding post was close to one quarter of a wavelength at the resonant frequency, which may not have been close enough to force a short circuit along the left edge of the patch. Hence, parts of the right side of the patch, particularly near the bottom, did not experience an open circuit condition and currents may have flowed to other areas of the patch.

As the frequency increases, this behaviour would likely be even more apparent, as the electrical distance between the grounding post and F_2 grows. Moving the feed points closer to the grounding post could alleviate this problem.

For the Clayoquot antenna (shown in Fig. 4.7) a number of modifications were made. The brass tube was replaced by a variable capacitor to remove any radiation at the ground point; also the feed points were moved closer to the grounding post to lower the input resistance and improve the short circuit condition. The grounding capacitor (T9175 from E.F. Johnson™) consisted of twelve half-disk plates (two sets of six) that were interleaved by turning a screw. Interleaving the plates varied the capacitance between 2.5 pF and 17.5 pF at low frequencies. The grounding capacitor connected the microstrip patch to the brass screw which was flush with the top of the dielectric.

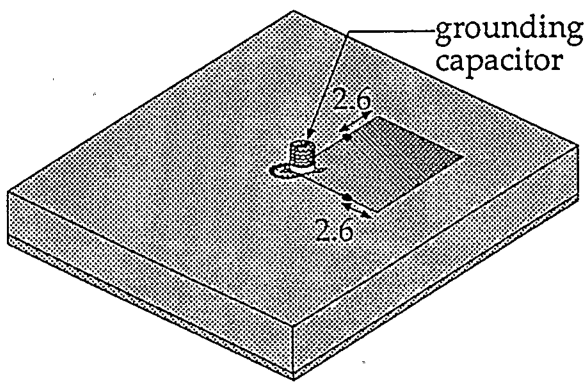

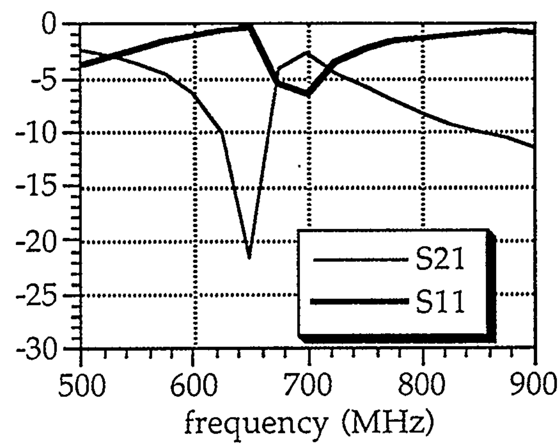

Fig. 4.7 Clayoquot antenna with S parameters. Grounding capacitor is set to 2% interleave.

Measurements were taken with seven different settings of the variable capacitor. The results given in this section are for a setting of roughly two per cent interleave.

Like Kutzmayteen, Clayoquot is very inefficient and the coupling tends to degrade whenever the return loss improves (see Fig. 4.7). In fact, Clayoquot is even less efficient than Kutzmayteen. At a 'resonant' frequency of 675 MHz, the power sum of the return loss and coupling is lowest at -2.33 dB. This compares with -2.85 dB for Kutzmayteen. The input impedance of Clayoquot with 2% interleave of the grounding capacitor is shown in Fig. 4.8. The mean input impedance is 1.0 + j2.1 ohms. Comparing this figure with a mean input impedance of 2.4 + j1.4 ohms for Kutzmayteen indicates that moving the feed points closer to the grounding post did decrease the input resistance as expected but at the expense of increasing the input inductance. As a result, the impedance match is weaker. Adding capacitors to the feed points should move the impedance curve towards the centre of the Smith chart and improve the match.

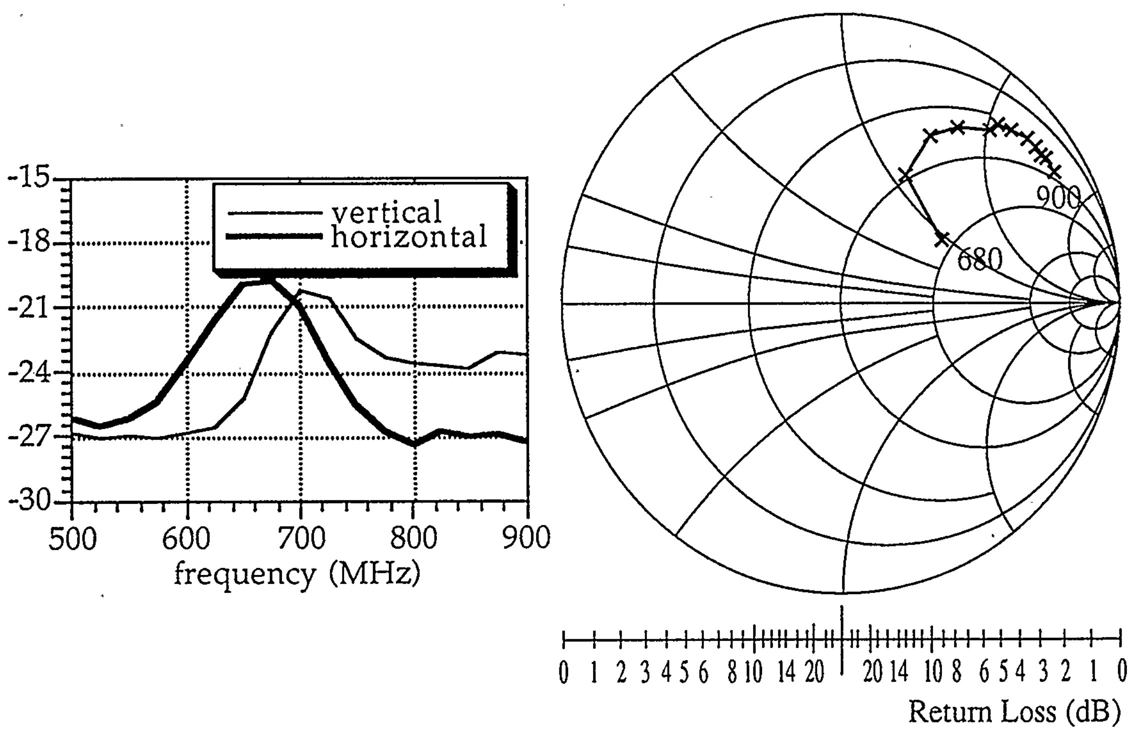

Fig. 4.8 Polarization and input impedance of Clayoquot (interleave = 2%).

The graphs of measured power in the vertically and horizontally polarized waves of Clayoquot when feed point F_1 is fed (Fig. 4.8) show a similar pattern to those of Kutzmayteen. The horizontal polarization dominates below the 'resonant' frequency but is quickly overtaken by vertical polarization at higher frequencies. In fact, the frequency at which the power in the vertical and horizontal polarizations cross over is very close to the 675 MHz 'resonant' frequency, indicating that the polarization at this frequency is closer to 45° than it is to horizontal. This measurement downplays the idea that radiation from Kutzmayteen's brass tube significantly distorted the antenna's performance and gives further weight to the second idea, which is that the assumption that the patch edge connecting F_2 to the grounding post was a short circuit is not valid.

The final version of the square patch antenna is Carmanah, illustrated in Fig. 4.9. A variable capacitor similar to the grounding capacitor was connected between each feed point and the square patch. For the sake of maintaining antenna symmetry, the two feed point capacitors were always set to the same value. Measurements at 4 different settings were taken while the grounding capacitor was fixed at 2% interleave. The best results were observed with the minimum capacitance setting (ie. where the plates were rotated so they were not interleaved).

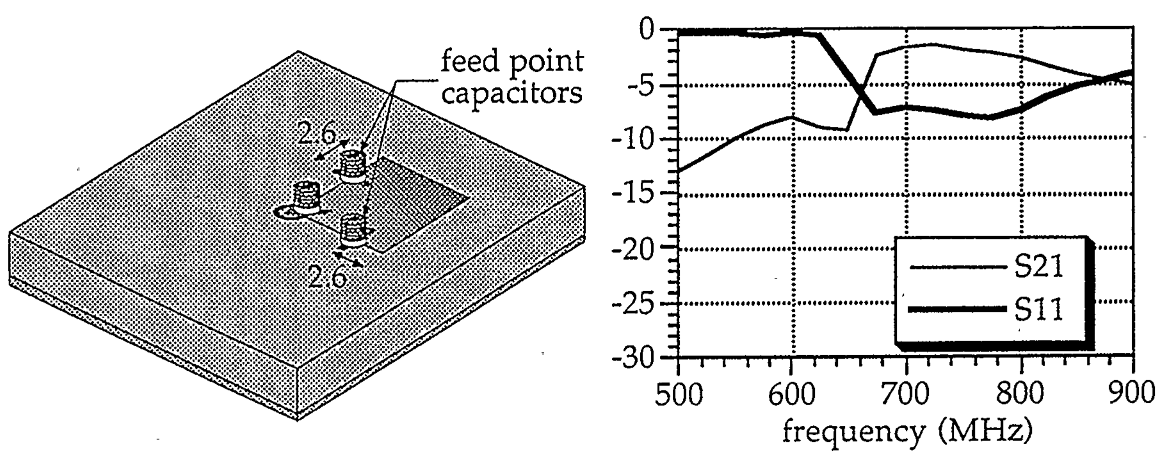

Fig. 4.9 Carmanah antenna with S parameters. Feed point capacitors are at a minimum setting, and the grounding capacitor is fixed at 2% interleave.

The effect of adding a capacitor to each feed point is to bring the impedance plot down from the top of the Smith chart, as shown in Fig. 4.10 (note that the lower frequency on the impedance measurements is now 600 MHz, not 680 MHz. As before, measurements were taken every 20 MHz). This lowered the return loss above 650 MHz (see Fig. 4.9) resulting in an improved efficiency over previous designs. At 650 MHz, the power sum of the return loss and coupling is now lowest at -3.95 dB.

Unfortunately, the impedance moved down the chart faster at the lower frequencies than at the high frequencies, causing the impedance characteristic to spread out. A single variable capacitor was a poor choice for a broad band matching circuit.

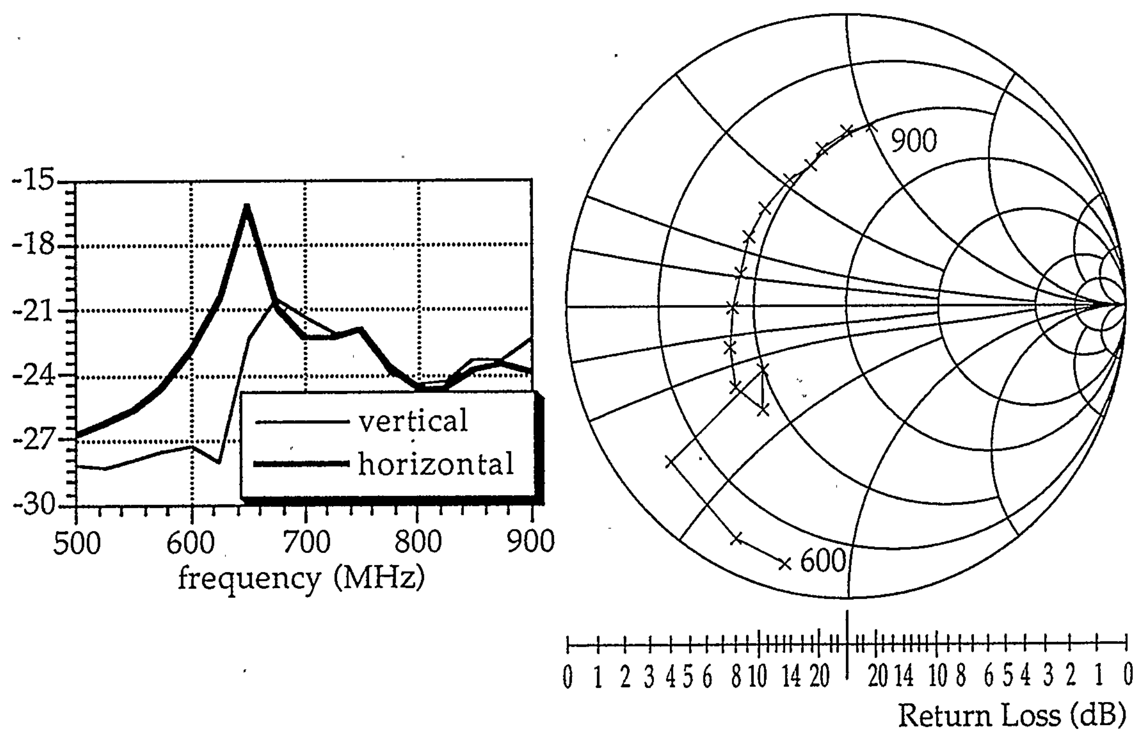

Fig. 4.10 Polarization and input impedance of Carmanah (interleave = -10%).

An interesting feature of the input impedance plot is that it has two regions of constant resistance which suggests that the antenna was acting like an impedance transformer. At the low frequencies (600 to 640 MHz), this resistance is very low (less than 10 ohms), suggesting that feed point F_1 was strongly coupled to the grounding post. At the middle and higher frequencies (680 to 900 MHz) the resistance is higher (near 25 ohms), suggesting that the strong coupling between the feed points (as illustrated in Fig. 4.9) is transforming the 50 ohm impedance at F_2 down at F_1. This further reinforces the argument that the edge of the patch between the ground post and the secondary feed point is not at ground potential.

Carmanah is the first antenna where horizontal polarization was not significantly overtaken by vertical polarization. As shown in Fig. 4.10, the horizontal polarization is strongest at the 650 MHz 'resonant' frequency, where it is more than 6 dB higher than the vertical polarization. Above this frequency, both the vertical and horizontal polarizations are very close. This indicates that the wave from the antenna is either linearly polarized at an angle near 45° or circularly polarized (no tests were done to determine whether linear or circular polarization was present, but circular polarization is unlikely). Notice that the horizontal and vertical polarizations overlap in the same frequency range where the coupling between feed points is strong (as shown by comparing Figs. 4.9 and 4.10).

It is possible that the variable capacitors were radiating, but because of their electrically small size, the radiation is likely negligible.

Months after the measurements of the square patch antenna were made, there was some question as to whether they were taken in the proper frequency range. Although the antenna was designed to operate between 829 MHz and 870 MHz, it may have actually worked above 900 MHz (the highest frequency that measurements were taken at). This quandary was aggravated by the fact that the triangle patch antenna (discussed in section 4.2) was designed to operate between 816 MHz and 855 MHz but resonated near 1.1 GHz. The U patch antenna, on the other hand, offers some comfort in that it operated at 856 MHz, very close to the 802 MHz to 842 MHz design range. Nevertheless, the question needed to be addressed and so the Clayoquot version of the square patch antenna was reassembled and measured over a broader frequency range. The results, measured by the HP 8510C Network Analyzer, are shown in Fig. 4.11.

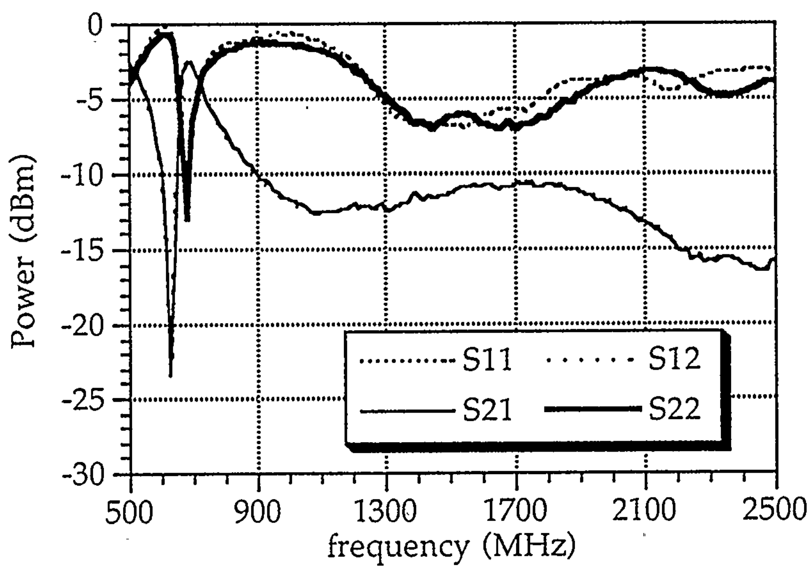

Fig. 4.11 S parameters of Clayoquot antenna over a wider frequency range.

There are no interesting features in the S parameters of Clayoquot between 900 MHz and 2500 MHz, which verifies that the original measurements were made in the proper frequency range. Neither of the return losses S_{11} nor S_{22} goes below -7.5 dB in this range, but more importantly, there is no sharp dip to indicate a resonance.

The results shown in the 500 MHz to 900 MHz range of Fig. 4.11 are very similar to the measurements shown in Fig. 4.7, with a few minor exceptions. The discrepancies between measurements are largely due to the finer resolution of the second measurement, where S parameters were measured every 5 MHz. The S parameters given in Fig. 4.7 were measured every 25 MHz.

All four S parameters are given in Fig. 4.11. The similarities between S_{11} and S_{22} and between S_{12} and S_{21} (they are nearly identical) indicate the symmetry of the square patch antenna. Thus, it was not necessary to measure all four S parameters in previous measurements.

4.1.4 Conclusions

The operation of the square patch antenna is based on the assumption that at the resonant frequency, the 'dead' port and the grounding post are both at a low potential and therefore force one edge of the patch to be short circuited. At this frequency, the opposite edge is one quarter of a wavelength away; hence, the structure should resonate. Because the opposite edge sees an open circuit in the direction of the short-circuited edge, current on the open circuited edge can only travel along the open-circuited edge (see Fig. 4.4). This current should then create an electric field between the open-circuited edge and the ground plane, exciting a horizontally-polarized wave.

Unfortunately, this assumption does not hold. S parameters, impedance plots and polarization measurements all indicate that the three versions of the square patch antenna radiated inefficiently with an unintended polarization. The strong coupling between ports and the grounding post was the main cause of these problems. None of the design improvements were successful in weakening the coupling, so the design was not pursued any further.

It is recommended that if any more work is to be done on the square patch antenna, a method of isolating the ports and the grounding post from each other must be found.

4.2 Triangle Patch Antenna

4.2.1 General Description

Following the results of the square patch antenna, a new antenna was designed to better isolate the feed points. The triangle patch antenna, shown in Fig. 4.12, consists of two copper, triangular patches atop a thick dielectric material that is glued onto a copper ground plane. The dielectric material used is different than that of the square patch antenna, so some of the dimensions have changed. Like the square patch, the triangle patches are made of copper tape.

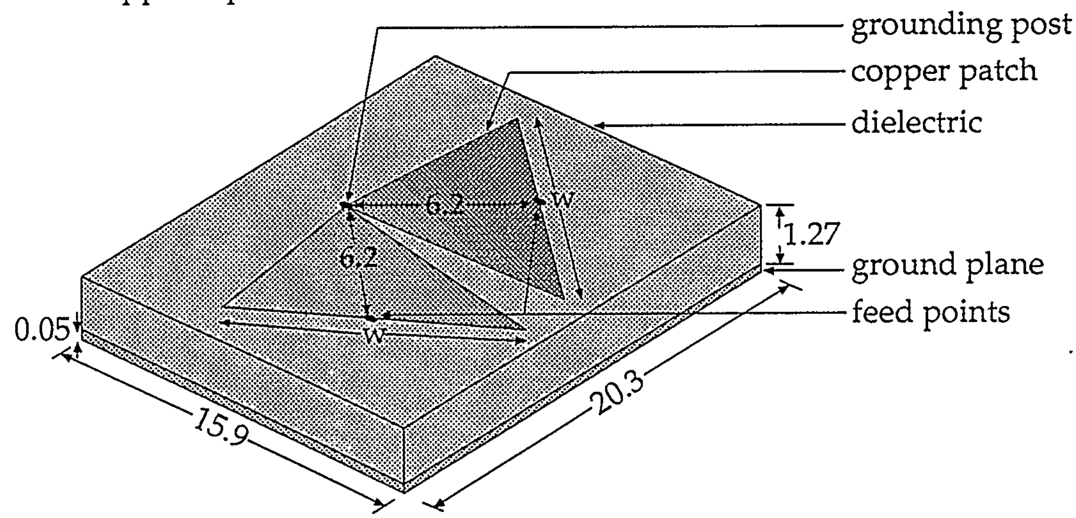

Fig. 4.12 Top view of triangle patch antenna (all dimensions are in centimetres).

The triangles are oriented so that their bases are orthogonal and their apexes meet at a common grounding post. Each patch is fed at the centre of its base. Each feed point is a thick copper wire (2 mm in diameter) that extends through the dielectric to an SMA connector underneath the antenna (see Fig. 4.13). The grounding post is a similar copper wire (a thick brass screw is not necessary) that is soldered directly to the ground plane. The distance between each feed point and the grounding post (i.e. the height of each triangle) is a quarter of a wavelength at the resonant frequency. With a height of 6.2 cm, the resonant frequency of each triangle is designed to be between 816 MHz and 855 MHz, as mentioned near the end of section 4.1.3. The base width, *w*, is adjustable.

Although this design should better isolate the feed points, it requires up to twice the area of copper compared to the square patch antenna.

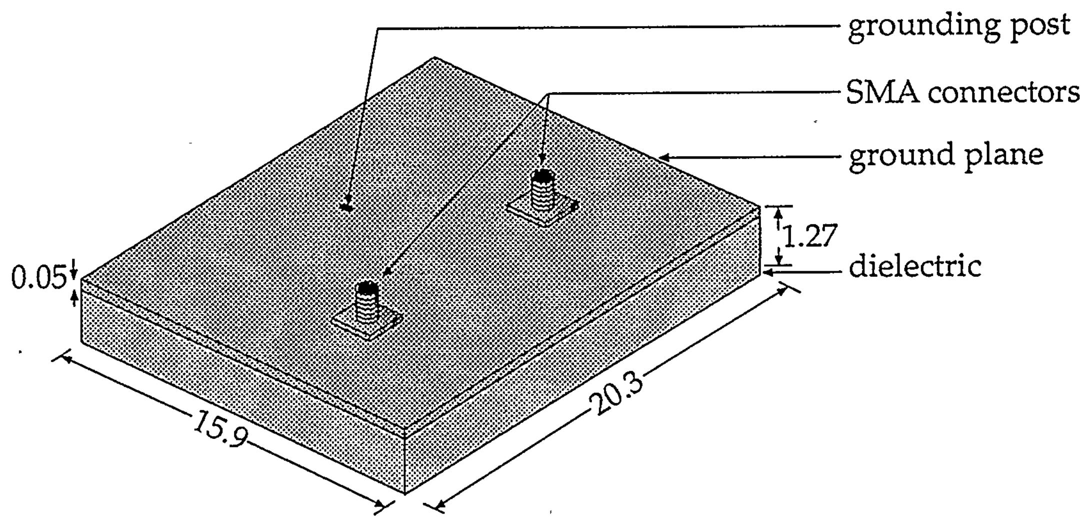

Fig. 4.13 Bottom view of triangle patch antenna (all dimensions are in centimetres).

4.2.2 Theory of Operation

Like the square patch antenna, the triangle patch antenna works on the principle that two edges, orthogonal to each other, each resonate with the ground plane beneath it, creating two orthogonally-polarized slot antennas.

Unlike the square patch, however, the feed points are physically separated by a gap in the copper tape. This gap eliminates most of the current paths between the feed points, thereby weakening the coupling between them. It also eliminates the condition that one feed should be at a low impedance and close to the grounding post while the other feed is in operation.

Because the electrical distance between each feed point and the grounding post is a quarter of a wavelength at the resonant frequency, each feed point should see an open circuit impedance in the direction of the grounding post. Therefore, current from the feed point cannot flow towards the ground post and must instead flow along the base of the triangle. This action excites an electric field between each base and the ground plane beneath it, radiating a linearly-polarized wave. Because the triangle bases are orthogonal, the two radiated waves are orthogonally polarized so that the antenna uses polarization diversity.

4.2.3 Results

The triangle patch antenna underwent a number of modifications, some of which are shown on Figs. 4.14 - 4.16, 4.18 and 4.19. A diagram of the copper patches of each antenna is shown together with its measured S parameters.

For the first antenna, newt 1, the two triangles were not separated. The coupling between ports is poor below 800 MHz and the return loss is poor above this frequency. The antenna is therefore very inefficient at all frequencies.

By separating the two triangles (newt 3) the coupling improved substantially, especially above 800 MHz. The return loss, however, is still high. It can be modified by cutting each triangle in a way that moves the feed point away from the centre of its base, thereby changing the input impedance. This was performed to make newt 5. The side of each triangle to the right of the feed point was cut closer to the feed point and the corner on the right side was cut off. Due to this latest modification, newt 5 was not symmetrical about a vertical line containing the ground post.

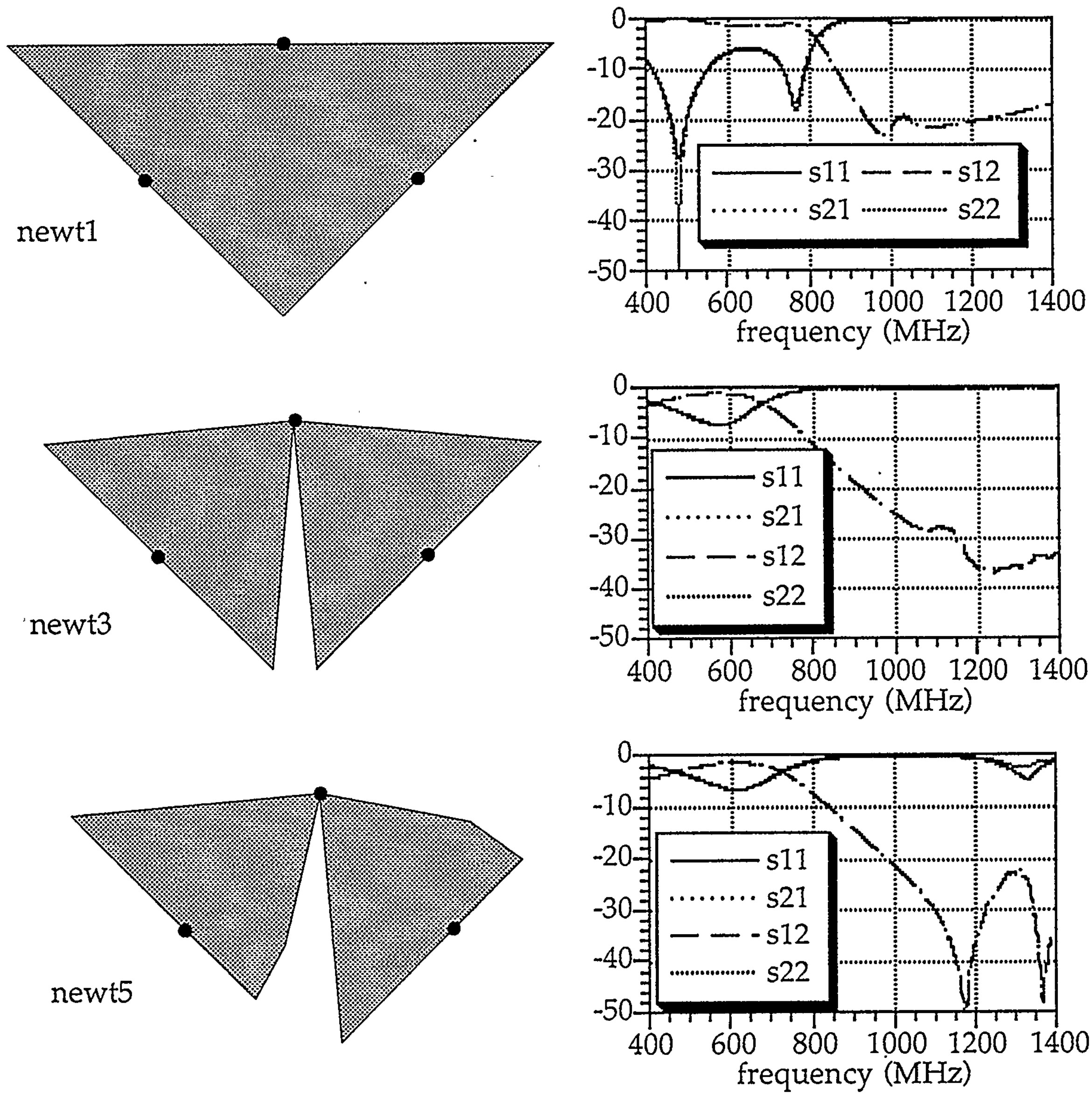

Fig. 4.14 Top view and measured S parameters of newt 1, 3, and 5.

A slight dip in the return losses of newt 5 near 1325 MHz suggests that both patches were resonating here. The return losses are not very good, but newt 5 represents a significant step forward in the design. The coupling improves remarkably at 1175 MHz and 1365 MHz but unfortunately rises near the two resonant frequencies. This rise is problematic as it tends to reside near the resonant frequency of the second patch in the remaining antennas. In future work, a way of eliminating this rise or moving it away from the resonant frequencies should be explored. Maintaining the symmetry of the antenna may accomplish this.

As explained in section 4.2.2, the operation of the antenna relies on the principle that an open circuit exists at the feed point in the direction of the ground post. This ensures that current from the feed point cannot flow towards the ground post and must instead flow along the base of the triangle. Maintaining the open circuit condition is difficult when there is so much copper area. With so many possible current paths, the feed point will see many impedances in the general direction of the ground post. The resulting impedance may therefore never be an open circuit.

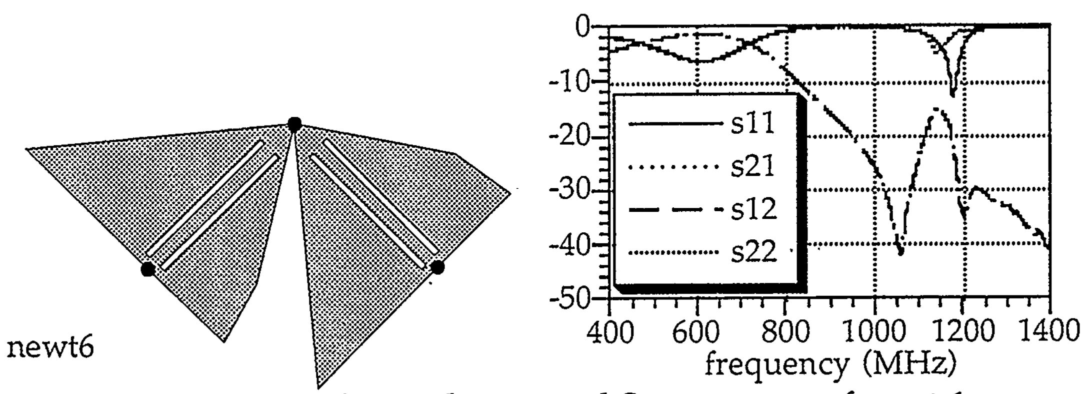

Fig. 4.15 Top view and measured S parameters of newt 6.

In order to force the open circuit condition, a transmission line was carved into each patch between its feed point and the ground post. As shown in Fig. 4.15, newt 6 had two long slots cut into each patch. The slots were situated on either side of the direct path between the feed point and the grounding post, making this path a transmission line.

Both patches appear to be radiating much better. Patch 1 has a return loss of -13.04 dB at 1177.5 MHz and patch 2 has a return loss of -5.01 dB at 1143.8 MHz. The antenna's asymmetry created the differences in centre frequency and return loss for the two patches.

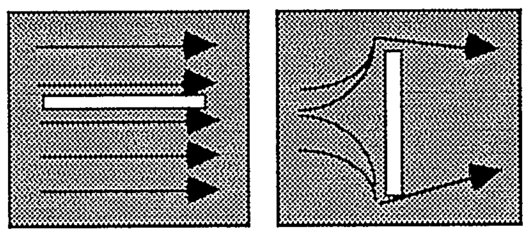

Fig. 4.16 The effect of a thin slot in a conducting surface on current distribution (arrows indicate current flow).

In the remaining modifications of the antenna, it was found that widening the two slots on either side of the feed-to-ground transmission line on each patch and adding other slots parallel to this line had a marked effect on the antenna performance. Adding slots perpendicular to this line, however, had very little effect. From these observations it was easy to determine how the current was flowing on the patches and how the slots affected this flow.

As shown in Fig. 4.16, a thin slot cut into the surface of a microwave antenna generally has little effect on the current distribution (and hence the radiation parameters) if it is cut in the direction of the current (indicated by arrows). If this slot is cut orthogonal to the current flow, however, the current has to redistribute and the antenna's radiating properties change. It is therefore likely that the current is flowing from the feed points out to the sides of the patches of newt 6.

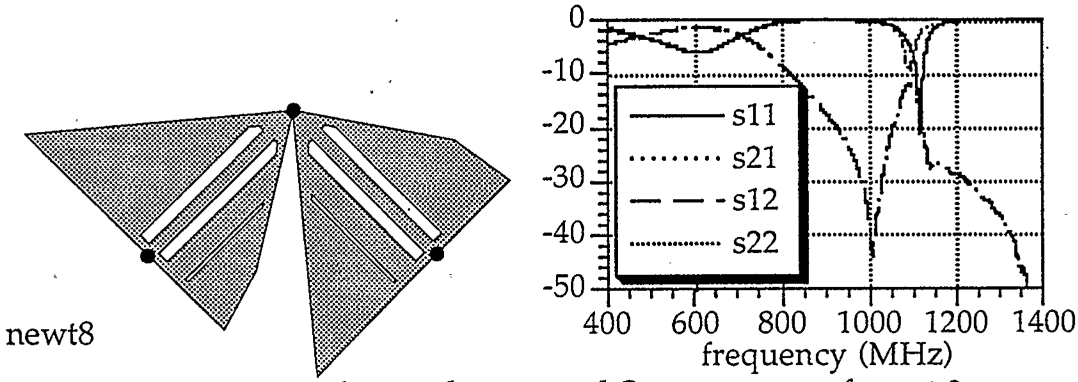

Fig. 4.17 Top view and measured S parameters of newt 8.

When slots are cut parallel to the feed-to-ground line as with newt 8, the current cannot flow to the sides of the patches in the same way. Some of it will flow beside the slot to the ground post, but more of it will flow closer to the base of the patch.

The added current along the base gave rise to a stronger electric field between the base and the ground plane, and the patches therefore radiated more efficiently, as shown in Fig. 4.17. The return losses are -21.11 dB and -9.39 dB at the respective centre frequencies of patch 1 and patch 2. Unfortunately, the coupling increased to -11.85 dB at the centre frequency of patch 2, but the overall efficiency (neglecting losses) improved over that of newt 6.

On newt 9, extending the thin slot of each patch to the inside edge severely degraded its performance. The modifications broke the current path along the inside edge, preventing the currents on the outside of the thin slot from flowing to ground. As seen on Fig. 4.18, the coupling has risen sharply at 1032 MHz, reducing the antenna's efficiency. A plausible explanation for this is that the currents on the outside of the thin slot, lacking a path to ground, have established an electric field in the gap between the triangle patches.

The S parameters of newt 11 are very close to those of newt 8, which as was explained earlier, is likely because currents were flowing in the direction of the new slots and were therefore unchanged.

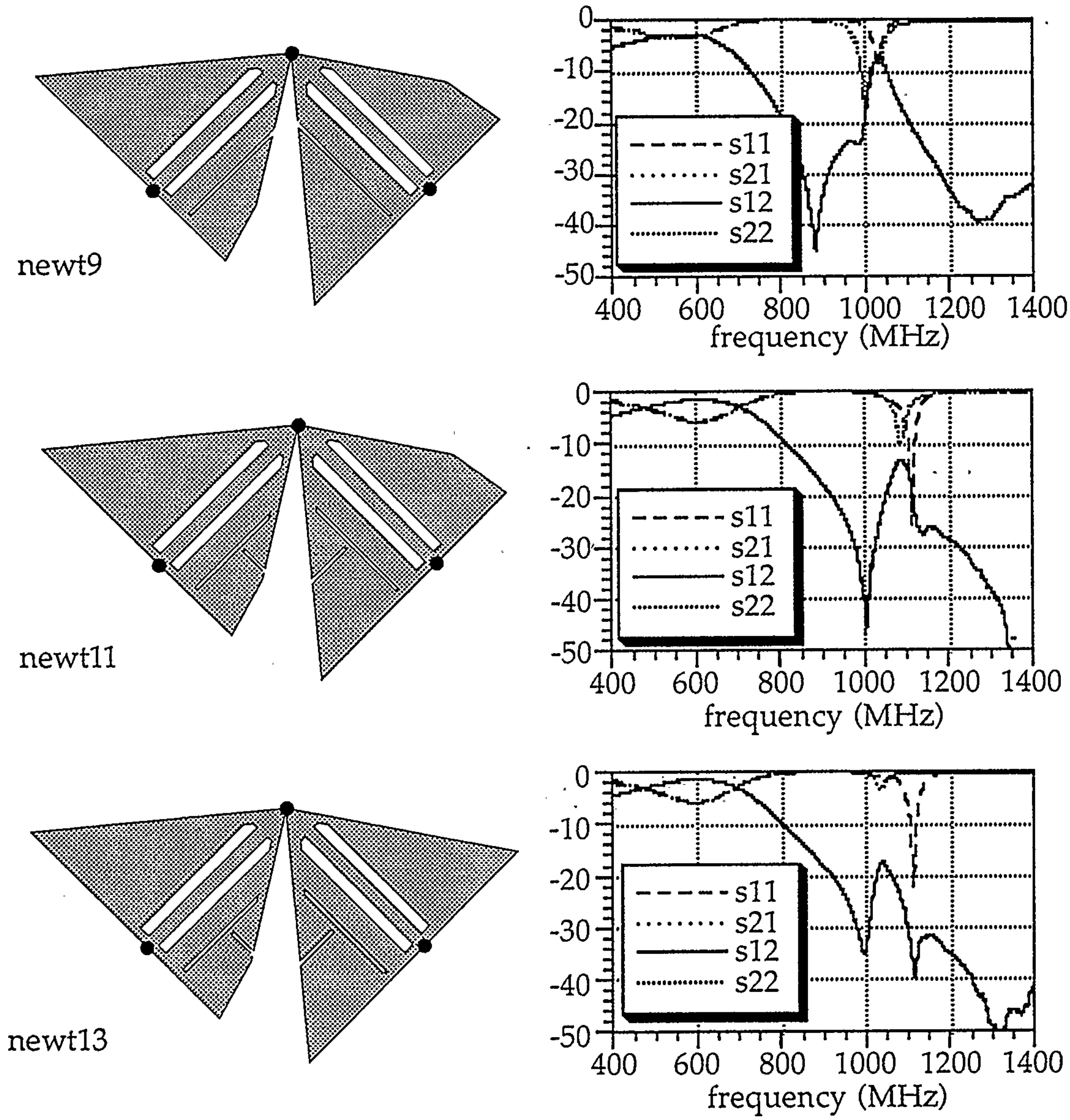

Fig. 4.18 Top view and measured S parameters of newt 9, 11 and 13.

Soldering a corner back onto the second patch (newt 13) resulted in lower coupling between the feed points but nearly destroyed the resonance of the second patch. The resonance of the first patch was not significantly affected. This corner was removed again for all subsequent modifications.

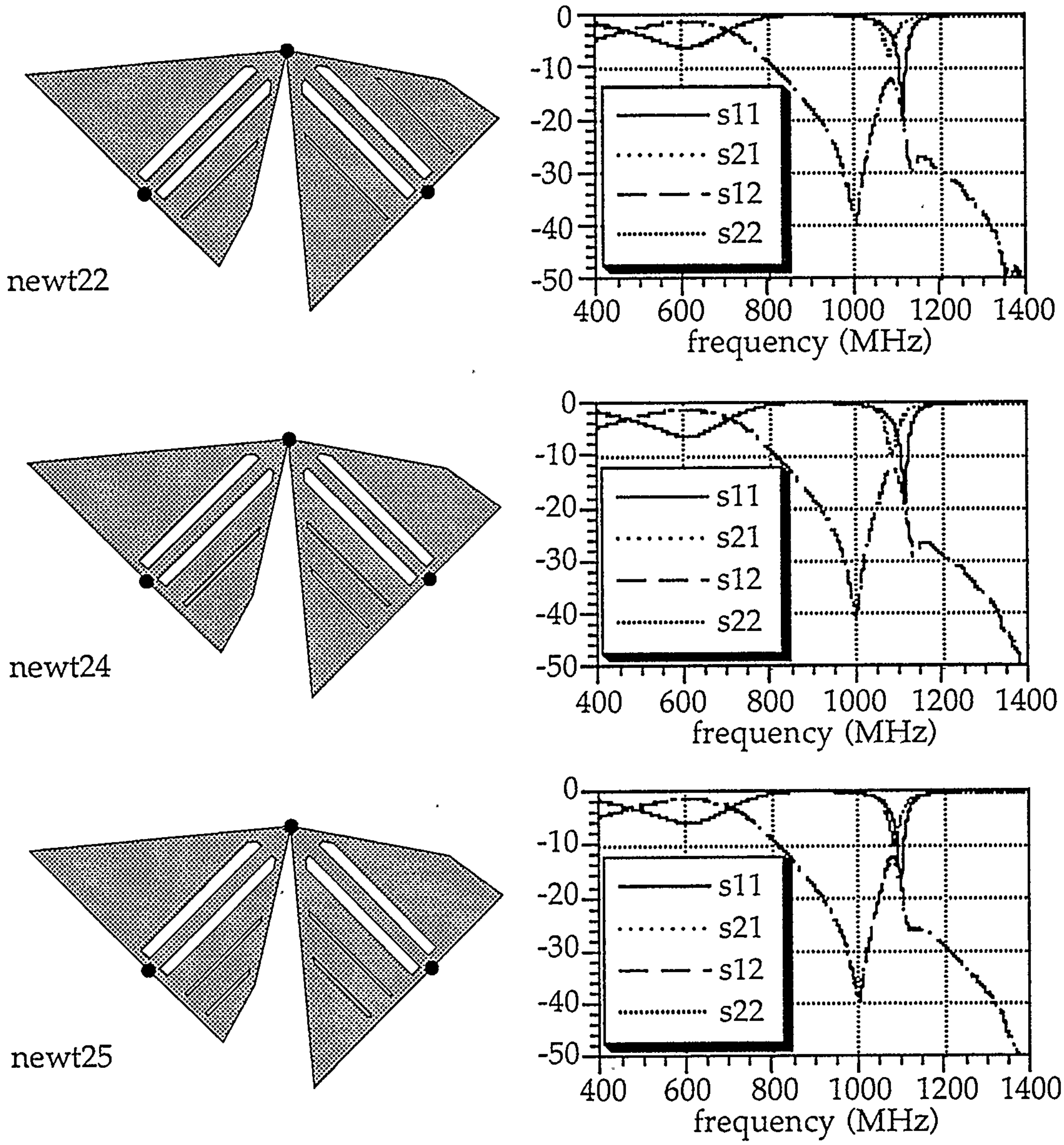

Fig. 4.19 Top view and measured S parameters of newt 22, 24 and 25.

For newt 22, 24 and 25, more slots were cut parallel to the feed-to-ground line. Compared to newt 8, each slot typically lowered the resonant frequency of the patch it was cut into. Slots cut in the area between the feed points (newt 24 and 25) also tended to improve the impedance matching (return loss) of the second patch while a slot cut outside this area (newt 22) worsened the matching. To further illustrate this, the measurements of newt 8, 22, 24 and 25 are tabulated for comparison.

Of the eleven antennas studied here, newt 25 has the best return loss of the second patch and the closest spacing of the resonant frequencies. The centre frequencies of the two patches of newt 25 are 13.8 MHz apart. They could be brought closer together by cutting more slots in patch 1 parallel to its feed-to-ground transmission line to lower its resonant frequency or by shortening the height of the second patch to raise its resonant frequency.

Antenna	centre frequency (MHz)		return loss (dB)	
	Patch 1	Patch 2	Patch 1	Patch 2
newt 8	1115.0	1091.3	-21.11	-9.39
newt 22	1113.8	1083.8	-18.98	-7.87
newt 24	1113.8	1085.0	-19.41	-10.11
newt 25	1098.8	1085.0	-18.66	-10.52

Table 4.1 Centre frequencies and return losses of newt 8, 22, 24 and 25.

The resonant frequencies of newt 25 are not within the useful range for the 800 MHz or 1.7 GHz cellular systems, but they can be adjusted by changing the size of the antenna.

The first patch had a bandwidth of 15.7 MHz. At its resonant frequency, it coupled -17.61 dB of energy to patch 2. Patch 2 had 8.7 MHz of bandwidth and at its resonant frequency it coupled -12.19 dB to patch 1 (the definition of bandwidth used throughout this thesis is that range of frequencies where the standing wave ratio is less than or equal to two, or, in other words, where the return loss is less than or equal to -9.54 dB). These bandwidths are too narrow for this antenna to be useful in current cellular systems. In the 800 MHz cellular band for instance, a receiving antenna should have at least 25 MHz of bandwidth. The bandwidth can be improved by using a thicker dielectric or a lower dielectric constant. The coupling between antennas is worse than the -20 dB desired to keep the patches comfortably isolated.

The radiation pattern and polarization of newt 25 were not measured due to time constraints.

4.2.4 Conclusions

The triangle patch antenna, although larger than the square patch antenna, performed much better. In theory, both antennas operate on the same principle; the quarter-wavelength size of each mode creates a resonant structure and because one end is grounded, the currents concentrate on the opposite edge, radiating a linearly-polarized wave.

There is, however, one fundamental difference. With the triangle patch antenna, a gap existed between the feed points which was intended to physically isolate them. According to experimental results, the feed points were in fact better isolated than those of the square patch antenna, particularly at higher frequencies.

Cutting thin slots into each triangle patch in a direction parallel to the direct path between the feed point and the grounding post greatly improved the return loss. The slots formed transmission lines within the patches which served two uses. First, they reduced the copper area on the triangles, thus creating less paths for current flow and therefore maintaining an open circuit condition at the feed points. Second, they forced the current to flow only in certain directions, and because of the open-circuit condition, most of the current flowed along the base edge of each triangle, increasing the electric potential between each base edge and the ground plane.

4.3 U Patch Antenna

4.3.1 General Description

The most general version of the U patch antenna is shown in Figs. 4.20 and 4.21. Two rectangular copper patches of the same size rest atop a thick dielectric material which is glued to a copper ground plane. Like the previous antennas, the patches are made of copper tape. There is also copper tape along the entire front side of the antenna, grounding the front edges of the rectangular patches. This antenna is called a U patch because the two rectangular patches and the grounded side form the shape of the letter 'U.' A gap of width g exists between the rectangular patches, forming a rectangular slot. The feed points on either side of the gap on the top of the 'U' are copper wires (1 mm in diameter). Each is soldered at one end to a rectangular patch and extends through the dielectric medium and the ground plane to SMA connectors at the other end. The length of each copper patch is 6.3 cm, equivalent to one quarter of a wavelength at the resonant frequency*. Its width, w, is variable.

The U patch antenna has a more complicated feed arrangement than the square or triangle patch antenna. Rather than being fed separately, the two feed points are fed together in phase or 180° out of phase. This phasing is easily provided by attaching a hybrid circuit to the SMA connectors of the antenna. The hybrid circuit used for this antenna was the Anzac™ H-183-4, illustrated in Fig. 4.22. It operates like two power splitters (one from port A, one from port B), except that one splitter also provides a phase reversal in one output. When fed

* This length is slightly larger than the 6.2 cm length of the triangle patches, only because the extra length was needed in case there were errors in cutting the copper tape. Afterwards, the author did not bother removing the extra length, which only means that the antenna is designed for a slightly smaller frequency.

into port B, a signal is split, with equal amplitude and phase, to ports C and D. If port A is fed instead, the signals at ports C and D are equal in amplitude, but the signal at port D is delayed 180° with respect to the signal at port C. Ports A and B are isolated from each other and port C is isolated from port D.

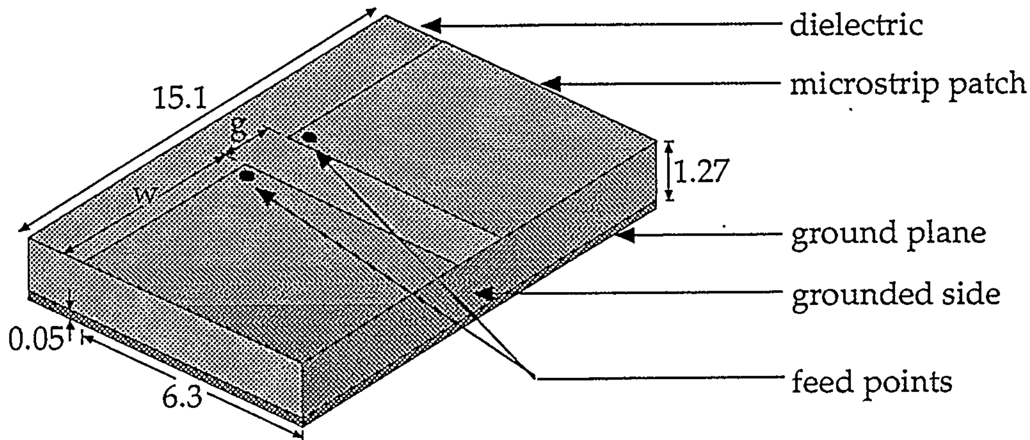

Fig. 4.20 Top view of U patch antenna (all dimensions are in centimetres).

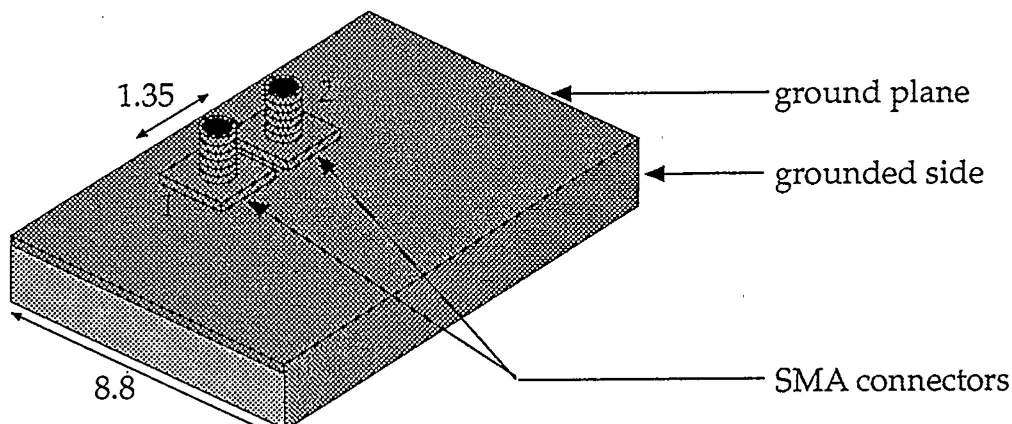

Fig. 4.21 Bottom view of U patch antenna (all dimensions are in centimetres).

The Anzac™ H-183-4 has a frequency range of 30 MHz to 3 GHz. On the HP 8510 Network Analyzer, data on the Anzac™ hybrid was measured for the 45

MHz to 1 GHz frequency range. When port A was fed, the maximum phase error between ports C and D was 0.5° and the maximum signal level difference was 0.103 dB. When port B was fed, ports C and D had a maximum phase error of 0.6° and a maximum signal level difference of 0.0662 dB. The maximum coupled power between ports A and B was -32.93 dB. For ports C and D, the maximum coupled power was -36.08 dB.

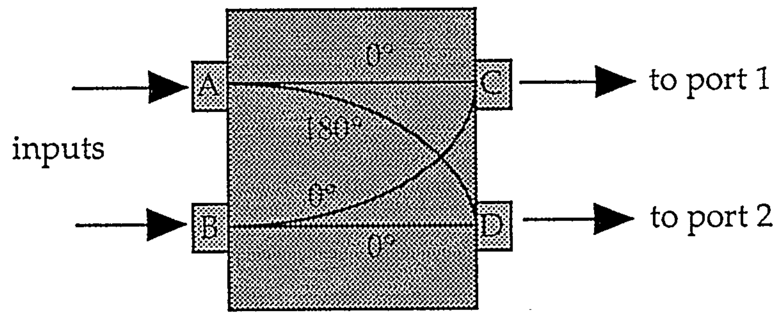

Fig. 4.22 Anzac™ H-183-4.

Ports C and D of the hybrid were connected to ports 1 and 2 of the antenna, respectively, via two short lengths or rigid coax. As measured on the HP 8510 Network Analyzer, the maximum differences in phase and amplitude out of the two lines were 0.809° and 0.017 dB respectively in the 45 MHz to 1 GHz frequency range.

4.3.2 Theory of Operation

The idea for the U patch antenna evolved out of some observations from the results of the triangle patch antenna, although the methods of operation of the two antennas are quite different. The slot antenna created between the base edge of each triangle patch and the ground plane radiated well, but the gap between the patches radiated also, increasing the coupling between feed points and therefore reducing its radiation efficiency. If the gap is used to enhance the antenna's performance rather than degrade it, the resulting antenna will be more efficient. In other words, it is desirable to have a diversity antenna where one polarization is created between a patch edge and ground, and the other polarization is created across the gap.

This can be achieved by cutting a gap through the centre of one triangle patch and removing the other patch, as shown in Fig. 4.23. To operate this antenna, the feed point at the base of the triangle is split into two feeds which are placed on either side of the gap. The U patch antenna is created from this modified triangle patch by spreading the grounded end out. This ensures that the top edges of the patch are at a constant distance of one quarter of a wavelength from ground potential.

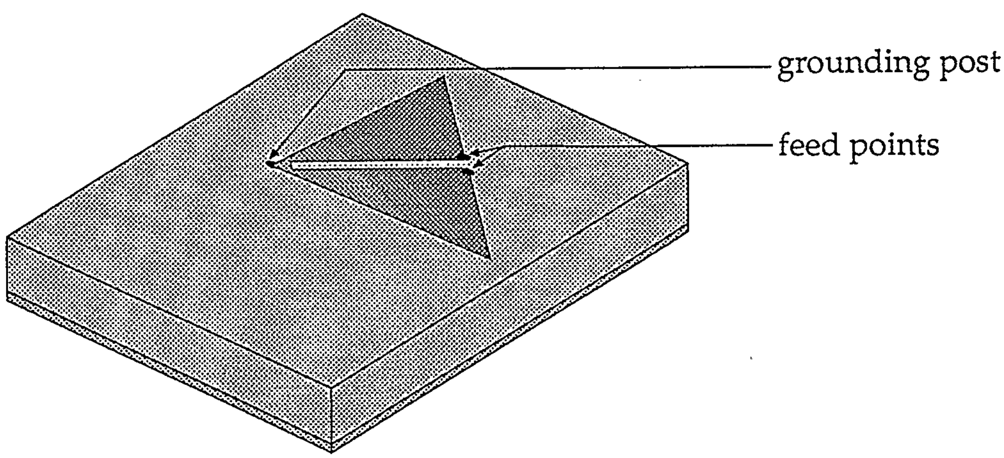

Fig. 4.23 Triangle antenna utilizing the gap.

As stated earlier, the two modes of the antenna are provided by exciting the feed points in phase or 180° out of phase. When they are excited in phase, an electric field is created across a slot between the top edges of the 'U' and the ground plane, as shown in Fig. 4.24. In this case, the radiated field has a polarization that is parallel to the direction of the gap between the patches.

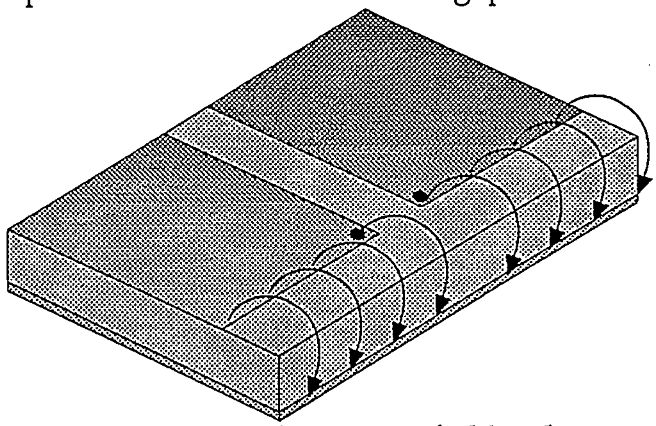

Fig. 4.24 U patch antenna fed in phase.

When the feed points are excited out of phase, the two patches are at different potentials. Therefore, an electric field is excited across the gap between them, as shown in Fig. 4.25. The radiated field from this gap has a polarization that is orthogonal to that of the radiated field when the feed points are excited in phase.

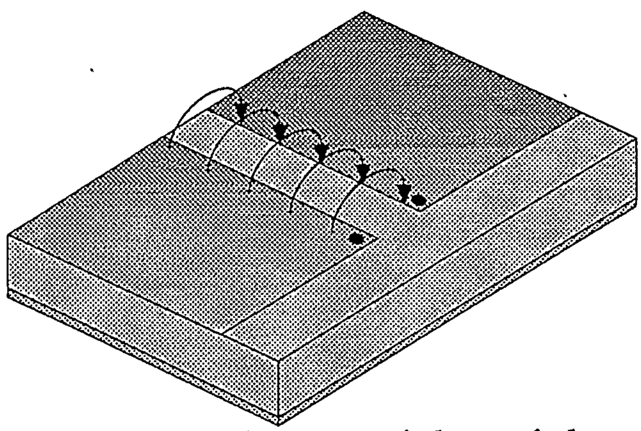

Fig. 4.25 U patch antenna fed out of phase.

Because of the design of the U patch antenna, its two modes are inherently isolated. For example, when the feed points are excited in phase, both patches are at the same voltage potential, so no electric field can exist across the gap, as it does when the feeds are excited out of phase. For the case when the feeds are excited out of phase, electric fields can exist between each patch and the ground plane, but because the fields of one patch are 180° out of phase with the fields of the other, they will cancel each other out before they propagate into the far field.

For ease of description, the gap between the patches is called "slot 1" and the slot between the top edges of the 'U' and ground is called "slot 2."

4.3.3 Results

Many variations of the U patch were studied. Some of them are shown in Figs. 4.26, 27, 29 and 30. A perspective view of each antenna is shown together with its four measured S parameters. Because the input signals were fed through the hybrid circuit before reaching the antenna, the definitions of these S parameters differ slightly from those of the previous antenna designs. Parameter S_{11} is the return loss at port A of the hybrid, S_{22} is the return loss at port B, S_{21} is the coupling from A to B and S_{12} is the coupling from B to A.

Tsitika is the unmodified antenna described by Figs. 4.20 and 4.21. As predicted, the coupling is low over the entire 400 MHz to 1400 MHz range. This antenna is a very inefficient radiator, however. The best return loss is -6.83 dB at port A and -4.39 dB at port B. Impedance matching reduces the return loss. It can be achieved by moving the locations of the feed points on the conductors or by connecting matching circuits to the feed points. The former method is more difficult because more holes have to be drilled through the ground plane, the dielectric and the copper patches. Also, these holes could have undesirable effects on the antenna performance. Matching circuits avoid these problems and can be simple to build. Two quarter-wave transformers were designed for this antenna, one of which is shown in Fig. 4.27. The quarter-wave transformer is a microstrip transmission line with a length of one quarter of a wavelength at the resonant frequency and a width determined by the desired matching impedance and the physical parameters of the line [4.1, 4.2].

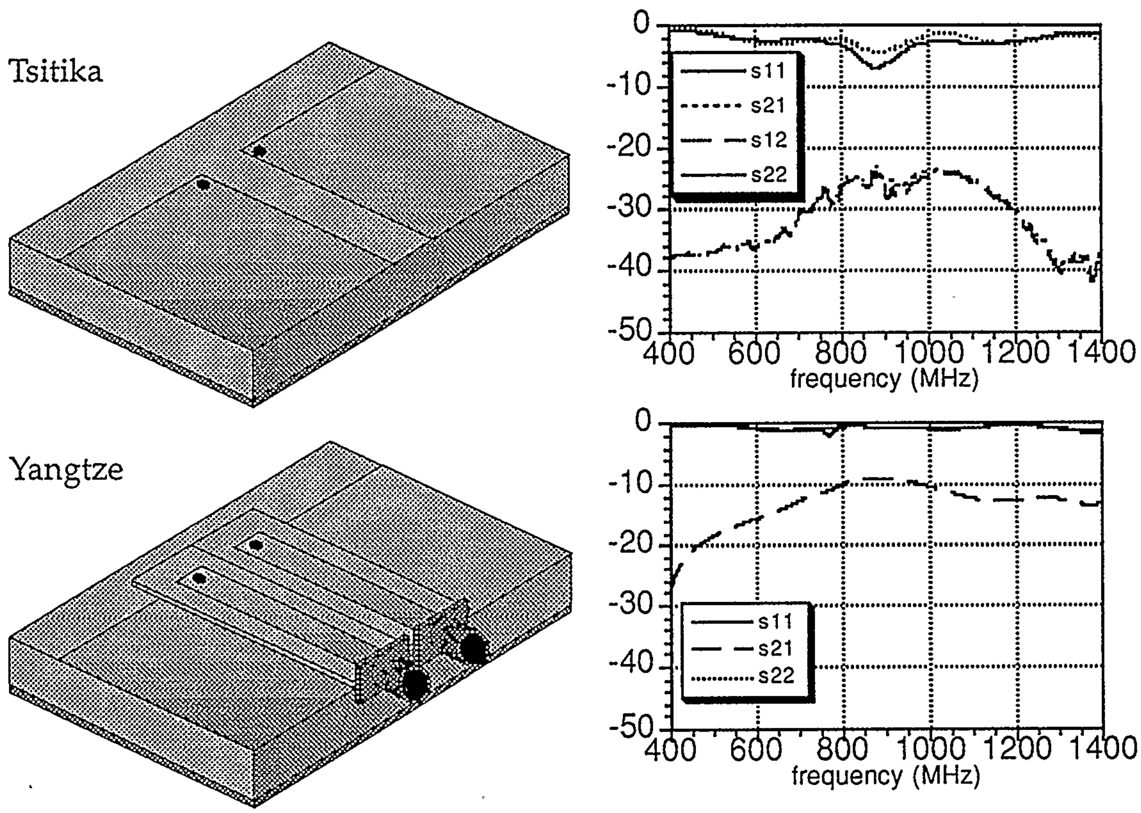

Fig. 4.26 Diagrams and S-parameters of Tsitika and Yangtze.

To provide impedance matching near the resonant frequency, the impedance of each line was set to the geometric mean of the antenna's total input impedance and the 50 ohm system impedance. The total input impedance of the antenna was defined as the arithmetic mean of the input impedances at ports A and B. At the resonant frequencies, the input impedances are purely resistive and can be calculated from the return loss measurements. Return losses of -6.83 dB and -4.39 dB give input impedances of 32.82 ohms at port A and 23.32 ohms at port B, respectively [4.3], for a total antenna impedance of 28.07 ohms. The quarter-wave transformer therefore needs an input impedance of 37.46 ohms to match the antenna to 50 ohms at resonance. However, when Tsitika was first tested, an error was made and the total antenna impedance was calculated to be 13 ohms, giving a quarter-wave transformer impedance of 25.5 ohms.

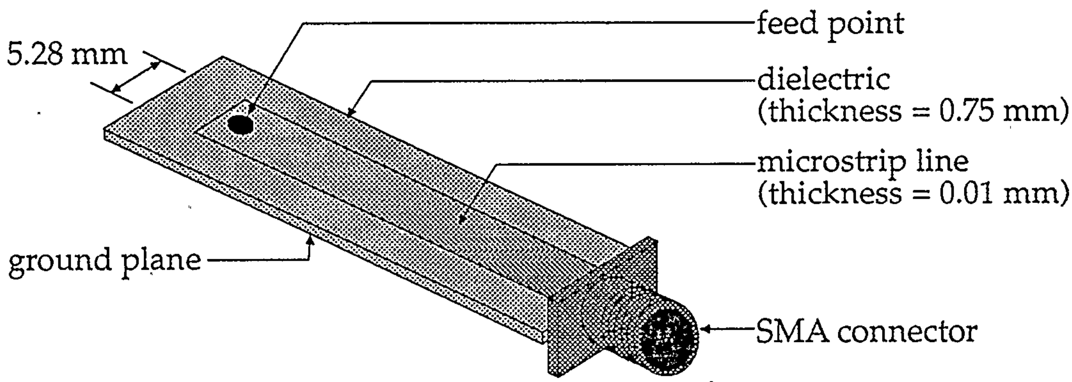

Fig. 4.27 Quarter-wave transformer.

Using a printed circuit board having a relative dielectric constant of 2.53, a dielectric thickness of 0.75 mm and a copper thickness of 0.01 mm, a width of 5.28 mm provides the 25.5 ohm impedance at the 880 MHz resonance frequency [4.2].

The two quarter-wave transformers were installed on the U patch antenna, replacing the SMA connectors on the ground plane. At first, the transformers were attached to the top of the antenna. The ground planes of the transformers were soldered to the copper patches of the antenna, making the top of the antenna act as the ground plane for the microstrip transformers (see Yangtze, Fig. 4.26). This ruined the return loss and substantially increased the coupling between feeds. There are a number of plausible explanations for this. For one, the copper patches were not at ground potential near the gap, especially close to the feed points. The patches therefore acted as poor ground planes for the transformers. Also, placing the transformers atop the most critical region of the antenna likely affected the electric fields there, preventing these fields from acting across the gap or through the dielectric to the ground plane as they should.

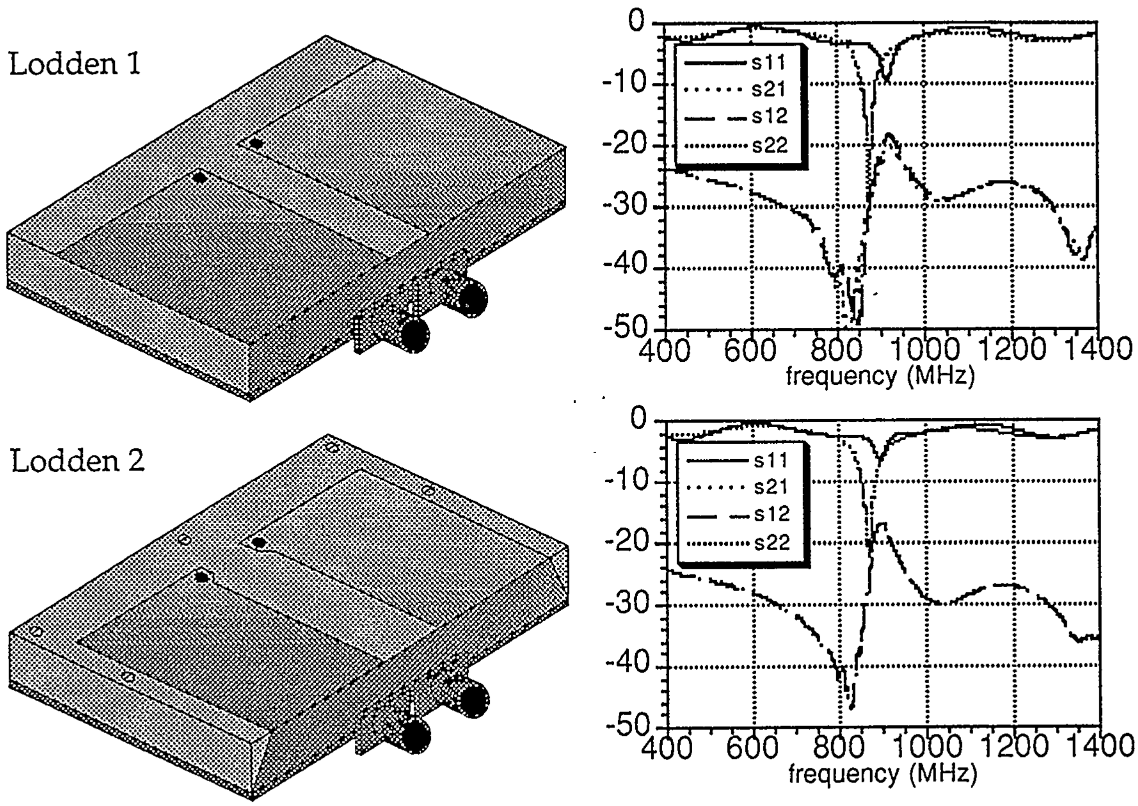

Fig. 4.28 Diagrams and S-parameters of Lodden 1 and Lodden 2.

Attaching the transformers to the bottom of the antenna produced much better results. The ground planes of the transformers were soldered to the antenna's ground plane and a wire extended from the end of each transformer through the dielectric to a feed point on the U patch. As shown in Fig. 4.28, Lodden 1 has a distinct resonant frequency for each slot and very low coupling over the entire frequency range. The impedance match of slot 2 is excellent (-30.34 dB at 873.75 MHz). The match of slot 1 is not as good (-9.64 dB at 915.00

MHz) but it is better than for Tsitika or Yangtze. The transformers were therefore reasonably successful in matching the antenna impedance to the system.

The other modification of Lodden 1 is the increased gap across slot 1 to 1 cm. This modification alone had a negligible effect on the antenna performance, as witnessed by other measurements not shown here. Even when the gap was further widened to 1.5 cm, no noticeable effect was seen (the gap was widened all along slot 1 except near the feed points, where the gap remained at 1 cm to keep the feeds attached to the patches).

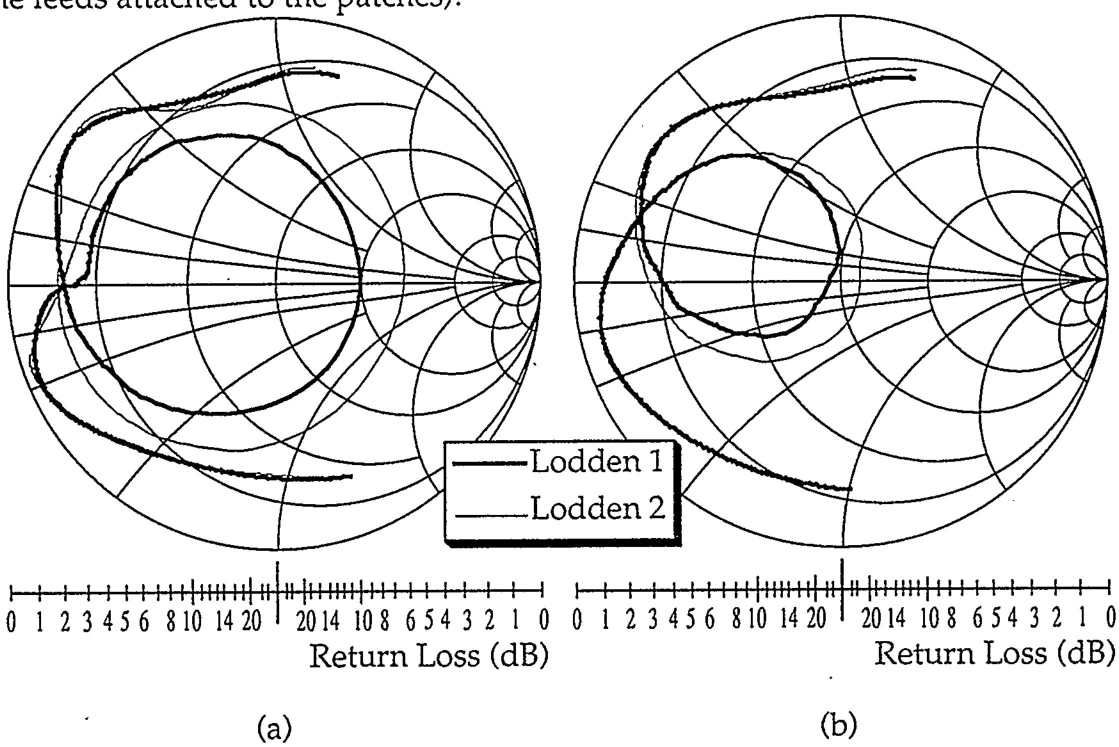

Fig. 4.29 Smith charts comparing Lodden 1 and Lodden 2. (a) S_{11} (b) S_{22}.

By the time Lodden 2 was designed, so much heat had been applied to the antenna from soldering and de-soldering that the glue could no longer keep the ground plane bonded to the dielectric. Screws were therefore inserted at five locations around the perimeter of the antenna to clamp it together (see Lodden 2, Fig. 4.28). Nylon screws were used instead of metal screws so that there was minimal disturbance of the electromagnetic fields. In order to make room for two of the screws on the sides of the antenna, each side of the U patch was recessed by 0.8 cm from the edge, as shown in Fig. 4.28 (Lodden 2). This had the effect of raising the return losses of both slots. Smith charts of the impedances for Lodden 1 and Lodden 2 (Fig. 4.29) reveal that the return losses are higher for Lodden 2 near resonance because the input impedances have increased away from the centre of the Smith chart. When the feeds are operated out of phase, the sides of the 'U' can be thought of as transmission lines whose characteristic impedance is inversely proportional to their width; as each side of the U patch is narrowed, its characteristic impedance increases.

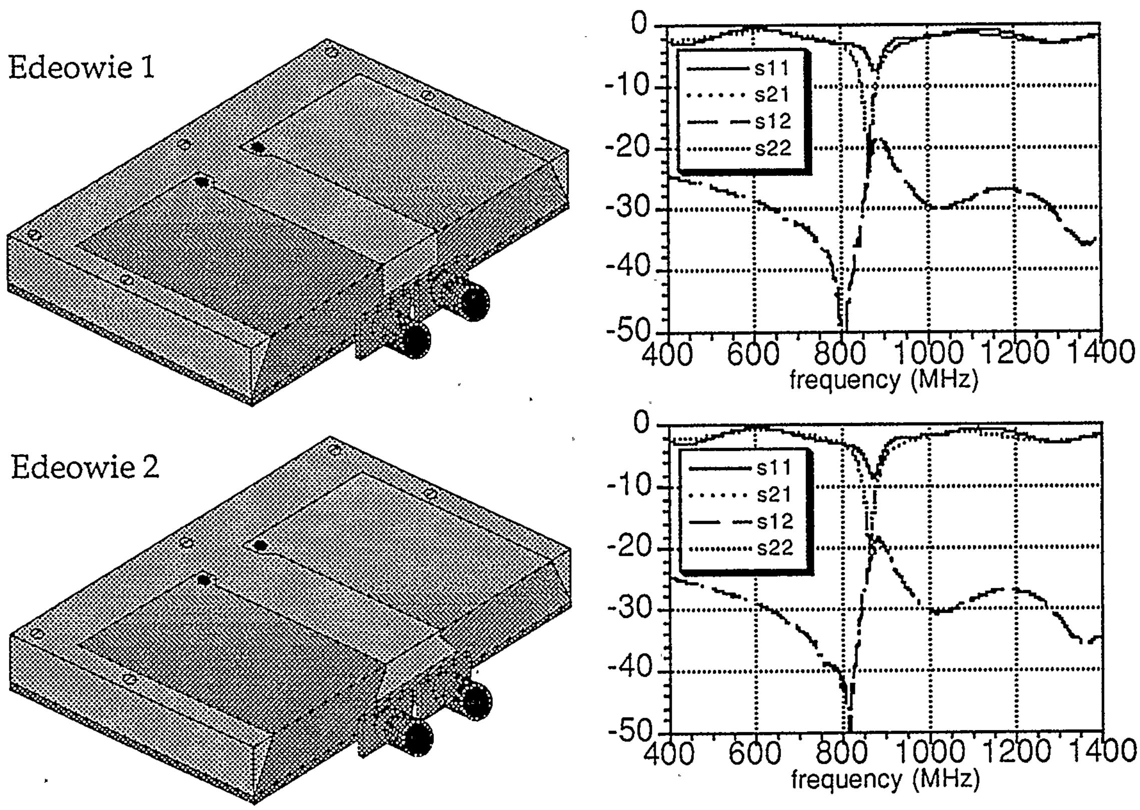

Fig. 4.30 Diagrams and S-parameters of Edeowie 1 and Edeowie 2.

This, however, does not explain why widening slot 1 did not also increase the input impedance unless it is also taken into consideration that the narrower a transmission line is, the greater is the effect of its width on its impedance. In other words, when slot 1 was widened, the transmission lines defined by the sides of the 'U' were so wide that the decrease in width was too small to effect the impedance.

When the feeds are operated in phase, the currents along slot 2 are strongest at the outside ends. These currents are impeded when the ends are cut in, resulting in a raised input impedance.

The modifications that led to the formations of Edeowie 1, 2 and 3 are based on the converse statement of the previous paragraph: when a slot is lengthened, its impedance will drop. Although Lodden 2 has low coupling between ports and a good impedance match for slot 2, the input impedance of slot 1 needs to be brought down substantially. The two slots must also operate at the same resonant frequency, so the resonant frequency of slot 1 must be brought closer to that of slot 2.

Lengthening slot 1 can accomplish both of these aims simultaneously. As shown in Fig. 4.30, slot 1 was lengthened by cutting down the front, towards the ground plane. The cutting was done in small steps, one or two millimetres at a time, and at first, it had no noticeable effect. The last few millimetres, however, gave a substantial improvement in return loss and resonant frequency, and so it seemed that cutting close to the ground plane was the way to go. After cutting the slot extension about as far as possible, it was tapered out, making it wider near the ground plane (see Edeowie 2). This further improved both the return loss and resonant frequency. Finally, thin horizontal slots were cut out from the base of the taper, close to the ground plane until the resonant frequencies were equal (see Edeowie 3, Fig. 4.31). The measured results of Lodden 2 and Edeowie 1, 2 and 3 are summarized in Table 4.2 for comparison.

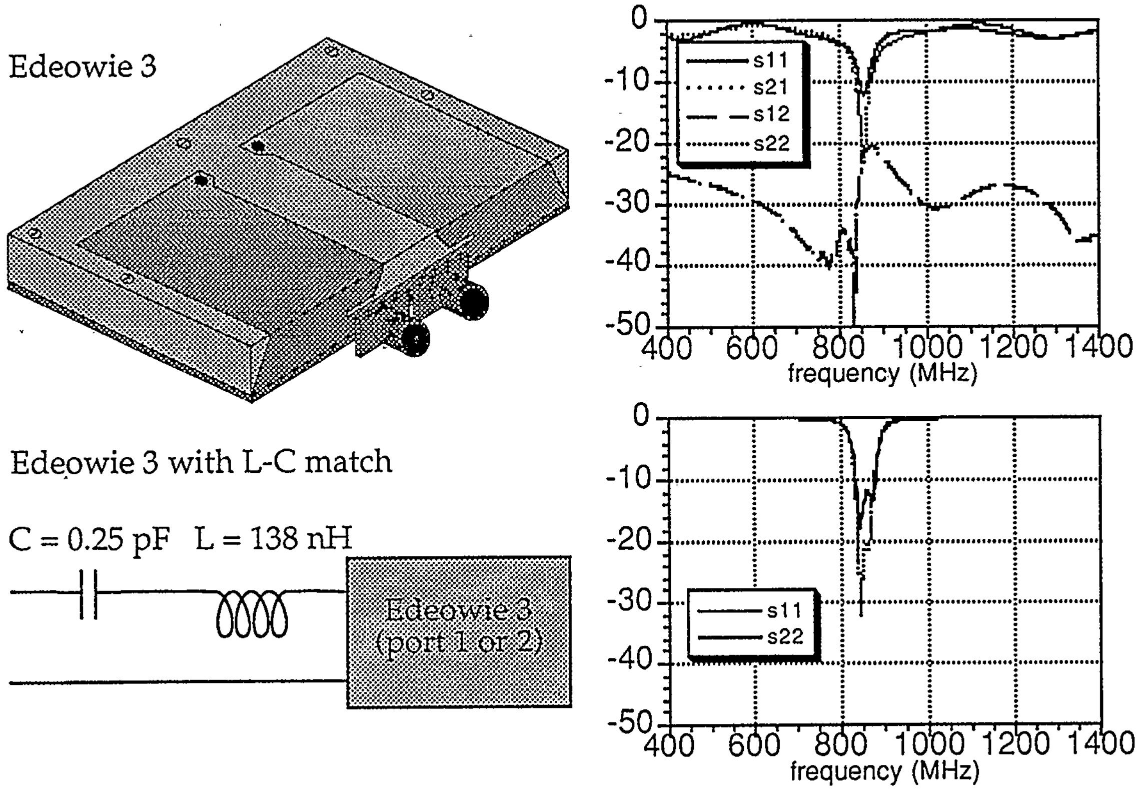

Fig. 4.31 Diagrams and S-parameters of Edeowie 3, unmodified and modified.

It is interesting to note that the coupling between ports improved as the return loss improved, although only slightly. This is different from the square and triangle patch antennas, where improvements in return loss were always in a tradeoff with stronger coupling.

Edeowie 3 is clearly the best antenna of the U patch designs. It is therefore the best antenna among all of the antennas tested. The coupling between ports is below the -20 dB mark, indicating that both ports were well isolated from each other. The return loss of slot 1 is good, the return loss of slot 2 is excellent and both modes of the antenna resonated at nearly the same frequency.

Antenna	Return loss (dB)		$f_{r1} - f_{r2}$ (MHz)	max. coupling (dB)
	slot 1	slot 2		
Lodden 2	-6.3	-22.3	27.50	-16.9
Edeowie 1	-7.4	-24.8	16.25	-18.3
Edeowie 2	-8.7	-21.0	8.75	-18.0
Edeowie 3	-12.0	-23.0	1.25*	-20.2

Table 4.2 Summary of S-Parameter results for Lodden 2 and Edeowie antennas (f_{ri} = resonant frequency of slot i).

Based solely on S parameter measurements, Edeowie 3 appears to have some potential for commercial use (although this claim cannot be substantiated without also looking at the radiation patterns, which are discussed shortly). However, there is still one problem which would limit its commercial use. Slots 1 and 2 have bandwidths of 17 MHz and 33 MHz, respectively. As mentioned in Section 4.2.3, each slot should have at least 25 MHz of bandwidth. The bandwidth of slot 1 is therefore too narrow. To widen the bandwidth, external matching circuits can be designed. These circuits can be connected to the input end of the transmission line matching circuits or integrated with them. Edeowie 3 has an impedance characteristic very similar to that of Lodden 1 or Lodden 2, shown on Fig. 4.29. Remembering that an impedance curve for a passive circuit rotates clockwise as the frequency increases, the impedance is inductive below the resonant frequency (f_r) and capacitive above it. With this in mind, a circuit that adds capacitive reactance below the resonant frequency, inductive reactance above it and zero reactance at the resonant frequency will tighten the impedance

* 1.25 MHz is the resolution of the measurement, so the resonant frequencies are very close.

curve around the centre of the Smith chart and thus widen the bandwidth of the antenna.

One simple circuit that provides these properties is the series-tuned resonant circuit, shown in Fig. 4.31. This circuit was built in software using the TOUCHSTONE® microwave computer aided design program [4.4]. Various capacitance and inductance values were programmed into the circuit until an optimal bandwidth for slot 1 was found. With a capacitance of 0.25 pF and an inductance of 138 nH slots 1 and 2 have bandwidths of 45 MHz and 43 MHz, respectively. Both of these bandwidths are comfortably above the 25 MHz requirement for commercial use.

For the TOUCHSTONE® program, the ideal capacitor and inductor were used. Practical capacitors and inductors are commercially available for the values required, but they have non-ideal characteristics (such as finite Q, self resonance and series resistance) that result in lower antenna bandwidths. Coilcraft™ offers ceramic chip inductors of 120 nH value. They have a minimum Q of 25, a maximum DC resistance of 0.63 ohms and self resonate above 900 MHz [4.5]. Since the self resonant frequency is so close to the operating frequency of the antenna (856 MHz), it is better to sacrifice bandwidth and use an inductor with a higher self resonant frequency. An 82 nH inductor self resonates above 950 MHz, which is comfortably above the antenna's operating frequency. Using this inductor, a capacitance of 0.42 pF is required to provide matching at 856 MHz. Porcelain Superchip™ capacitors are available at microwave frequencies from American Technical Ceramics™ ranging from 0.1 pF to 100 pF [4.6].

When entered into the TOUCHSTONE® program, the new values of inductance and capacitance give bandwidths of 41 MHz and 48 MHz for slots 1 and 2, respectively. The bandwidth of slot 1 is reduced slightly but still substantially above the 25 MHz criterion. A practical circuit will have even less bandwidth, but it is likely to stay above 25 MHz.

Two dimensional slices of Edeowie 3's radiation patterns are shown in Figs. 4.32 to 4.37. On these graphs, radiated power is measured outwards from -50 dB to 0 dB, with 0 dB referenced to the maximum radiated power. The first three graphs, 4.32 to 4.34, display the radiation in different planes when the antenna's feed points are excited in phase (0 dB = 8.97 mV). Figs. 4.35 to 4.37 show the radiation when the feed points are excited out of phase (0 dB = 11.1 mV). The vertical and horizontal polarizations are displayed separately, as parts (a) and (b) of each figure, respectively.

An interesting observation about these measurements is that the antenna worked best when rotated onto its side. The orientation of Edeowie 3 that was used for Figs. 4.32 to 4.37 is illustrated in Fig. 4.38.

The experimental results of the antenna in this orientation are superb. When the feed points were excited in phase (ie. slot 2 is in use), the horizontal polarization was strong and nearly omnidirectional in the horizontal (yz) plane (ϕ_{HP} = 315°) while the vertical polarization was much weaker (ϕ_{HP} is explained in section 3.1.2). On average, the horizontal polarization was 23.6 dB stronger than the vertical.

A similar situation was found when the antenna was fed out of phase (slot 1 is in use); the vertical polarization was strong and fairly close to omnidirectional in the horizontal (yz) plane (ϕ_{HP} = 199°) while the horizontal polarization was 19.9 dB weaker on average.

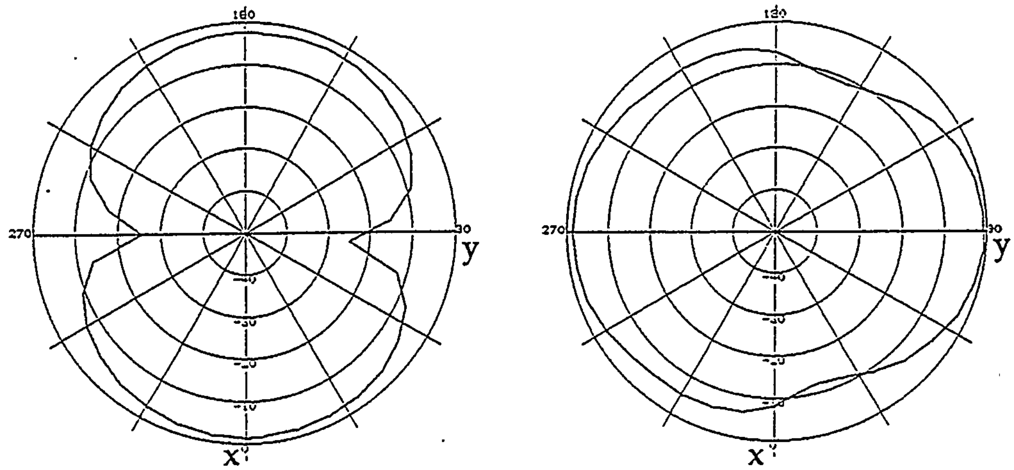

(a) (b)

Fig. 4.32 (a) Vertical and (b) horizontal radiation in xy plane, fed in phase.

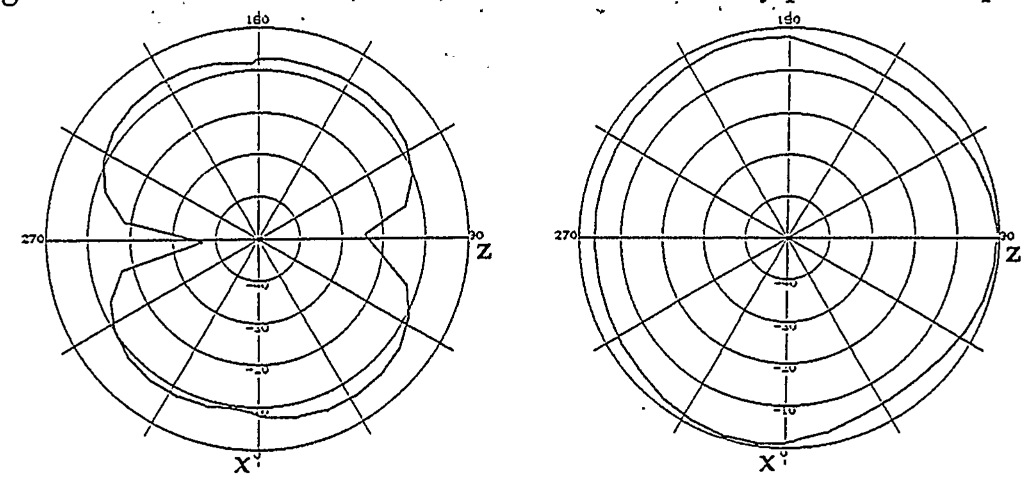

(a) (b)

Fig. 4.33 (a) Vertical and (b) horizontal radiation in xz plane, fed in phase.

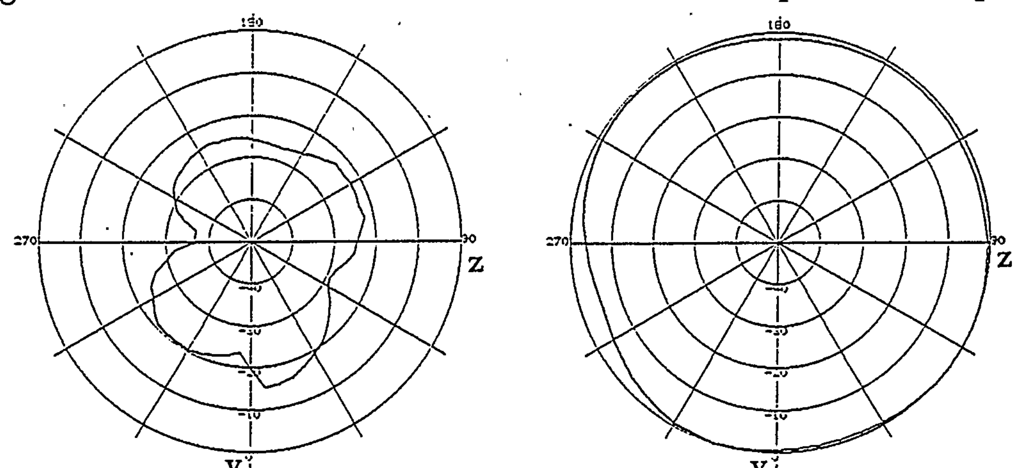

(a) (b)

Fig. 4.34 (a) Vertical and (b) horizontal radiation in yz plane, fed in phase.

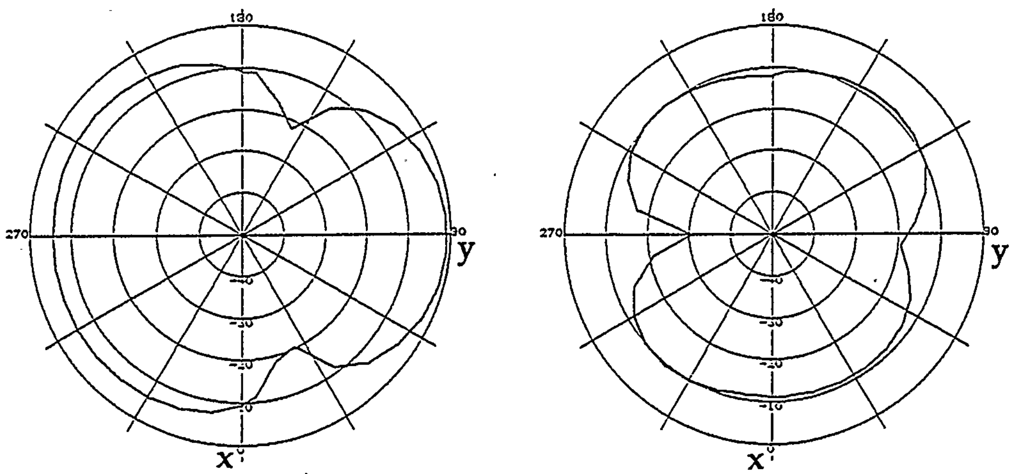

(a) (b)

Fig. 4.35 (a) Vertical and (b) horizontal radiation in xy plane, fed out of phase.

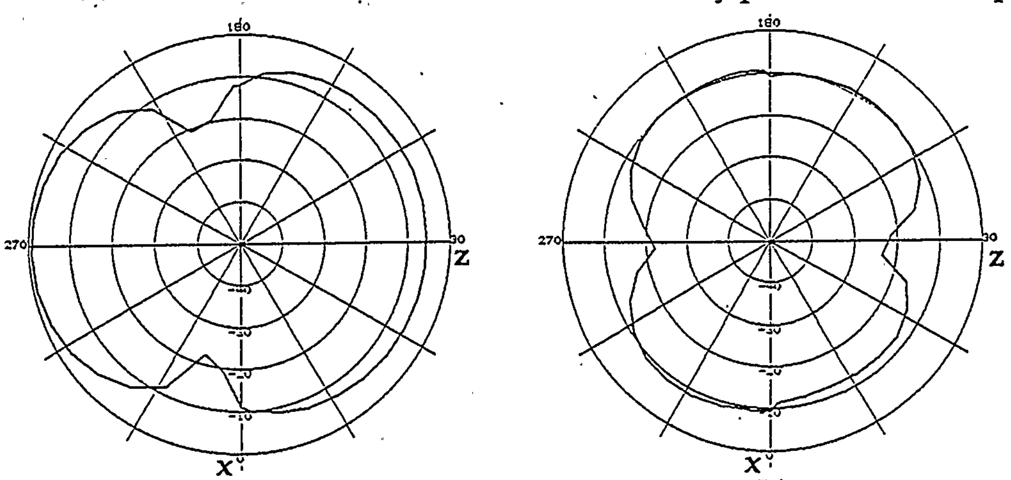

(a) (b)

Fig. 4.36 (a) Vertical and (b) horizontal radiation in xz plane, fed out of phase.

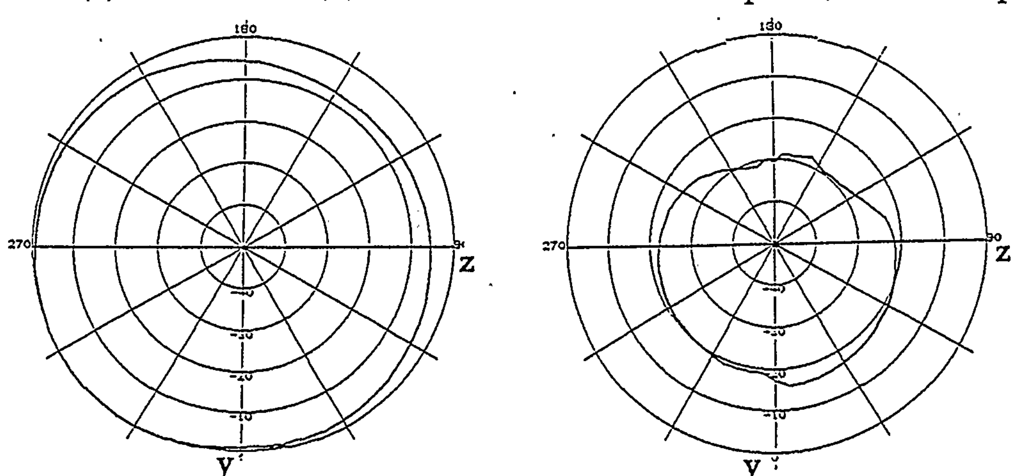

(a) (b)

Fig. 4.37 (a) Vertical and (b) horizontal radiation in yz plane, fed out of phase.

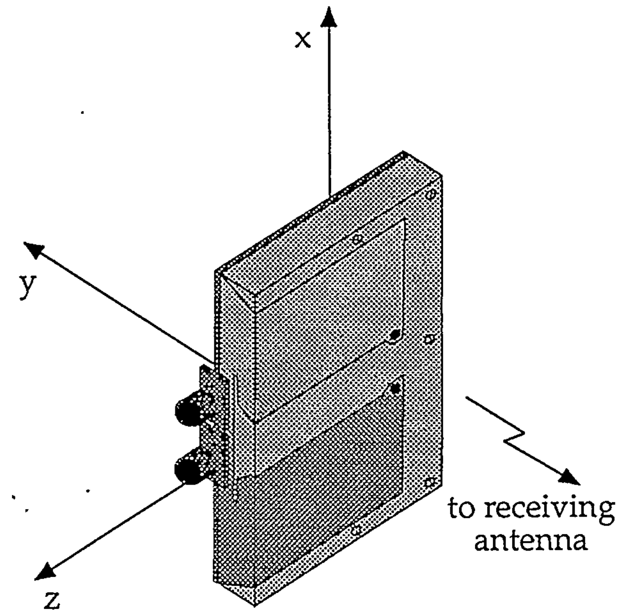

Fig. 4.38 Orientation of Edeowie 3 (origin of axes is in the geometric centre of the antenna).

In the forward vertical (xy) and side-looking vertical (xz) planes, the antenna has more than the required 30° beamwidth above the horizontal necessary to capture the bulk of the multipath signals in a cellular environment. The beamwidths of the dominant polarization of the antenna when fed in phase and out of phase are tabulated in Tables 4.3 and 4.4 respectively.

Beamwidth	xy plane	xz plane
Total	60.5°	73.2°
Above Horizon	30.5°	37.5°

Table 4.3 Beamwidths of the horizontal polarization when the antenna is fed in phase.

Edeowie 3 has a fairly directional radiation pattern that has slightly less gain than an omnidirectional antenna. The gain and directivity of the horizontally-polarized radiation pattern when the antenna was fed in phase are

0.97 (-0.15 dB) and 3.8 (5.8 dB) respectively. When Edeowie 3 was fed out of phase, the vertically-polarized radiation pattern had a gain of 0.99 (-0.05 dB) and 5.16 (7.13 dB) of directivity.

Beamwidth	xy plane	xz plane
Total	66.5°	70.6°
Above Horizon	34.8°	36.6°

Table 4.4 Beamwidths of the vertical polarization when the antenna is fed out of phase.

Edeowie 3 has many excellent features that make it attractive for commercial use. Because of its size, it can be used in a vehicular mobile system, but it is not yet small enough for use in a portable hand held unit. As indicated in Figs. 4.20 and 4.21, the antenna is 15.1 cm long, 8.8 cm wide and 1.27 cm high in its current form. This size is clearly too large for a hand held system, but there are a number of ways to reduce it. For example, substrates with higher dielectric constants can be used, as discussed in section 2.1. Also, the antenna can incorporate reactive loading in the antenna structure or at the feed points to offset the reactance that exists when an antenna is smaller than its optimal size. An example of this is found in the cellular 'whip' antennas mounted on vehicles. An inductive coil is incorporated part of the way up the monopole to tune out the capacitance that exists because of its smaller than ideal size.

Each of the above methods imposes new challenges, however, as the bandwidths and efficiency will decrease. Smaller antennas are also more sensitive to design tolerances (substrate homogeneity, impedance discontinuities and dirty or rough copper surfaces) which means that manufacturing must be done meticulously.

The antenna can also be made smaller if it is designed to operate at higher frequencies. All other things equal, an antenna built to operate at 2.0 GHz instead of 856 MHz would have its size reduced by a factor of 2.34. In other words, the antenna operating at 2.0 GHz would be 6.5 cm long, 3.8 cm wide and 0.54 cm high -- a practical size for a hand held unit.

4.3.4 Conclusions

Although the measurements of the triangle patch antenna are better than the square patch antenna, still too much power was coupled between the feed points. By observing some of the design flaws in the triangle patch antenna, some minor design changes were made. The result of these changes is the U patch antenna, which provides inherent isolation between its two modes of operation and uses the gap between the patches to its advantage rather than its detriment.

The latest model of the U patch antenna, Edeowie 3, has excellent radiating characteristics and has commercial potential. The vertically- and horizontally-polarized modes resonated at frequencies within 1.25 MHz of each other and were coupled by only -20.2 dB, slightly below the recommended -20 dB ceiling.

The two modes of operation had bandwidths of 17 MHz and 33 MHz. Although one of these bandwidths is smaller than the 25 MHz bandwidth needed for the receive band of the 800 MHz cellular system, it can be improved with a simple, series-tuned LC circuit.

The radiation patterns of Edeowie 3 indicate good discrimination between the vertically-polarized and horizontally-polarized radiation of both modes in the yz plane. In both modes, the dominant polarization was nearly omnidirectional in the horizontal plane and roughly 20 dB stronger than the weaker polarization.

4.4 Summary of Results

Three antennas were designed and built over the course of the Master's thesis work in an attempt to provide polarization diversity.

The first antenna, the square patch, was meant to provide the operation of a cross slot antenna with one quarter of the copper area. With two feed points situated near opposite corners of a square microstrip patch and a thick post grounding a third corner, the antenna was designed to independently excite a horizontally-polarized or vertically-polarized field by creating an electric potential between one edge of the square and the ground plane. This antenna did not work very well. Strong coupling between the feed points prevented the structure from radiating efficiently, which called into question whether the fundamental assumptions regarding its operation held.

As the coupling between the feed points was the main challenge with the square patch antenna, the triangle patch antenna was designed specifically to overcome this challenge. Each feed point of this second antenna was soldered to its own triangular radiating patch and both patches were physically separated from each other, except at one common grounding point.

This design did in fact reduce the coupling between the feed points and resulted in a much better antenna. The latest model of the triangle patch antenna, newt 25, radiated with fairly good return losses (-18.66 dB and -10.52 dB for patch 1 and patch 2, respectively) at centre frequencies that are quite closely spaced (1098.8 MHz and 1085.0 MHz). The coupling from patch 2 to patch 1 is

-12.19 dB at 1085.0 MHz. This parameter is much better than that of the square patch, but coupling of at least -20 dB is necessary to ensure sufficient isolation between the two modes of operation.

The best solution to the coupling problem was met with the final design, the U patch antenna. Coupling across the gap between patches was seen as a significant contributor to the total coupling between the two feed points of the triangle patch antenna, so the U patch antenna used the gap to its advantage. Exciting the feed points 180° out of phase created an electric field across this gap, radiating a vertically-polarized wave. By operating two feed points in phase, this structure excited an electric field across the slot between the patches and the ground plane, creating a horizontally-polarized wave.

The result is a very attractive antenna that has some commercial potential. The maximum coupling between the feeds is -20.2 dB. As well, the two modes resonated within 1.25 MHz of each other. They had 17 MHz and 33 MHz bandwidths, one of which is not large enough to make the antenna viable for use in the 800 MHz cellular system but can be improved with a series-tuned LC resonant circuit.

For the U patch antenna, vertically-polarized and horizontally-polarized radiation patterns were measured at NovAtel's Antenna Test Range. These patterns show that the dominant polarization was nearly omnidirectional in the horizontal plane and roughly 20 dB stronger than the weaker polarization.

The last model of the U patch antenna, Edeowie 3, is viable for use in vehicular mobile systems in its current form. Because of its large size, it is not compact enough to be used in hand-held systems, but the size can be reduced through design changes or by operating it at higher frequencies.

Chapter 5
Conclusions

The telephone has played a very influential role in the industrialized world but its life has been slow to progress. Although it was born in the late 1800s, it took us nearly a century to cut its umbilical cord. Wireless telephony is a very difficult concept to realize, and even now that it is here, there are still many challenges lying in its path to progress. One challenge is providing consistent high-quality voice or data amidst the multipath fading effects inherent in the mobile environment. It is well known that diversity reception can help in meeting this challenge and this thesis is therefore an attempt to provide antennas that employ diversity reception and are also compact enough to be used with today's portable communicators. The three sections of this chapter summarize the experimental results of three diversity antennas, debate the merits and drawbacks of the antenna measurement systems and recommend the direction of future research in this area.

5.1 Experimental Results

Microstrip antennas were used throughout the thesis because they are light, compact, and relatively easy to manufacture [5.1]. Each antenna was designed to provide polarization diversity which substantially reduces signal fading in mobile environments, particularly when there is no line-of-sight propagation [5.2, 5.3, 5.4]. The first design uses a square microstrip patch antenna, fed near opposite corners to provide both vertical and horizontal polarization. This design did not work well, as strong coupling between the feed points prevented the structure from radiating efficiently or with the proper polarization. The next design, the triangle patch antenna, operates on the same principles as the square patch antenna with the exception that the feed points were physically separated to reduce the coupling. This antenna performed much better than the square patch antenna, but its coupling is still insufficient to isolate the two modes of operation. Some radiation across the gap between the two triangle patches contributed to the coupling.

The final design, the U patch antenna, solved the coupling problem by using the gap to its advantage. It performed very well and has some commercial potential. Both the vertically-polarized and horizontally-polarized modes of the latest model of the U patch antenna resonated well and there was very low coupling between them. The bandwidth of one mode is low but can be improved with a series LC resonant circuit. Measured radiation patterns indicate strong discrimination between the two modes and almost omnidirectional radiation in the horizontal plane. The latest form of the U patch antenna is viable for use in vehicular mobile systems but is not compact enough for hand-held units. The size can be reduced significantly if the antenna is designed for higher frequencies.

5.2 Measurement Systems

The three antennas were evaluated based on their scattering parameters, which indicate how the power incident at an antenna is used and indirectly give some idea of how well an antenna radiates. In addition, the radiated fields of the square patch and U patch antennas were measured either at one position in front of the antenna over a broad frequency range or at many locations all around the antenna at one frequency. These measurements, particularly the latter type, provide an understanding of the strength and polarization of the fields and in doing so outline the diversity of the polarizations. However, none of these measurements can determine the most important feature, which is how much the signal fading is reduced in a typical mobile environment. To do this, the antenna must be set up to receive signals in a number of typical mobile environments and the measured signals at each antenna in diversity should be compared to the diversity signal which is produced by standard selection or combining methods. If this method is too time consuming or resource intensive to be practical, a computer model can estimate the improvement due to diversity based on radiation pattern measurements [5.5].

5.3 Future Research

Although the square patch and triangle patch antennas did not perform very well, further research on them is recommended as they are so compact. So much work needs to be done to improve the square patch antenna that it alone is not worth pursuing. However, judging from the relative success of the triangle patch antenna and its foreseeable potential if more research on it is carried out, the next logical antenna design would combine the function of the triangle patch with the smaller size of the square patch.

The U patch antenna performed very well and has commercial potential. The next step for this antenna is to evaluate how much it reduces signal fading in mobile environments by one of the methods described in section 5.2. There should also be some work done to find ways of reducing its size given a fixed operating frequency. This can be achieved with reactive loading or by using substrates with higher dielectric constants.

References

Chapter 1

[1.1] H. Hashemi, "Simulation of the urban radio propagation channel," *Doctoral Dissertation*, University of California, Berkeley, 1977.

[1.2] B. Davies, "In-Building UHF Propagation Studies," *M.Sc. thesis*, Dept. of Electrical and Computer Engineering, University of Calgary, 1990, p. 110.

[1.3] G.A. Deschamps, "Microstrip Microwave Antennas," *3rd USAF Symposium on Antennas*, 1953.

[1.4] I.J. Bahl and P. Bhartia, *Microstrip Antennas*, Dedham, Massachusetts: Artech House, 1980.

[1.5] W.C.Y. Lee, *Mobile Communications Engineering*, New York: McGraw-Hill, 1982, pp. 275-280.

[1.6] Ibid., p. 283.

[1.7] Ibid., pp. 159-163.

[1.8] Ibid., p. 165.

[1.9] S.A. Bergman and H.W. Arnold, "Polarization Diversity in Portable Communications Environment," *Electronics Letters*, Vol. 22, No. 11, 1986.

[1.10] K. Nishikawa and K. Sato, "Low Profile Antenna for Land Mobile Communications," *U.S. Patent*, Patent No. 5,146,232, Sept. 8, 1992.

[1.11] K. Tsunekawa, "Diversity Antennas for Portable Telephones," *39th IEEE Vehicular Technology Conference*, Vol. I, May 1989, pp. 50-56.

[1.12] H. Arai, H. Iwashita, N. Toki and N. Goto, "A Flat Energy Density Antenna System for Mobile Telephone," *IEEE Transactions on Vehicular Technology*, Vol. 40, No. 2, May 1991, pp. 483-486.

[1.13] F. Lalezari and R.E. Munson, "Dual Polarized, High Efficiency Microstrip Antenna," *United States Patent*, Patent No. 4,464,663, Aug. 7, 1984.

Chapter 2

[2.1] I.J. Bahl and P. Bhartia, *Microstrip Antennas*, Dedham, Massachussets: Artech House, 1980, p. 32.

[2.2] G.J. Burke and A.J. Poggio, *Numerical Electromagnetics Code (NEC) - Method of Moments, Part III: User's Guide*, Lawrence Livermore National Laboratory, Jan. 1981.

[2.3] I.J. Bahl and P. Bhartia, *Microstrip Antennas*, Dedham, Massachussets: Artech House, 1980, p. 57.

[2.4] P.A. Rizzi, *Microwave Engineering: Passive Circuits*, Englewood Cliffs, NJ: Prentice-Hall, 1988, p. 77.

Chapter 3

[3.1] D. Harrison, NovAtel Communications Ltd., Calgary, Alberta, Canada, Private Communications, 1992.

[3.2] W.C.Y. Lee, *Mobile Communications Engineering*, New York: McGraw-

Hill, 1982, p. 3.

[3.3] P.A. Rizzi, *Microwave Engineering: Passive Circuits*, Englewood Cliffs, NJ: Prentice-Hall, 1988, p. 34.

[3.4] Ibid., p. 40.

[3.5] T. Taga, "A Method of Estimating the Correlation Coefficient of Antenna Diversity in Mobile Radio Communications," *Third Nordic Seminar*, Copenhagen, Denmark, 1988.

[3.6] I.J. Bahl and P. Bhartia, *Microstrip Antennas*, Dedham, Massachussets: Artech House, 1980, p. 75.

[3.7] Ibid., p. 65.

[3.8] B. Davies, "In-Building UHF Propagation Studies," *M.Sc. thesis*, Dept. of Electrical and Computer Engineering, University of Calgary, 1990.

[3.9] M. G. Douglas, "A Computer Program to Calculate the Correlation Between Two Antennas in Diversity," *course project report*, Dept. of Electrical and Computer Engineering, University of Calgary, Dec. 1990.

[3.10] G.J. Burke and A.J. Poggio, *Numerical Electromagnetics Code (NEC) - Method of Moments, Part III: User's Guide*, Lawrence Livermore National Laboratory, Jan. 1981.

[3.11] C.W. Trueman and S.J. Kubina, "Automated Radius Calculation for Wire-Grid Models," Electromagnetic Compatibility Laboratory, Concordia University, Montreal, PQ, 1990.

[3.12] *HP 8510C Network Analyzer Operating and Programming Manual*, Santa Rosa, CA: Hewlett-Packard Co., Mar. 1991.

[3.13] D. Goulbourne, P. Camwell, A. McGirr, J. McRory and G. Schmidt, "Automated Antenna Test Range For Small Antennas," *Symposium on Antenna Technology and Applied Electromagnetics (ANTEM)*, Aug. 1990.

Chapter 4

[4.1] P.A. Rizzi, *Microwave Engineering: Passive Circuits*, Englewood Cliffs, NJ: Prentice-Hall, 1988, p. 142.

[4.2] E.O. Hammerstad and Ø. Jensen, "Accurate Models for Microstrip Computer-Aided Design," *ELAB report*, Trondheim, Norway.

[4.3] P.A. Rizzi, *Microwave Engineering: Passive Circuits*, Englewood Cliffs, NJ: Prentice-Hall, 1988, p. 77.

[4.4] *EESof TOUCHSTONE® User's Manual*, Pub. 1.4-01186, Jan. 1986.

[4.5] *Microwaves & RF: Product Data and Directory Issue*, Cleveland, OH: Penton Publishing, 1991, p. 247.

[4.6] Ibid., p. 235.

Chapter 5

[5.1] I.J. Bahl and P. Bhartia, *Microstrip Antennas*, Dedham, Massachusetts: Artech House, 1980.

[5.2] S.A. Bergman and H.W. Arnold, "Polarization Diversity in Portable Communications Environment," *Electronics Letters*, Vol. 22, No. 11, 1986.

[5.3] B. Davies, "In-Building UHF Propagation Studies," *M.Sc. thesis*, Dept. of Electrical and Computer Engineering, University of Calgary, 1990, p. 110.

[5.4] W.C.Y. Lee, *Mobile Communications Engineering*, New York: McGraw-Hill, 1982, pg. 165.

[5.5] M. G. Douglas, "A Computer Program to Calculate the Correlation Between Two Antennas in Diversity," *course project report*, Dept. of

Electrical and Computer Engineering, University of Calgary, Dec. 1990.

Appendix
NEC Simulations

The initial thesis plan was to complement experimental results with NEC computer simulations, particularly in the initial design stages. As, during the course of the NEC work, the models became better understood, they could be relied on more heavily. The NEC modeling would then be more expedient and versatile than physical design. After more than five months of simulations, however, the models did not prove to be reliable enough to use and the work had to be abandoned.

Two NEC models will be used in this appendix to illustrate the point. They are both prototypes of the U patch antenna, described in Section 4.3. As NEC cannot model planar surfaces unless they compose an enclosed object, the two NEC prototypes must instead be described as a grid of wires (see Fig. A.1). NEC also cannot model dielectric materials and so the prototypes were designed to operate in an air dielectric medium. The ground plane of each antenna is not shown but was modeled as an infinitely large, perfect conductor lying in the -zx plane.

The length of the antennas, ℓ, is 9.375 cm which is the electrical equivalent to one quarter of a wavelength at 800 MHz. The other dimensions (the height, width and gap across slot 1) are given in Fig. A.1. Both prototypes are symmetric about a line that cuts through the middle of slot 1 and is normal to the electric wall that connects the top patches to the ground plane.

For each model, the input impedances as calculated by NEC are displayed in Figs. A.2 and A.3 with the measured impedance of the Tsitika antenna. Fig. A.2 represents the case when the two feed points are fed out of phase and Fig. A.3 is the case when they are fed in phase. Tsitika is the simplest of the U patch antennas and therefore most closely resembles the NEC models.

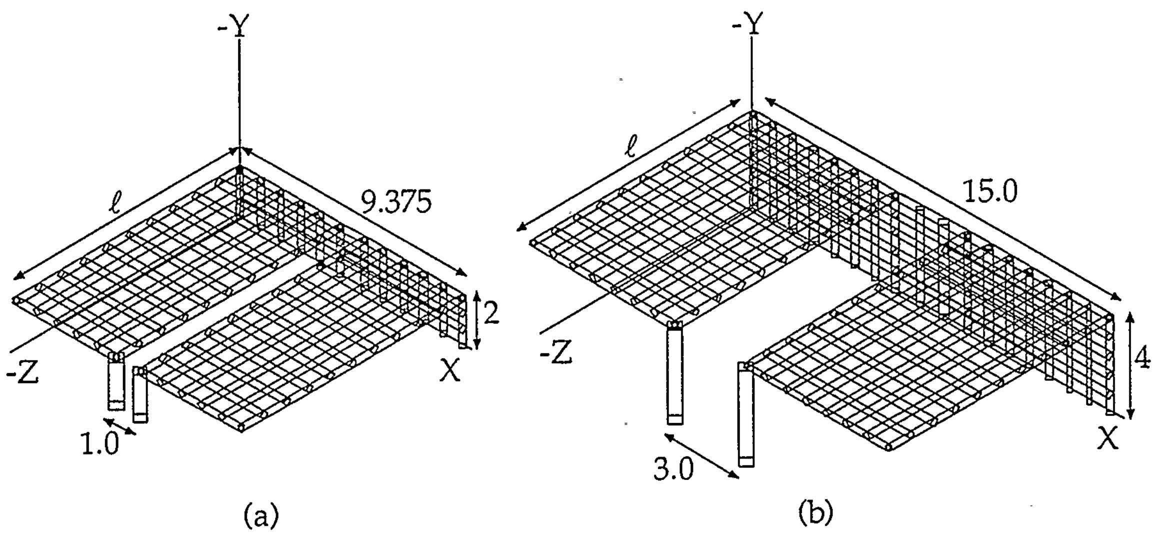

Fig. A.1 (a) NEC model 1 and (b) NEC model 2 of the U Patch antenna (all dimensions are in centimetres).

It should be noted that the NEC calculations and the experimental results of Tsitika are slightly different. The input impedance from NEC was calculated at the feed points (both feed points have the same impedance, so the total input impedance of the antenna is the same as the impedance at one feed point) while the input impedance of Tsitika was measured at an input port of the hybrid circuit (see Fig. 4.20). However, although they are different measurements, they should give the same results. For example, there was a time (phase) delay of 2.353 nanoseconds between the feed points and the input ports to the hybrid circuit, but this delay was removed in the experimental measurement. The hybrid circuit also splits or combines the signals into or from the antenna, respectively, but because all ports of the hybrid are matched to 50 ohms, this should not alter the input impedance from what would be seen at the feed points.

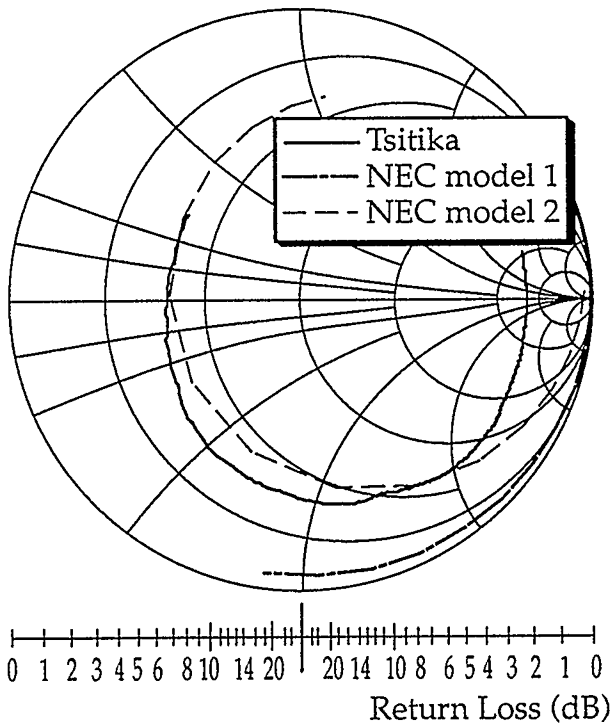

Fig. A.2 Input impedances of Tsitika and two NEC models, feed points fed out of phase.

The input impedances of the NEC models are both very different from the experimental results, or, more importantly, each pair of input impedances for one NEC model does not even closely approximate the pair of measured impedances of Tsitika. The S_{11} values of NEC 2 and Tsitika come fairly close to each other, but the S_{22} values are very different. This is typical of all of the

NEC models studied. By varying the height, width and gap across slot 1, one impedance can be brought closer to the experimental curve, but always at the expense of moving the other impedance farther away.

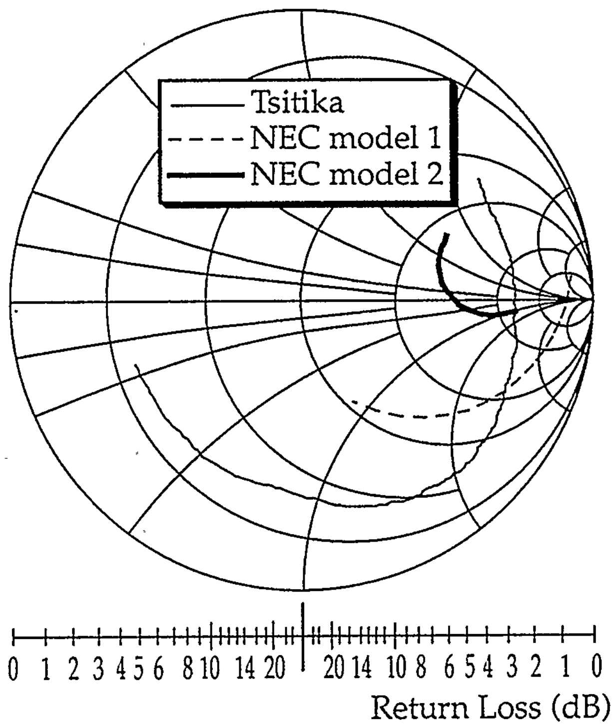

Fig. A.3 Input impedances of Tsitika and two NEC models, feed points fed in phase.

The computed radiation patterns are even more different from those measured in reality. Shown in Figs. A.4 and A.5, the radiation patterns of both polarizations of the antenna when the feed points were fed out of phase and in phase, respectively, clearly do not even resemble the radiation patterns of Edeowie 3, given in Figs. 4.32 to 4.37 (only the radiation above the -zx plane is shown because there is no radiation below an infinitely large ground plane).

A more reasonable comparison to make would be between the radiation patterns of NEC model 1 and those of Tsitika, but radiation patterns of Tsitika were not measured, and even if they were, they are not expected to be significantly different from those of Edeowie 3, as many of the modifications from Tsitika to Edeowie 3 would only affect the antenna's internal parameters such as impedance matching.

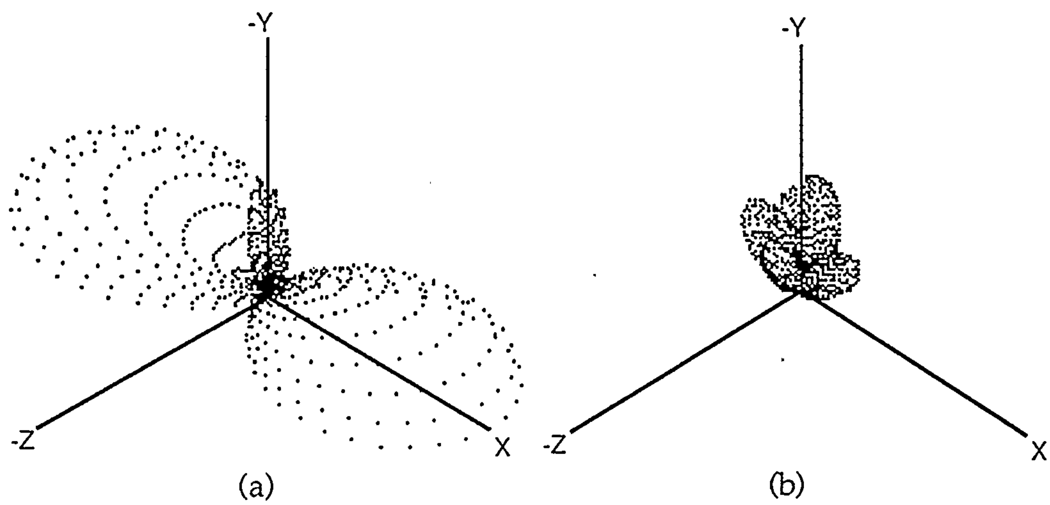

Fig. A.4 (a) Vertically-polarized and (b) horizontally-polarized radiation patterns of NEC model 1, feed points fed out of phase.

The NEC radiation patterns show that the horizontally-polarized radiation is much weaker than the vertically-polarized radiation, the vertical components radiate mainly in the -zx plane whereas the horizontal components do not radiate in that plane at all, and the vertical components are weakest along the -y axis, precisely where the horizontal components are strongest. None of these properties are true of the measured radiation patterns of Edeowie 3.

All of the differences between NEC calculations and experimental results do not mean that NEC cannot analyze antennas well, but rather in five months the author could not design one well. Being an all-purpose electromagnetic analysis program, NEC's manuals did not offer tips for antenna designers. The author also did not find many articles that could offer assistance (aside from [3.6]) and therefore, time and experience were the only tools available to make some progress with this complex program. Five months did not prove to be enough time for this author, but any more time seemed like a waste.

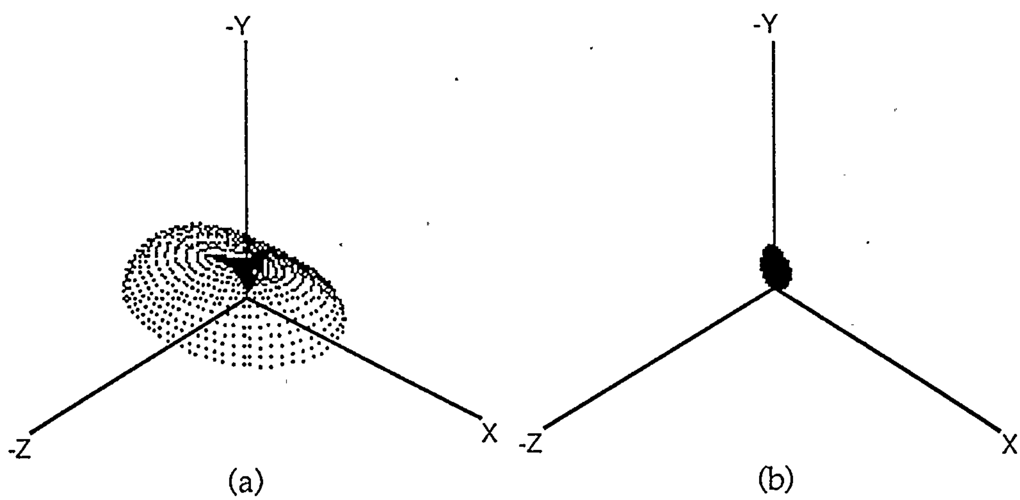

Fig. A.5 (a) Vertically-polarized and (b) horizontally-polarized radiation patterns of NEC model 1, feed points fed in phase.

The main difficulty with using this program is that there are so many variables to simultaneously manipulate. The wire radii, the spacing between wires, the wire grid pattern and the shape of the antenna are all of concern, as is the question of whether the dielectric should be approximated with an array of capacitors or whether the size of the antenna should be enlarged to work with an air dielectric.

In retrospect, all of these concerns were addressed as thoroughly as possible aside from one: the wire grid pattern. As the wire mesh must approximate as closely as possible a planar conductor, it is important that the currents on the mesh flow as they would on the planar conductor. Care must therefore be taken to orient the wires in the directions of current flow, which is more likely to be radially outward from the feed points than along straight lines parallel to the x and -z axes. Modifying the pattern of the wires in this way could significantly affect the calculated input impedances and radiation patterns.